UCLA
UCLA Electronic Theses and Dissertations

Title

Drug Release Kinetics from Poly(ethylene glycol) Hydrogels for Wound Dressings

Permalink

https://escholarship.org/uc/item/1wr9p0z6

Author

Cook, Kaitlyn A

Publication Date

2020

Peer reviewed|Thesis/dissertation

UNIVERSITY OF CALIFORNIA

Los Angeles

Drug Release Kinetics from Poly(ethylene glycol) Hydrogels for Wound Dressings

A thesis submitted in partial satisfaction

of the requirements for the degree Master of Science

in Bioengineering

by

Kaitlyn Alexis Cook

2020

ABSTRACT OF THESIS

Drug Release Kinetics from Poly(ethylene glycol) Hydrogels for Wound Dressings

by

Kaitlyn Alexis Cook

Master of Science in Bioengineering

University of California, Los Angeles, 2020

Professor Andrea Kasko, Chair

Prolonged field care (PFC) for treatment of battlefield and trauma injuries requires the advancement of wound management techniques in order to prevent loss of life or limb prior to hospitalization in austere combat locations where medical evacuation is delayed. The goal of this project is to design a hydrogel wound dressing capable of providing sustained release of antibiotics, analgesics, and hemostatic agents over a three-day period. Poly(ethylene glycol) (PEG) hydrogels were fabricated through crosslinking using redox initiators – ammonium persulfate (APS) and tetramethylethylene diamine (TEMED). Hydrogels were characterized through the mass swelling ratio (q_m) to determine the mesh size (ξ) and thus qualitatively predict the release kinetics of the therapeutic drugs. Hydrogels with incorporated therapeutic drug were placed in known volumes of deionized water, from which aliquots were taken at set

time intervals. A UV Visible Spectrophotometer determined the aliquots' absorbance which

determined the cumulative release kinetics. Ultimately, three-day sustained release of the

therapeutic drugs from the PEG hydrogel was achieved through retarding the diffusion of the

therapeutic drugs by incorporating acrylic acid.

The thesis of Kaitlyn Alexis Cook is approved.

Nicholas Bernthal

Stephanie Seidlits

Andrea Kasko, Committee Chair

University of California, Los Angeles

2020

I would like to dedicate this thesis to my parents, Matthew and Catherine Cook, who have given

me a passion and desire for continuous learning. Thank you for the endless knowledge and

support you have provided throughout my academic career. Thanks to my siblings, Madison,

Allison, and Keegan, who always challenge me to be better. My family's competitive nature has

held me accountable and pushed me to be my absolute best. I love you all!

The day I stop learning is the day I stop growing. I continue to learn to continue to grow.

The cream will always rise to the top, it just takes time to get there.

Table of Contents

vii

List of Figures

List of Tables

List of Symbols and Acronyms

ξ – mesh size

η – viscosity of the solution

ρ_{BD} – bulk density for each molecular weight PEG

$(r_0^2)^{1/2}$ – RMS end to end distance of polymer chains between two neighboring crosslinks

ρ_s – density of the solvent

A – absorbance

AOR – area of responsibility

APS – ammonium persulfate

c – molar concentration (mol/L)

C_n – polymer specific characteristic ratio

CSF – cerebrospinal fluid

D_0 – diffusion coefficient for a therapeutic drug molecule in free solution

DCM – Dichloromethane

D_g – diffusion coefficient for a therapeutic drug molecule in the hydrogel

DI H_2O – with deionized water

DMA – Dynamic Mechanical Analyzer Q-800

E – modulus

ε – molar absorption coefficient (L*mol^{-1}*cm^{-1})

FDA – Food and Drug Administration

IED – improvised explosive device

k_B – Boltzmann Constant

K_b – diffusion retardation factor based on affinity interactions

L – height of thin film

l – length of the bond along the polymer backbone

l – optical path length (cm)

M_c – molecular weight between crosslinks

M_d – dry mass of the hydrogel

M_D – mass of the dried hydrogel

M_n – molecular weight (g/mol)

M_r – molecular weight of repeating units

M_S – mass of swollen hydrogel

M_s – swollen mass,

MW – molecular weight

N – number of links in the chain (N)

NMR – Nuclear magnetic resonance

PAA – polyacrylic acid/sodium polyacrylate

PEG – poly(ethylene glycol)

PEGDA – poly(ethylene glycol) diacrylate

PFC – prolonged field care

q_m – mass swelling ratio

q_m – mass swelling ratio

Q_v – volumetric swelling ratio

RMS – root mean square

R_s – radius of therapeutic drug solute

r_s – Stokes Einstein hydrodynamic radius

T – Temperature

t – Time

TEA – Triethylamine

TEMED – tetramethylethylene diamine

UV – ultraviolet

UV-Vis – UV-Visible Spectrophotometer

v – specific volume of polymer

V_1 – molar volume of DI H_2O

$v_{2,s}$ – polymer volume fraction

$v_{2,s}$ – polymer volume fraction

wt% – weight percent

X_1 – Flory Huggins polymer-solvent interaction parameter

Y – ratio of critical volume required for successful translational movement of solute to average

free volume per molecule of liquid

Acknowledgements

The views expressed in this thesis are those of the author and do not reflect the official policy or position of the United States Air Force, Department of Defense, or the U.S. Government.

1 Background

1.1 Focus Area

Throughout the past several decades there has been a shift in the nature of war. The battlefield has moved to a diffuse global stage compared to previous regional conflicts. The widespread geographic area of wars results in conflicts that occur rapidly, are short in duration, are high intensity, and thus leave little to no lead time for planning and establishing proper evacuation routes or medical care facilities.[1] Consequently, medical evacuations and access to proper medical facilities have become increasingly difficult due to the nature of such conflicts.

As such, the onus of responsibility now falls on the far forward care to provide hospital level care in austere environments. Prolonged field care (PFC) will require that combat medics play a larger role than simply bandaging a wound prior to transport to a hospital. In the field, management of wounds needs to be quick and prevent infection. Historically, the job of a battlefield medic is to apply a wound dressing that applies pressure and thus is a temporary fix prior to reaching a field hospital. However, the austere conditions of combat can hinder quick and easy access to hospitals. It may take many hours to days before the injured receive proper care.

The three fundamental challenges to extremity trauma in the field are: 1) hemorrhage, 2) pain control, and 3) infection. Therefore, it is necessary for PFC to provide hemorrhage control, pain management, and infection prevention in order to increase effective treatment and decontaminate the wound prior to arrival at the hospital for battlefield and combat injury victims. A strategy to seal and passively protect the wound in addition to actively

decontaminating and preventing proliferation of limb-threatening infection is a critical unmet

need in PFC that requires a novel solution. Thus, this research focuses on creating a low-

complexity, versatile, rugged, hydrogel wound dressing for PFC. This research requires the

innovation of a long-lasting wound dressing that delivers therapeutics and is easily able to be

applied by medics or the injured individual themself while in the field. The wound dressing is

designed to last three days so that no wound dressing change is required between injury and

evacuation, and therapeutics are continually delivered to the wound dressing. The ultimate

goal is to create a hydrogel platform capable of sealing the traumatic wound, preventing

bleeding with hemostatic agents, enhancing wound decontamination through sustained release

of antibiotics, and providing pain management with analgesic release. This hydrogel platform is

a biochemical tool aiming to improve patient outcome after battlefield and trauma injuries and

can be applied in the austere combat environments in the case of delayed medical evacuation.

Simply put, the overall goal is to design a field-polymerizable hydrogel that is usable in

far-forward, austere environments enabling sustained release of antibiotics, analgesics, and

hemostatic agent over a three-day period to provide maximum treatment until the person is

able to be evacuated to a medical facility.

There are several criteria to make this hydrogel wound dressing applicable for PFC. First,

is mobility. The wound dressing needs to be light weight in order to make it nonburdensome to

carry in the already heavy rucksacks of individuals in combat. The hydrogel solute needs to

require no additional equipment except for the potable water, which allows the hydrogel to

swell. Secondly, the hydrogel needs to form quickly (less than 60 seconds) as time is not a

luxury afforded to combat personal. The rapid formation of the hydrogel allows the liquid gel

solution to fill the wound shape, gel, and begin to release the hemostatic agent, antibiotics, and analgesics. Third, the hydrogel must also be customizable in the variety and combinations of therapeutics due to the nature of the wound. This allows for modularity and interoperability. The fourth criteria is ruggedization. The hydrogel needs to be able to withstand the harsh conditions and varied environments in which military personnel operate. Therefore, this hydrogel platform is a technological advancement in PFC that has many different avenues for optimization and application in either combat or trauma scenarios.

The hydrogel was designed with the limitations of austere combat zones. Therefore, the hydrogel itself is a lightweight powder that simply requires potable water, carried by all combat personal, as the solvent to form the hydrogel. The polymerization of the hydrogel is able to take place without the need for additional equipment, such as an UV light, by using biocompatible chemical reactions that allow for rapid polymerization. The polymerization is also able to occur within the wound itself. Thus, making the polymer versatile to many wounds regardless of the shape or size.

1.2   The Needs of the Military

Extremity injuries account for 54 percent of the combat wounds suffered by the military personal on the battlefield.[2] Additionally, musculoskeletal injuries are the most common injury and the costliest. Musculoskeletal injuries contribute to the greatest loss of strength for the injured individual.[2] Furthermore, the extremities have high rates of infection complications. Of those patients with extremity injuries, approximately 15 percent will develop osteomyelitis.[3] Osteomyelitis is an infection of the bone. The risks with extremity wounds are able to be mitigated in the field with proper wound treatment by combat medics prior to evacuation from

the austere location to established treatment facilities. However, it is the supplies and procedures for how these injuries are treated that contribute to the survival and recovery of the wounded individual.

There are a multitude of compounding factors that increase the challenge with in-field medical care. A few of the challenges for combat related injuries include detonation of high energy explosives, the environmental contamination, evacuation procedures, and level of medical care available.[4] In recent combat operations, of the individuals with extremity wounds, more than half were classified as penetrating soft tissue wounds.[4] Early and aggressive management of soft tissue wounds are key factors to decreasing the infection rates and improving the healing outcomes. Treatment with antibiotics contributes to wound management. Furthermore, the timing of antibiotic application is important. Antibiotics given after the three-hour mark of the injury incur an infection rate of 7.4%. However, when given within the first three hours, the infection rate is significantly lower, 4.7%.[5] Additionally, the lower extremity is more likely to sustain a serious extremity injury compared to the upper extremity; 47.8%and 41.6% respectively.[6] Compounded with the science that supports infection is more common in the lower extremity than the upper extremity, the need for infection control is critical.[6]

Despite the increase in medical advancements and care available to combat personnel in the austere conditions of combat, the amputation rates have remained roughly the same for major extremity injuries in the past 50 years.[6] The amputation rate was and still is between 7 and 8 percent of those who suffer from major extremity injuries.[6] Advancements in modern weaponry, such as improvised explosive devices (IEDs) have increased the degree of primary

4

tissue destruction. Explosive devices are the mechanism of injury in 87.9% of the individuals who received amputations.[6] Amputations performed early in the evacuation chain account for 95% of major amputations. This means amputations were performed prior to reaching the site of definitive care.[6] However, infections are the driving factor in late amputations.[7] Despite the improvement of potential evacuations times in the current wars, the environmental and combat conditions are still variable and can cause for substantial delays.[4] Larger areas of responsibility (AOR) result in rapid, short, high intensity conflicts, thus leaving little to no lead time for planning and establishing proper evacuation routes or medical care facilities.[1] Consequently, medical evacuations and access to proper medical facilities have become increasingly difficult due to the nature of such conflicts. Therefore, the austere conditions may prevent individuals from reaching even established care facilities early in the evacuation chain. This is where hemorrhage control, pain management, and antibiotics become an important factor in limiting surgical complications due to infection.

Hemorrhage is another issue that individuals with combat wounds face. Tourniquets are often the solution to hemorrhaging of a traumatic wound. Studies show that the quicker the tourniquet was applied the better the patients did. [8] This is especially true if the tourniquet was able to be applied prior to shock. Shock is defined as the weak or absent pulse in an uninjured limb without a tourniquet, and is due to the loss of blood and inability to circulate throughout the body.[8] While tourniquets are often associated with saving the lives of trauma victims, the long-term effects are not as promising. The tourniquet is an effective hemorrhaging tool to stop bleeding for major limb trauma, but this is only a temporary measure.

Despite the literature for tourniquets being effective, it is also recognized that the longer the tourniquet is in place, the increase in potential complications. Generally skeletal muscle is not tolerant to ischemia after six hours.[9] Additionally, tourniquets can cause nerve palsies and skin injury. Therefore with the potential long evacuations times in austere environments, a wound dressing that supplements the need for long term tourniquet use would be helpful.[9]

Currently, the military supplies medics with QuikClot, a combat gauze that is used for hemorrhage control. However, this technology still lacks the ability to completely control the bleeding, and hemostasis without limb ischemia remains a gap in the QuikClot technology. In the deaths that occur prior to evacuation, 50 percent are accounted for by uncontrolled hemorrhage and this continues to be the leading cause of death for those that are transported to a medical facility.[10] Furthermore, QuikClot does not provide additional therapeutics such as analgesics and antibiotics. Hemorrhaging that is uncontrolled due to traumatic events is often the major cause of complications and death.[10] Treating hemorrhages with hemostatic agents is an easy and effective treatment.

Pain management is also a critical component for treating combat injuries. Military personnel often carry "wound packs" that contain a mixture of oral medications including acetaminophen, rofecoxib, and fluoroquinolone for use in the event of an injury.[11] These "wound packs" allow the individual to self-treat prior to medical care. In the event of delayed medical evacuation, it is important to control the pain especially as the adrenaline of the event causing the injury wears off. Studies have even shown that local analgesics used in combination within adrenal have greater efficacy in reducing pain.[12] Therefore a wound dressing, with

6

analgesics incorporated, should be immediately applied while there is an increased amount of adrenaline in the body to better manage the pain. The concept of self-treatment for pain management can thus be translated to the wound dressing by application of analgesics at the site of injury.

1.3 Hydrogels as Wound Dressing

Hydrogels are an insoluble hydrophilic material that are made from synthetic polymers. They have a high water content, between 70-90 percent.[13] Hydrogels are moist, conformable, and soft. They also are able to transport oxygen and metabolites. The hydrogel is able to be conformed to the wound itself, keep the wound hydrated, while also providing a protective barrier layer typically provided by the skin. This protective barrier prevents against bacterial infection. The hydrogel is also able to match the modulus of the skin and deliver additional metabolites and oxygen to promote wound healing. The hydrogel is able to be easily removed from the skin when healing is complete, or a new dressing is needed to be applied. Most importantly the hydrogel is sterile, non-toxic and non-allergic.[13]

There are currently several commercial hydrogel wound dressings on the market. Some of these products include Intrasite™, Nu-gel™, and Aquaform™. Intrasite™ is known for creating a hydrate wound environment that enhances autolytic debridement in necrotic tissues. This product comes in a preformed hydrogel that is able to be excreted through a syringe.[14] Nugel™ is a preformed hydrogel that comes in a syringe like package. The product claims to provide moisture that contributes to the enhancement of necrotic tissue debridement.[15] Aquaform™ is known for providing moisture.[16] These hydrogel products are prescribed for individuals with diabetic ulcers, burns, and minor skin lacerations. However, the issues with the

translation of these hydrogels to the military application is that the hydrogels are pre-formed. This means that the hydrogels already contain the water. This is an issue because the water is 70 to 90% of the product, which is unnecessary weight to carry in an already heavy rucksack. The pre-formed hydrogel also limits the quantity able to be carried, since the packaging takes up space and has a limited amount of product inside. Preformed product decreases the products shelf life and stability, reducing the combat viability. Therefore, the products may not be able to withstand the dramatic temperature fluctuations and movement experienced in the austere environments.

There are also antimicrobial hydrogels reported in the literature. Some of these include poly(HEMA), dextran, chitosan, and other chemistries. The poly(HEMA) platform was combined with ciprofloxacin, and the release kinetics studied were based on variations in concentration of cross linker. The greater the concentration of crosslinker, the greater the release time of the drug release.[17] Another drawback is that this technique utilized ultraviolet (UV)-radiation to incorporate the drugs into the pHEMA membrane.[17] This product therefore does not meet the mobility requirement. However, it is possible to incorporate antimicrobial peptides into pHEMA, but research still needs to be refined to match the release profile of the device for the time spent in vivo.[18] Dextran based hydrogels with absorbed antifungal drugs were analyzed for antifungal properties. These hydrogels are possible to prevent biofilm formation on coated medical devices.[19] Dextran was also used in an injectable gel that had extended antifungal activity. The drug release was able to be sustained for an 11 day period without adverse side effects.[20] A thermosensitive hydrogel made of chitosan with the drug chlorohexidine was used in periodontal treatment as a drug delivery system.[21] There are several other chemistries

possible for creating antimicrobial hydrogels.[22] The major issue with these antimicrobial hydrogels is that the majority of the drug is released within the first 24 hours of the application of the hydrogels. The desired time scale for the therapeutic drug release is three days.

Wound dressings made from synthetic hydrogels, poly(ethylene glycol) (PEG), are comprised of many properties required for the in-field wound dressing. First, the synthetic hydrogel is also able to be a sealant. Therefore, the PEG hydrogel is able to withstand arterial pressure greater than 100 mmHg without leaking due to the ability to both chemically and physically mimic properties of native extracellular matrix.[23] The synthetic hydrogel made of PEG is both more chemically and thermally robust than the native proteins and polysaccharides. Second, PEG hydrogels can have high water content similar to that of eukaryotic cells.[24] PEG hydrogels also have a tunable modulus to match that of the soft tissue found in the skin.[25] PEG hydrogels have also demonstrated biocompatibility as a result of low protein absorption.[24] Instead of small molecules that form poly(HEMA), poly(NIPPAm) and other hydrogel polymers, PEG is formed from high molecular weight polymers that are water soluble.[24] The water solubility of PEG hydrogels is advantageous as it allows the PEG hydrogel to be formed while in the presence of living cells, tissues, and fragile biomolecules such as DNA and proteins.

There are many examples of PEG hydrogels being used as wound sealants and dressing for surgical operations. Creating new products for surgeries decreases the need for sutures, wires, staples, and other closing devices.[26] The problem with the existing surgical techniques is that they do not provide immediate closure of the wound, thus allowing for the possibility of infection or further tissue damage.[26] Wound sealants create a sealed environment that prevents bodily fluid leakage and exposure to contaminants in the surrounding environment.[26]

The PEG-based hydrogel as a wound dressing and sealant would not only prevent further infection but would also shorten the healing time, create less pain for the patients, and eliminate removal.[26] Issues with existing sealants are the difficulty to create a strong adhesion given the soft tissue environment of application. Additionally, the environment is wet due to bodily fluids such as blood, which creates additional adhesion challenges.[26] One example is κCA-nanosilicate hydrogels that are able to be injected into the wound site in order to accelerate the clotting and deliver therapeutics for wound healing.[27] Another example is Progel, a PEG and albumin based hydrogel, that was created to stop air leaks from the lungs. Progel was able to successfully demonstrate that it caused no adverse tissue reactions and was able to help seal the lungs after pulmonary surgery.[28] However, it is important to note that sealants are difficult as no one sealant can be universal for the different tissue types in the body.[28] Therefore careful optimization is necessary for specific applications. Future work is also needed to create a sealant that also has the ability to actively promote growth and repair of the tissue.[28]

DuraSeal® from Integra is a surgical hydrogel adhesive that is formed from a PEG diester and a trilysine amine crosslinking agent. DuraSeal® is used after spinal and cranial surgeries to prevent cerebrospinal fluid (CSF) from leaking.[29] One issue with Duraseal® is it is not designed for large defects. Furthermore, DuraSeal® is not able to be applied if adequate hemostasis is not achieved. The Baxter corporation produced Coseal® which is also a PEG-based sealant. Coseal® is intended to be a sealant for high pressure environments and thus can be used to secure anastomotic suture line hemostasis and to prevent adhesion.[30] Grinstaff and fellow researchers reported a PEG-based hydrogel sealant for *ex vivo* vein punctures. This

covalently crosslinked dendritic thioester hydrogel is able to form within seconds due to the multiple thioester linkages between the thiol residues and PEG macromer.[23] The issue here is that the component to crosslink the hydrogel, poly(lysine), is only biocompatible at low concentrations. Grinstaff's hydrogel system, when tested on mice, saw a decrease in blood loss of 33% when applied to severe hepatic hemorrhage and 22% when applied to an aortic injury.[31] The hydrogel was also able to act as a sealant preventing leaks for pressures up to 120 mmHg.[31] This is higher than the arterial pressures experienced in vivo which is between 70-100 mmHg and significantly higher than venous pressure of 8-12 mmHg.[31]

The majority of surgical sealants and dressings discussed are crosslinked in a step-growth condensation reaction mechanism. Step growth kinetics have a longer cure time, upwards of 10 minutes and tend to be softer due to a lower crosslink density. Conversely, PEG-based hydrogels experience chain growth reaction mechanisms making them valid for wound dressings and sealants.[28] One issue is that UV light is required to crosslink the materials. The UV light is not desired for combat operations as it is additional equipment, meaning additional weight, and also tactically disadvantageous.

These examples demonstrate that PEG-based hydrogels for wound dressings and sealants are feasible. The issue is the current existing PEG hydrogel wound dressings and sealants have areas of improvement and limitations that would not allow for direct transfer to a combat environment. Therefore, further research is needed to develop a combat capable wound hydrogel dressing.

The ideal hydrogel is one that is synthetic, made of PEG, that is able to act as both a wound dressing and a sealant for combat injuries. Therefore, the hydrogel would need to be

lightweight and portable, require no additional equipment or medical training, and rapidly polymerize (fast crosslinking kinetics). The hydrogel should not produce significant heat while crosslinking. This hydrogel would be able to seal traumatic wounds due to both sufficient mechanical and adhesive properties.

1.4   Hydrogels for Drug Delivery

PEG hydrogels have been extensively researched not only for wound dressing and sealants but also for delivery of soluble therapeutics.[32] The hydrogel release kinetics for therapeutics is based on many compounding factors. Such factors include molecular size of the therapeutic agent, the crosslink density of the hydrogel, the concentration and phase of the therapeutic drug, and the method to incorporate and load the therapeutic drug into the hydrogel. These factors are individually discussed in greater detail below.

1.4.1   Molecular Size

The hydrogel wound dressing releases the incorporated therapeutic drugs through a diffusion-based process. Diffusion based release indicates that the mass of the therapeutic drug impacts the way in which the therapeutic drug is able to diffuse. The diffusion coefficient is inversely proportional to the molecular radius.[33] Smaller, lower mass therapeutic drugs will have a smaller molecular radius and larger, higher mass therapeutic drugs will have a larger molecular radius. The common trend is for these small molecule therapeutic drugs to diffuse out of the hydrogel faster than large molecule therapeutic drugs. However, some small molecules may not diffuse out as fast if there are specific interactions between the therapeutic drug and the hydrogel that retard the diffusion. Typically, small molecule therapeutic drugs have a burst release from the hydrogel due to rapid diffusion. The small molecule therapeutic

12

drugs will then have a sub therapeutic level of sustained release over a longer period of time due to a dramatic decrease in therapeutic concentrations with the burst release. Moderate molecular weight therapeutic drugs exhibit behavior similar to the small molecular weight therapeutic drugs, however, the larger size increases the time it takes to release. On the contrary, higher molecular weight therapeutic drugs such as therapeutic proteins are much slower to diffuse out of the hydrogel often giving an extended-release profile.

1.4.2   Crosslink Density

Diffusion of the therapeutics is also limited by the mesh size (ξ) of the hydrogel. The mesh size of a hydrogel is dependent upon the crosslink density within the hydrogel.[34] The crosslinked mesh of the hydrogel impedes the release of the therapeutic drugs. The crosslink density is able to be controlled in PEG hydrogels by three different mechanisms.[35] One mechanism is to vary the molecular weight (MW) of the PEG used. The second mechanism is to alter the volume fraction ($v_{2,s}$) of PEG used in the hydrogel. The third mechanism is to change the mechanism of crosslinking. Lower molecular weight PEG has shorter chains and therefore a tighter cross link network, thus, increasing the crossing density. Higher molecular weight PEG has longer chains and therefore a less dense crosslinking network. It is also possible to modify the crosslink density as time passes.[36] This is possible through incorporating degradable linkages into the network backbone and therefore as time passes, and the concentration of therapeutic drug within the hydrogel decreases, the crosslink density will also decrease through degradation of the degradable linkages to allow for greater diffusion of the entrapped therapeutic drugs.[36–38]

The diffusion coefficient for a therapeutic drug molecule (D_g) in the hydrogel relative to the diffusion coefficient in free solution (D_0) is a function of three different factors.[39] These factors include the radius of the therapeutic molecule (R_s), the mesh size of the hydrogel (ξ), and the polymer volume fraction in the hydrogel ($v_{2,s}$).[35]

1.4.3 Method of Therapeutic Drug Sequestration

Three different techniques exist to secure the therapeutic drugs within the hydrogel network. These three techniques are 1) physical entrapment, 2) covalent tethering, and 3) affinity-based sequestration. Physical entrapment means the therapeutic drug is free to diffuse out immediately, because the therapeutic drug is sequestered into the hydrogel and not actually covalently linked to the network. Therefore, the larger the therapeutic drug, the slower the diffusion out of the hydrogel. The hydrogel does not have much effect on the diffusion of small molecules and therefore does not retard the small molecule diffusion from the hydrogel. Thus, small molecule therapeutic drugs will diffuse out of the hydrogel in a matter of hours, making sustained release more difficult. Thus, additional methods to obtain sustained release are necessary for small molecule therapeutic drugs. Additional methods include covalent tethering or affinity interactions. Covalent tethering requires a degradable linkage used to covalently bind the therapeutic drug to the polymer network. Over time the hydrolytic linker degrades, in turn releasing the therapeutic drug from the hydrogel. The linkers can either be hydrolysable, meaning they have a predictable rate of release, or a short peptide sequence that is susceptible to enzymatic degradation. Often the different therapeutic drug chemistries require their own specific conjugations making covalent tethering difficult. This approach is impractical when dealing with several different therapeutic drugs within the same hydrogel due

14

to having to covalently tether each therapeutic drug independently. Furthermore, this method

requires a more complicated Food and Drug Administration (FDA) approval process due to the

classification as a combination product. A more advantageous alternative to this covalent

conjugation is affinity interactions. These interactions are able to be used to sequester and

release molecules of the therapeutic drugs from the hydrogel. Despite being more transient

than covalent bonds these non-covalent interactions, if sufficiently strong, can retard the

diffusion of this therapeutic drugs out of the hydrogel. There are many different types of

affinity interactions that are capable of controlling the release of the therapeutics from the

hydrogel. Some of these interactions include hydrophobic interactions,[40] ionic interactions,[41–43]

and other non-covalent interactions . An advantage to using this affinity-based release method

is that the therapeutics are not covalently bound to the hydrogel, and thus the therapeutic

drugs are able to be interchanged freely without worrying about the specific interactions. Using

affinity-based methods the therapeutic drugs are retarded from diffusion with a change in

molecular diffusivity by a factor of K_b+1 where $K_b=[L]/K_d$. K_b represents the equilibrium

concentration between the bound and free ligands. K_b is also described as the ratio of free-

receptor concentration, L, to the dissociation constant, K_d.[44]

1.4.4   Therapeutic Drug Concentration and Phase

Both the initial therapeutic drug concentration and phase of the therapeutic drug are

potential tools to alter the release kinetics of the therapeutic drugs. It is possible to alter and

extend the release time of the therapeutic drug using a concentration of the therapeutic drug

higher than the solubility limit within the system.[45] The therapeutic drug is only able to dissolve

when a sufficient amount of the therapeutic drug leaves the hydrogel up until the solubility of

15

the therapeutic drug within the hydrogel. The phase of the insoluble therapeutic drug also alters the release. Crystalline drugs dissolve slower into solution than amorphous drugs. Additionally, some crystalline phases are less stable which also plays an effect on the dissolution rate.[46]

1.5   Objective of this Work

The objective of this work is to create and characterize PEG hydrogels with varied mesh size to analyze therapeutic drug release properties and kinetics. Using this characterization, the four therapeutics, tranexamic acid, bupivacaine, tobramycin, and vancomycin, will be able to be loaded into the hydrogel, and the sustained therapeutic drug release of the therapeutic drugs optimized for three-day release profile. Ultimately, the PEG macromer and initiators, and therapeutic drugs will be in powder form, combined with potable water, form into a liquid that is able to be applied to the wound and will solidify rapidly (within 90 seconds). Once accomplished, the project requirements will be met, and research can move forward to animal model testing.

1.6   Overview

Chapter two will discuss the computational models, conducted using MATLAB, to understand the correlation between mesh size and therapeutic drug release kinetics. The computational models will examine the cumulative therapeutic drug release verse time and how the release can be extended with the size of the polymer mesh and additional on functional groups to the PEG chains. Chapter three will then describe the methods and materials for the in-lab verification of the computational models. Thus, it will cover the PEG diacrylate (PEGDA) synthesis, hydrogel preparation, characterization, and therapeutic drug

release characterization. Chapter four describes the results from the mesh size characterization and therapeutic drug release kinetics. Chapter five explains the conclusions drawn from both the computational models and in lab experimentation. Chapter six elucidates the future work that still needs to be accomplished in order to finalize the hydrogel wound testing and make commercially available.

2   Computational Modeling

2.1   Background

Computational modeling provides an insight into the hydrogel characteristics and therefore how such hydrogel characteristics influence the release kinetics of therapeutic drugs. To characterize the hydrogel structure, the volumetric swelling ratio (Q_v), polymer volume fraction ($v_{2,s}$), and specific volume of polymer (v) are calculated. The molecular weight between crosslinks (M_c) can then be calculated. Using the respective values for M_c the mesh size (ξ) can be calculated. Given the mesh size for each PEG hydrogel, the release kinetics and cumulative release can be modeled.

2.2   Calculations for Mesh Size

Excel was used as a storage database for all the pertinent collected data and values obtained from scientific papers. MATLAB was then used to calculate the cumulative release of each of the four therapeutic drugs, tranexamic acid, bupivacaine, tobramycin, and vancomycin. The molecular weights of linear PEG used for the models range from 200 to 10,000 g/mol, shown in **Table 2.1**.[47]

Table 2.1: Bulk density of poly(ethylene glycol) with varied molecular weights and the number of repeats within the chain.

M_n (g/mol)	Bulk Density (g/mL)	Number of repeats (n)
200	1.124	4
300	1.13	6
400	1.13	9
575	1.13	12
600	1.13	13
700	1.13	15
1000	1.2	22
1500	1.2	33
2000	1.21	45
3000	1.21	67
4000	1.2	90
6000	1.2	135
8000	1.2	181
10000	1.2	226

The hydrogel network structure, degree of crosslinking, and hydrophilicity are all variables to the degree in which the hydrogel can swell. For purposes of the models, the swelling ratio based on hydrogel mass (q_m) was chosen to be set between 2 and 15. This is a controllable variable that can be experimentally varied in the lab. Where q_m is: [36]

$$q_m = \frac{M_S}{M_D}$$

where M_S is the mass of the hydrogel swollen and M_D is the mass of the hydrogel dried. The swelling ratio based on hydrogel mass is then applied to the volumetric swelling ratio, Q_v:[36,48]

$$Q_v = 1 + \left(\frac{\rho_{BD}}{\rho_s}\right) * (q_m - 1) \qquad \textit{Equation 2.2}$$

The bulk density (ρ_{BD}) is known for each molecular weight PEG and varies between 1.124 and

1.21 (**Table 2.1**)[36,47]. The density of the solvent (ρ_s), deionized water (DI H_2O), at 37 degrees

Celsius, is known to be 0.993 g/cm^3.[36,49] q_m is found from **Equation 2.1**.

The polymer volume fraction in equilibrium swollen hydrogel ($v_{2,s}$) is:[36,44]

$$v_{2,s} = \frac{1}{Q_v} \qquad \textit{Equation 2.3}$$

Where Q_v is found in **Equation 2.2**. The specific volume of the polymer (v) is:[36]

$$v = \frac{\rho_s}{\rho_{BD}} \qquad \textit{Equation 2.4}$$

The molecular weight of the polymer chains between two neighboring crosslinks (M_c)[36,44,50]:

$$M_c = \frac{1}{\left(\frac{2}{M_n}\right) - \left(\frac{\frac{v}{V_1} * \left(\log(1 - v_{2,s}) + v_{2,s} + X_1 * v_{2,s}^2\right)}{v_{2,s}^{1/3} - \frac{v_{2,s}}{2}}\right)} \qquad \textit{Equation 2.5}$$

Here, M_n is the molecular weight (g/mol) of the PEG used in the computational modeling. The

molar volume of DI H_2O (V_1) is a constant of 18 cm^3/mol.[34] The Flory Huggins polymer-solvent,

DI H_2O, interaction parameter (X_1) used was 0.426 as determined by Merrill et al.[34,36,51] Where

$v_{2,s}$ and v are found from **Equation 2.3** and **Equation 2.4** respectively. Therefore, M_c has units of

g/mol.

The number of links in the chain (N) will vary for each molecular weight PEG where N

is:[44]

$$N = \frac{2 * M_c}{M_r} \qquad \textit{Equation 2.6}$$

where the molecular weight of the repeating units (M_r) from which the polymer chain is composed equals 44.05 g/mol.[34] M_c is known from **Equation 2.5**.

The root mean square (RMS) end to end distance of the polymer chains between two neighboring crosslinks ($(r_0{}^2)^{1/2}$) has units in angstroms.[34,44,50]

$$(r_0{}^2)^{\frac{1}{2}} \; = \; l * (C_n * N)^{\frac{1}{2}}$$

Equation 2.7

The length of the bond (l) along the polymer backbone is approximated as 1.54 A.[34,39,50] This is calculated from the weighted average of a single carbon-carbon bond and two carbon-oxygen bonds. The polymer specific characteristic ratio (C_n) is approximated at 4.[39,52,53] **Equation 2.6** provides the value for N.

Mesh size (ξ) is then able to be calculated: [34,44,50]

$$\xi = v_{2,s}{}^{-1/3} * (r_0{}^2)^{\frac{1}{2}}$$

Equation 2.8

where $v_{2,s}$ and $r_0{}^2$ are known from **Equation 2.3** and **Equation 2.7** respectively.

2.3 Calculations for Diffusion from Hydrogel

Table 2.2 includes information about the four therapeutic drugs used in the hydrogel. The r_s values for tranexamic acid, bupivacaine, and tobramycin were estimated using a hydrodynamic radius converter.[54] The r_s value for vancomycin was published.[55]

Therapeutic Drug	Drug Effect	Solubility	MW (g/mol)	MW (kDA)	r_s (Å)
Tranexamic Acid	hemostatic agent	water soluble at 167 mg/mL	157.21	0.15721	4.86
Bupivacaine	analgesic	freely water soluble	288.435	0.288435	5.92
Tobramycin	cationic antibiotic	water soluble	467.515	0.467515	6.93
Vancomycin	antibiotic	water soluble > 100 g/mol	1449.3	1.4493	10

The therapeutic drug diffusion coefficients (D_0) were solved using **Equation 2.9**, the Stokes Einstein equation.[35] The units are m^2/s.

$$D_0 = \frac{k_B T}{6\pi\eta\, r_s}$$
Equation 2.9

The Boltzmann Constant (k_B) is $1.38064852*10^{-23}$ J/K.[35] Temperature (T) is 310.15 Kelvin.[35] The viscosity of the solution (η), DI H_2O, at 37 degree Celsius is $6.915*10^{-4}$ Ns/m^2.[35] The Stokes Einstein hydrodynamic radius (r_s) of the therapeutic drug is converted from **Table 2.2** into meters.[35]

Using D_0 solved for in **Equation 2.9**, the diffusion of each therapeutic drug from the hydrogel (D_g) is calculated independently.[35]

$$D_g = D_0 * \left(1 - \left(\frac{r_s}{\xi}\right)\right) * e^{-Y\left(\frac{v_{2,s}}{1-v_{2,s}}\right)}$$
Equation 2.10

Y is the ratio of critical volume required for successful translational movement of solute to average free volume per molecule of liquid and is approximated to be 1.[35] The equation also requires, r_s, $v_{2,s}$, and ξ found from **Table 2.2**, **Equation 2.3**, and **Equation 2.8** respectively . D_g is then calculated individually for each therapeutic drug using the drugs' respective D_0 and r_s values. The charge of each drug is not necessary for the computational release kinetic models; however, drug charges will play a role in extending their release profiles from the PEG hydrogel.

2.4   Calculations for Summation of Therapeutic Drug Released from a Thin Film

Thin film summation of therapeutic drug release calculations were completed for a hydrogel with thickness of 0.2 cm and radius of 0.3 cm. The radius value was selected because a 6 mm biopsy punch is used in laboratory experiments. A height of 0.2 cm meets the assumptions for the equations used in modeling thin film release kinetics and is the thickness of a thin film created in a lab.

The amount of therapeutic drug released at some time (t) versus the total amount of therapeutic drug released at time infinity is:[44]

$$\frac{M_t}{M_\infty} = 1 - \sum_{n=0}^{\infty} \left(\frac{8}{(2n+1)^2\pi^2}\right) * e^{\left(\frac{-D_g(2n+1)^2\pi^2 t}{L^2}\right)} \qquad \text{Equation 2.11}$$

where n is a symbolic variable used for the summation from 0 to infinity and t is also a symbolic variable for time used to solve in seconds from 0 to 3 days. The height of the thin film, L, is variable. However, for modeling purposes 0.2 cm was maintained. **Equation 2.11** was then evaluated for a three-day time period to determine the time it takes for all the therapeutic drug to be released. From the calculated data, the cumulative release graphs of the therapeutic drug over time (t) is produced.

2.5 Cumulative Release Graphs

Figures 2.1, **2.2**, **2.3**, and **2.4** display the theoretical diffusion of tranexamic acid,

bupivacaine, tobramycin, and vancomycin respectively from PEG hydrogels of varied molecular

weights. The molecular weights displayed on the graphs are 575, 700 and 2000 g/mol. The

general trend is that the lower the molecular weights of the hydrogel the slower the diffusion

of the therapeutic drug. Therefore, PEG 575 hydrogels should have the longest therapeutic drug

release and PEG 2000 hydrogels should have the fastest therapeutic drug release. Due to the

similar theoretical release profiles of PEG 575 and PEG 700 it may be hard to experimentally

determine the release kinetic differences between PEG 575 and PEG 700.
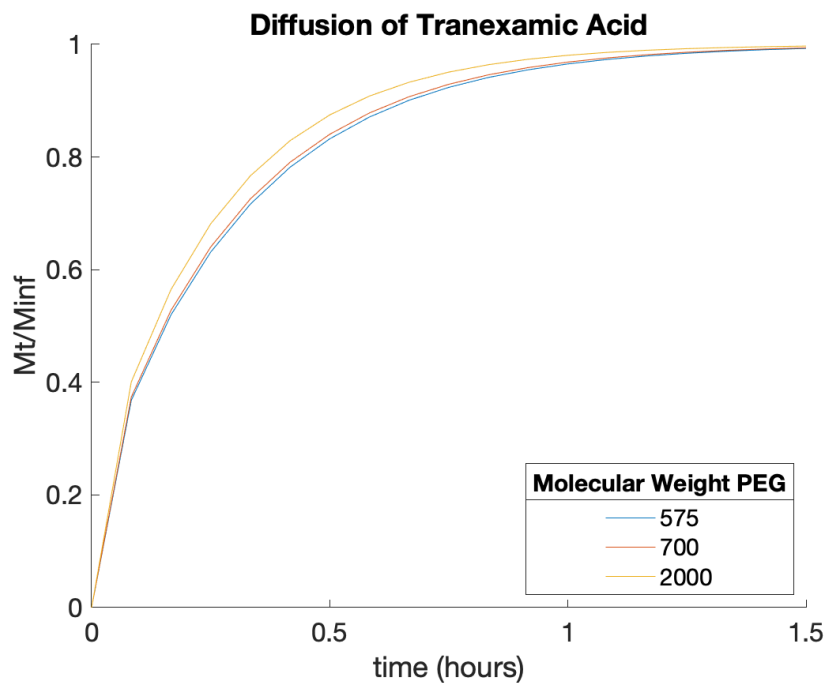
Figure 2.1: Cumulative release computational model of tranexamic acid diffusion in varied molecular

weight PEG hydrogels (n=12, 15, 45) with 2 mm thickness.
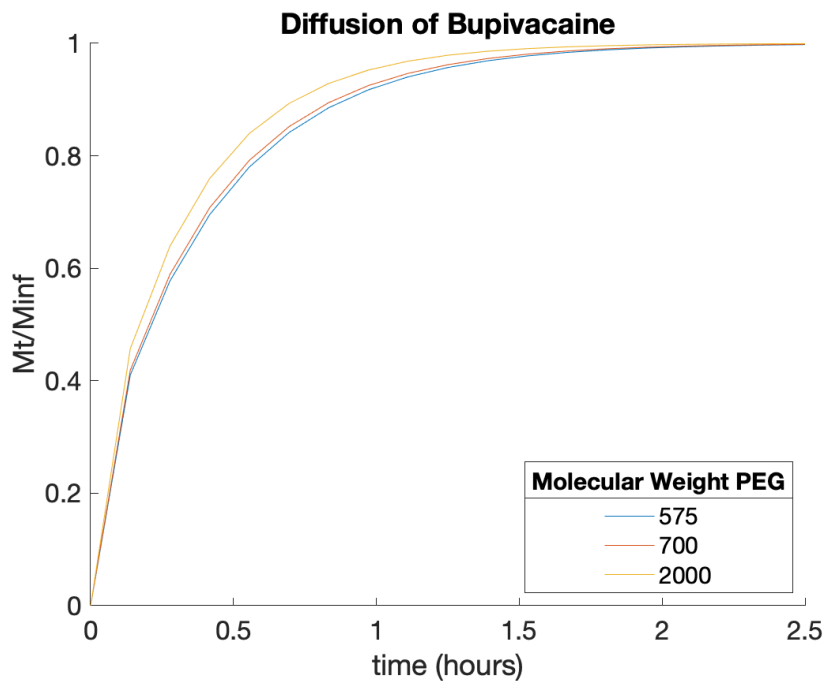
Figure 2.2: Cumulative release computational model of bupivacaine diffusion in varied molecular weight

PEG hydrogels (n=12, 15, 45) with 2 mm thickness.
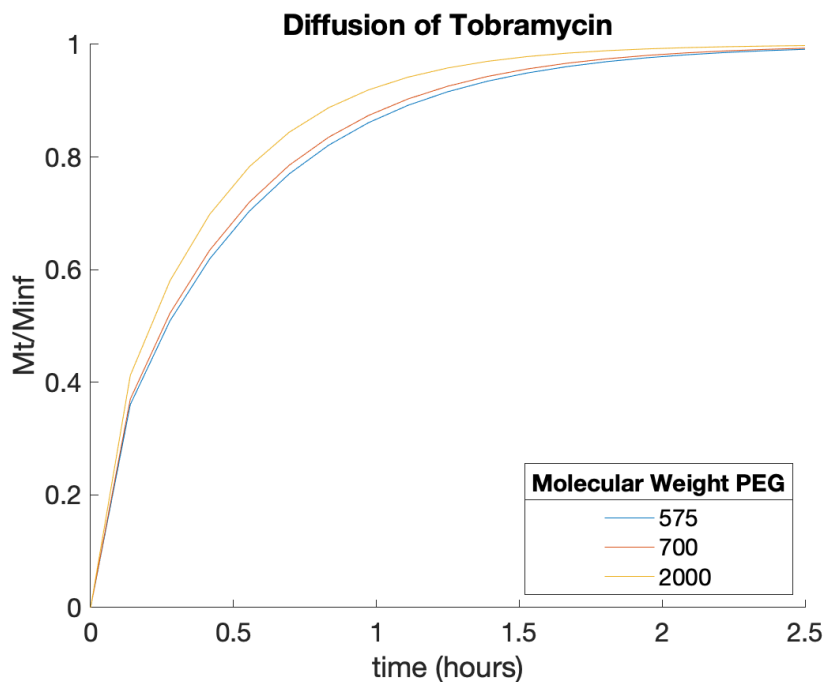
Figure 2.3: Cumulative release computational model of tobramycin diffusion in varied molecular weight

PEG hydrogels (n=12, 15, 45) with 2 mm thickness.
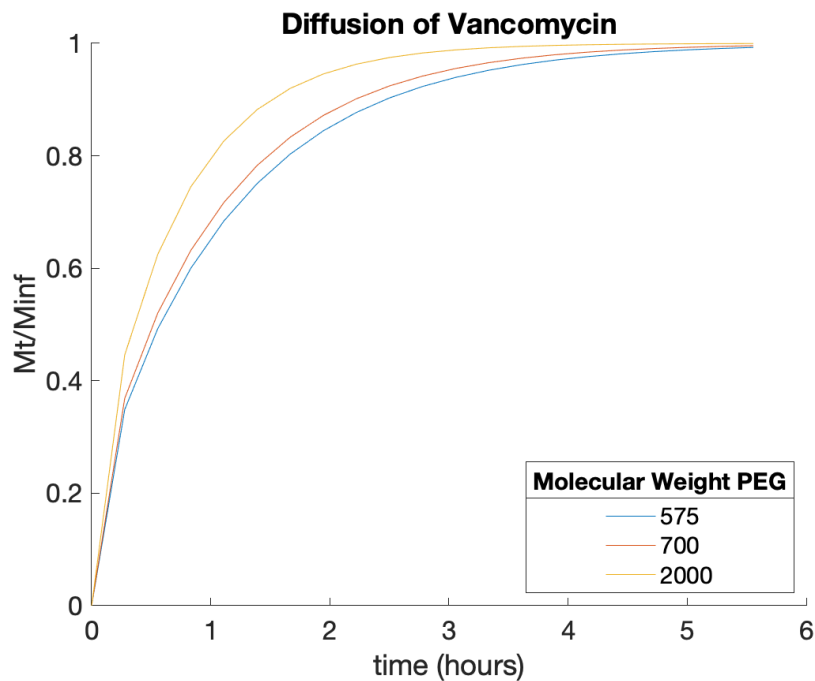
Figure 2.4: Cumulative release computational model of vancomycin diffusion in varied molecular weight PEG hydrogels (n=12, 15, 45) with 2 mm thickness.

Figures 2.5, **2.6**, **2.7** compare the theoretical release kinetics of each therapeutic drug within a specific molecular weight PEG hydrogel. Regardless of the molecular weight PEG hydrogel, the vancomycin released the slowest, followed by tobramycin, then bupivacaine, and the fastest was tranexamic acid. This correlates with the molecular weight and hydrodynamic radius of each therapeutic drug. The larger the molecular weight and the larger the hydrodynamic radius, the slower the therapeutic drug will diffuse out of the hydrogel.
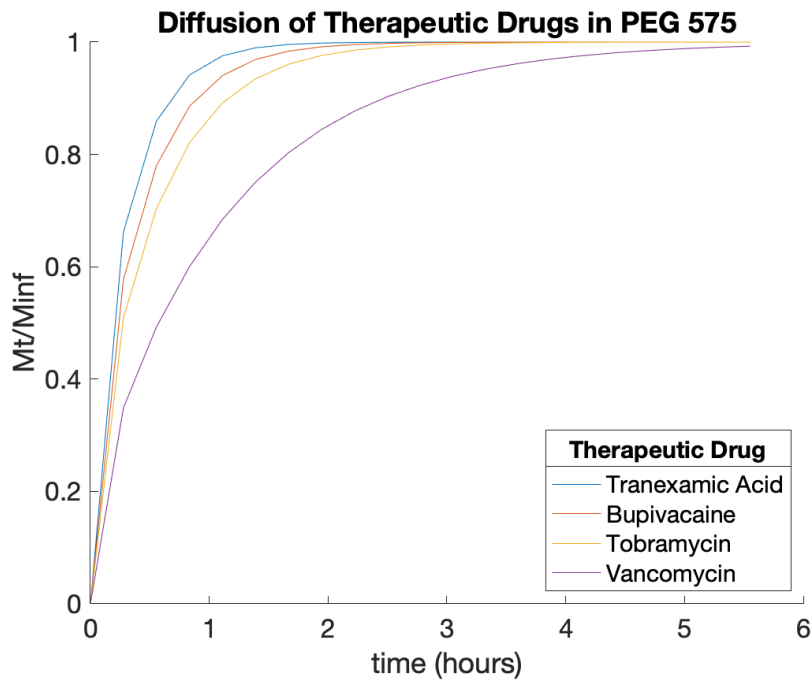
Figure 2.5: Computational model for the comparison of cumulative therapeutic drug release for 2 mm thick PEG 575 hydrogels (n=12).
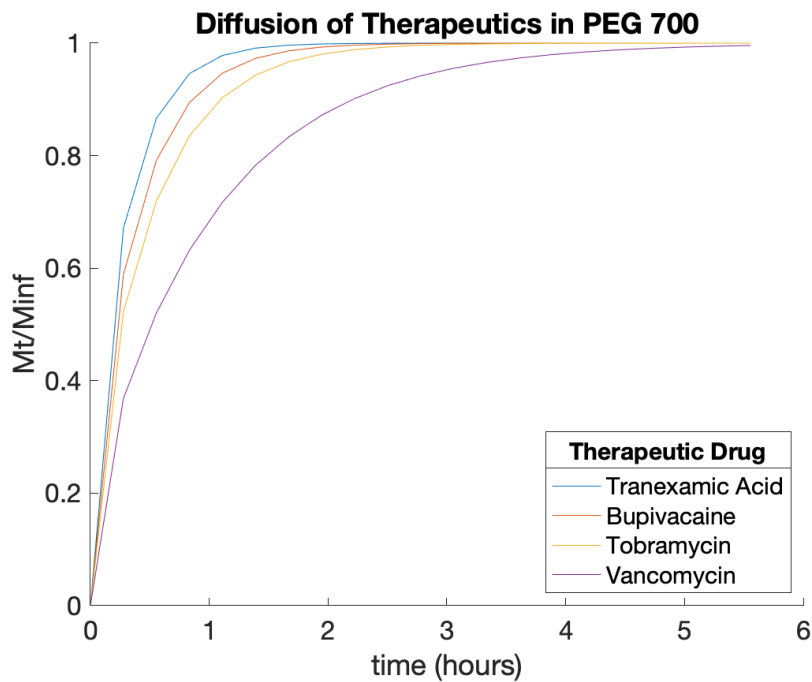
Figure 2.6: Computational model for the comparison of cumulative therapeutic drug release for 2 mm thick PEG 700 hydrogels (n=15).
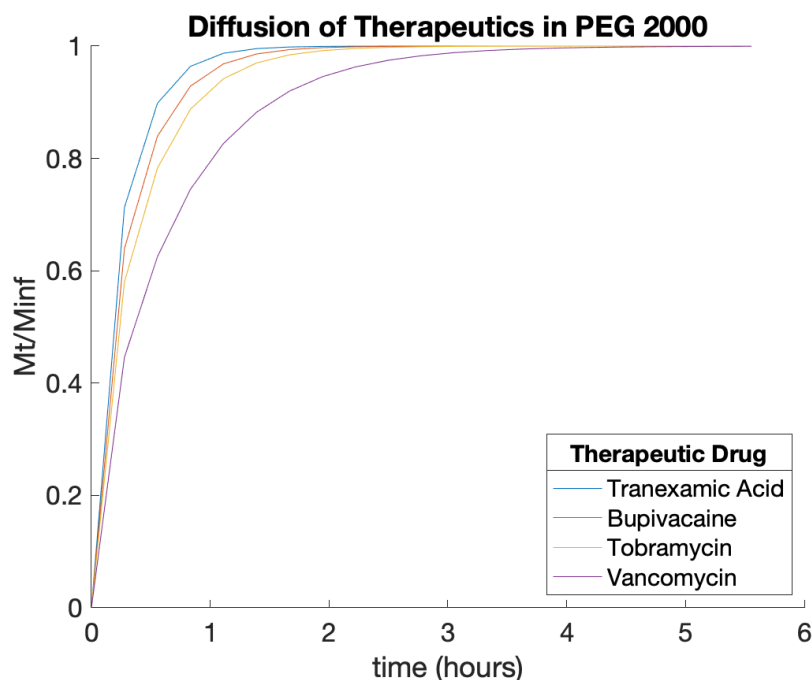
Figure 2.7: Computational model for the comparison of cumulative therapeutic drug release for 2 mm thick PEG 2000 hydrogels (n=45).

2.6   Conclusions

The computational models were used as a tool to be able to predict the therapeutic drug release kinetics. These models gave a starting point to which PEG molecular weight hydrogels should be created in the lab to get the longest therapeutic drug release without additional chemical modifications to the hydrogel. The key takeaway from the modeling is that even the lowest molecular weight PEG hydrogel will not result in a three-day therapeutic drug release with the largest drug, vancomycin. Therefore, some chemical modifications will need to be made to retard the diffusion of the therapeutic drug from the hydrogel and obtain an extended-release profile. However, it is important to note that computational models are in an ideal laboratory and the release profiles will vary for the hydrogels due to the nature of a model versus an actual laboratory procedure.

3   Materials and Methods

3.1   Materials

Poly(ethylene) glycol (PEG) with molecular weight 2000 was obtained from Alfa Aesar (Ward Hill, Massachusetts) for poly(ethylene glycol) diacrylate synthesis. Dichloromethane (DCM) HPLC grade was obtained from Acros Organics (Fair Lawn, New Jersey) and distilled from calcium chloride and stored over 3 Angstrom molecular sieves. Triethylamine (TEA) was obtained from Alfa Aesar (Ward Hill, Massachusetts) and distilled from KOH. Acryloyl chloride was obtained from Alfa Aesar (Ward Hill, Massachusetts). Diethyl ether was obtained from Acros Organics (Fair Lawn, New Jersey) and kept cold in the freezer. Poly(ethylene glycol) diacrylate (PEGDA) with molecular weights 575 and 700 were obtained from Sigma Aldrich (St. Louis, Missouri). All PEGDA reagents used in the reactions were in their linear form.

For the gelation reactions, Ammonium persulfate (APS) and Tetramethylethylene diamine (TEMED) were obtained from Amresco (Solon, Ohio). The APS came in pre-weighed 150 mg tablets. The therapeutic drugs vancomycin hydrochloride, tobramycin, and tranexamic acid were all obtained from Acros Organics (Fair Lawn, New Jersey), and bupivacaine hydrochloride monohydrate was obtained from Sigma Aldrich (St. Louis, Missouri). Tranexamic acid requires Iron (III) Chloride hexahydrate, obtained from Acros Organics (Fair Lawn, New Jersey), to be detectable by a UV Visible Spectrophotometer. To extend the therapeutic drug release from the hydrogel, sodium polyacrylate (also known as polyacrylic acid) (PAA) was obtained from Ward's Science (Rochester, New York), and acrylic acid was obtained from Acros Organics (Fair Lawn, New Jersey).

Other materials used for the gelation reactions include Eppendorf tubes from Celltreat Scientific Products (Pepperell, Massachusetts), glass slides with dimensions 75x25x1 mm from VWR (Radnor, Pennsylvania), and Gel Slick® Solution from Lonza (Rockland, Maine). Additionally, micropipette tips were obtained from VWR (Radnor, Pennsylvania) and 48 well cell culture cluster flat bottom plates were obtained from Costar (Corning, New York).

A variety of different plastic cuvettes were used for the UV-Visible Spectrophotometer. Disposable methacrylate semi-micro cuvettes were obtained from Fisherbrand™ (Ottawa, Ontario). Both semi-micro and ultra-micro UV cuvettes were obtained from Chemglass Life Science (Vineland, New Jersey). Additionally, a reusable 6mm biopsy punch with plunger from World Precision Instruments (Sarasota, Florida) was used to cut the hydrogels and Fisherbrand™ Trace Calipers were used to measure the width of the hydrogels.

Nuclear magnetic resonance (NMR) was used to confirm the PEG diacrylate synthesis for PEG 2000. ^{1}H NMR was used indicating the NMR was taken with respect to the hydrogen-1 nuclei within in molecules of the PEG 2000 sample. A Dynamic Mechanical Analyzer Q-800 (DMA) from TA Instruments was used to measure the elastic modulus of the hydrogels. A Biomate 3S UV-Visible Spectrophotometer (UV-Vis) from Thermo Scientific was used to measure the absorbance of solutions with and without therapeutic drugs.

3.2 PEG Diacrylate Synthesis

Poly(ethylene) glycol diacrylate was made according to published protocols.[34] A one neck round bottom flask twice the size of the total reaction solution was used. A known amount of PEG 2000 was added to the one neck round bottom flask with a stir bar inside. The one neck round bottom flask with attached addition funnel was then flushed with argon. DCM was added

to the addition funnel using a syringe followed by three equivalents of TEA. The addition funnel was then slowly added to the round bottom flask. The stir plate was then turned on to dissolve the PEG. The round bottom flask was then placed in an ice bath while stirring continued. DCM was again added to the addition funnel followed by three equivalents of acryloyl chloride. The addition funnel was added dropwise to the round bottom flask. The reaction was left to run overnight. 24 hours later the reaction was then removed from the ice bath and argon gas. Using a rotary evaporator, approximately half of the DCM was removed from the round bottom flask. The remaining reaction solution was then pipetted from the round bottom flask into centrifuge tubes. The round bottom flask was rinsed with DCM and the rinsed solution was then added to the centrifuge tubes to ensure that all product was removed. Cold diethyl ether was added to the centrifuge tubes. The centrifuge tubes were then centrifuged in order to precipitate the reaction product out from the cold diethyl ether. The diethyl ether was then decanted off the top of the centrifuge tube. A small amount of DCM was then added to the centrifuge tube to redissolve the pellet. In order to redissolve the pellet vortexing was necessary. The diethyl ether precipitation process was repeated for a total of three times. The centrifuge tubes were then covered with a Kim wipe and secured with rubber band and then placed in a vacuum trap for 24 hours to remove excess diethyl ether and DCM. The PEG diacrylate product was then analyzed and confirmed using ^{1}H NMR. Chloroform was used as the solvent for ^{1}H NMR testing.

3.3   Hydrogel Preparation

1 M stock solutions of both APS and TEMED were prepared. Therefore, one 150 mg pre-weighed APS tablet was combined with 660 µL of DI H_2O to create a 1 M APS stock solution. A

ratio of 3:20 TEMED to DI H$_2$O creates a 1 M TEMED stock solution. Thus, a 1 M TEMED stock solution was prepared with 90 μL of TEMED combined with 600 μL of DI H$_2$O.

Three different molecular weight PEG diacrylates (PEGDA) were used in the experiments, either 575, 700, or 2000 g/mol. The hydrogels were prepared using PEGDA, but for simplicity the gels will be referred to as PEG 575, PEG 700, and PEG 2000. PEGDA of known molecular weight was placed into a pre-weighed glass vial, and the PEGDA was then weighed. Based on the weight of PEGDA, a calculated volume of DI H$_2$O was then added to create a 35.5 wt% solution.

The amount of initiators, APS and TEMED, were systematically varied between 0.05 – 0.5 wt% for the hydrogel solution. The amount of macromer, PEGDA, varied between 5 – 30 wt%. Optimization of the hydrogel occurred via the hydrogel characterization conducted as described below. Optimization of the hydrogel was first completed sans therapeutics. Thus, modifications to the weight percents of macromer or initiator may be necessary following the incorporation of therapeutics into the hydrogel which may result in changes to the polymerization of the hydrogel.

Ultimately, hydrogels with 24.14 wt% PEG were the best. The 1000 μL hydrogels were synthesized by adding 680 μL of 35.5 wt% PEG stock solution to an Eppendorf tube followed by 260 μL of DI H$_2$O. Then, 30 μL of 1 M APS stock was added followed by 30 μL of 1 M TEMED stock. The Eppendorf tube was then quickly vortexed, and solution pipetted, using a glass pipette, onto a gel slick glass slide. The glass slide had two 1 mm thick glass slide spacers on either end creating a 2mm space between the glass cover slide. The 2 mm thick hydrogels then formed within 1 minutes and were removed from the slide. The hydrogels were cut using a 6

mm biopsy punch with plunger. Each 6 mm punched hydrogel was then placed in their own well

within a 48 count well plate. 1000 μL DI H_2O was added using a volumetric pipette to each well.

3.4 Characterization

Characterization of the hydrogels included three separate, experimentally determined

components. The first characterization found the mass and the volumetric swelling ratio of the

hydrogels. The second characterization experiment found the elastic modulus. Both the

volumetric swelling ratio and the elastic modulus were then used to calculate a predictive mesh

size of the hydrogel. Lastly, the calculated mesh size allowed for further analysis of the hydrogel

and was used as a predictive measure for the release kinetics of the therapeutic drugs. The

predictions were eventually compared to the release kinetic data collected using the UV-Visible

Spectrophotometer.

3.4.1 Volumetric Swelling Ratio (Q)

Hydrogels were created as described in 3.3, *Hydrogel Preparation*. The uniform 6 mm

hydrogel punches were placed in a 48 count well plate with 1000 μL of DI H_2O and allowed to

swell for 30 minutes. No statistical difference was found when the hydrogels were allowed to

swell for 24 hours. For each experimental variation of hydrogel, three samples (n=3) were

completed to allow for statistical analysis of the data. The hydrogels were then removed from

the well plate using tweezers and weighed to obtain the swollen mass, M_s. Each hydrogel was

then placed in an Eppendorf tube, covered with a Kimwipe and secured by a rubber band. In

order to freezer the hydrogels they were either placed in the -80°F freezer overnight or placed

in a liquid nitrogen bath for 20 minutes. Once frozen, the Eppendorf tubes were then placed

into a beaker on the lyophilizer to dry. The hydrogels were left on the lyophilizer for 24 – 48

hours, until dry. After the drying process was complete, the hydrogels were weighed again to obtain the dry mass of the crosslinked polymer network, M_d. The mass swelling ratio, q_m, was then calculated from M_s and M_d:[36]

$$q_m = \frac{M_s}{M_d}$$

<div align="right">Equation 3.1</div>

The formula to solve for the volumetric swelling ratio, Q_v, is[36,48]

$$Q_v = 1 + \left(\frac{\rho_{BD}}{\rho_s}\right) * (q_M - 1)$$

<div align="right">Equation 3.2</div>

where PEG bulk density, ρ_{BD}, is known for each molecular weight PEG and varies between 1.124 and 1.21 g/cm^3 (**Table 2.1**).[36,47] The density of the DI H_2O, ρ_s, at 37 degrees Celsius, is 0.993 g/cm^3.[36,49]

3.4.2   Elastic Modulus (E)

The elastic modulus is characterized by uniaxial compression. A TA Instruments Q-800 Dynamic Mechanical Analyzer with a submersible compression clamp was used, however the hydrogel was not submersed. The diameter of the hydrogel was measured using Fisherbrand™ Trace Calipers. The hydrogel diameter measurement was taken from three different points, recorded and the average value determined. The height of the hydrogel was measured prior to the run using the *Measure* feature within the DMA program. The initial preload force was 0.001 N, and the initial strain was 0.5%. The run time for the hydrogels varied for each molecular weight. **Table 3.1** displays the ramp strain rate, max strain, and ramp de-strain rate parameters used for the DMA.

Table 3.1: DMA parameters for uniaxial compression testing.

MW of Hydrogel	Ramp Strain Rate (%/min)	Max Strain (%)	Ramp De-strain Rate (%/min)
PEG 575	2.5	-10	2.5
PEG 700	2.5	-10	2.5

The stress-strain curve produced by the Q-800 DMA was analyzed in the TA Instruments Universal Analysis 2000 program. The slope of the stress-strain curve was recorded from -2% to -8% strain for PEG 575 and PEG 700 hydrogels. The range for the percent strains were chosen as they were the linear region within the graphs produced by the Q-800 DMA. The modulus has units of KPa found from the slope of the graph times the maximum strain on the run. The modulus (E) is recorded for each sample. These modulus values were used as additional supporting evidence for the mesh size values found from the volumetric swelling ratios.

3.4.3 Mesh Size (ξ)

The values calculated from the volumetric swelling ratio allow for a cascade of calculations that yield the mesh size (ξ) of the hydrogel. These calculations parallel those used for the computational models found in Chapter 2. The polymer volume fraction, $v_{2,s}$ is:[44]

$$v_{2,s} = \frac{1}{1 + \left(\frac{\rho_{BD}}{\rho_s}\right) * (q_m - 1)}$$ *Equation 3.3*

where q_m is the mass swelling ratio, ρ_{BD} is the dry bulk density of hydrogel at 1.12 g/cm^3 and ρ_s is the density of solvent 0.993 g/cm^3. The value for $v_{2,s}$ can also be found using Q_v, the volumetric swelling ratio, where: [36,44]

$$v_{2,s} = \frac{1}{Q_v}$$ Equation 3.4

Using $v_{2,s}$, the molecular weight of polymer chains between two neighboring crosslinks, M_c, is able to be calculated where:[36,44,50,56]

$$\frac{1}{M_c} = \left(\frac{2}{M_n}\right) - \left(\frac{\frac{v}{V_1} * \left[\ln(1 - v_{2,s}) + v_{2,s} + X_1 * v_{2,s}^2\right]}{v_{2,s}^{\frac{1}{3}} - \left(\frac{v_{2,s}}{2}\right)}\right)$$ Equation 3.5

M_n is the molecular weight of polymer either 575, 700, or 2000. V_1 is the molar volume of water[34], 18 cm³/mol, and X_1 is the polymer water interaction parameter[34,36,51], 0.426. The specific volume of polymer, v, is:[36]

$$v = \frac{\rho_s}{\rho_{BD}}$$ Equation 3.6

Then $(r_0^2)^{1/2}$, the root mean square end to end distance of polymer chains between two neighboring crosslinks, is:[34,44,50]

$$(r_0^2)^{1/2} = l * (C_n * n)^{1/2}$$ Equation 3.7

where l is the length of bond along polymer backbone of 1.54 Å,[34,39,50] and C_n is the characteristic Flory ratio of 4 Å.[39,52,53] The number of links, n, is found from:[56]

$$n = \frac{2 * M_c}{M_r}$$ Equation 3.8

where M_r is the molecular weight of repeating unit of which the chain is composed (g/mol).

Finally, the mesh size (ξ) is calculated where: [34,44,50]

$$\xi = (v_{2,s})^{-1/3} * (r_0^2)^{1/2}$$ Equation 3.9

3.5   Release Kinetics using UV Visible Spectrometer

A UV Visible Spectrometer was used to find the absorbance values of solution after therapeutic drug had diffused from the hydrogel into solution. The values for absorbance were able to determine the cumulative release of the therapeutic drug determining the overall release kinetics from the hydrogel.

3.5.1   Therapeutic Drug Calibration Curves

Four different therapeutic drugs were used in the experiments including tranexamic acid, a hemostatic agent, bupivacaine, an analgesic, and tobramycin and vancomycin, both antibiotics. For each therapeutic drug, stock solutions were created by measuring a known amount of therapeutic drug into a 10 mL beaker and combined with deionized water (DI H_2O). Approximately half the total amount of DI H_2O for the solution was added to the 10 mL beaker, stirred on a stir plate, and then pipetted into a volumetric flask. Then additional DI H_2O was used to rinse the 10 mL beaker and then also pipetted into the volumetric flask to ensure all therapeutic drug was transferred. DI H_2O was then added to the volumetric flask until solution reached the fill line. An aliquot of the stock solution was then placed into a cuvette and scanned on the UV-Visible Spectrometer to determine the wavelength of maximum absorbance. The blank used for the scan was DI H_2O. The determined maximum absorbance values were compared to the published literature values for maximum absorbance. Published maximum absorbance values are 281 nm[57] for vancomycin, 210 nm[58] for tobramycin, 262 nm[59] for bupivacaine, and 375 nm[60] for tranexamic acid with Iron(III) Chloride. Using the maximum absorbance found, the molar absorptivity of the therapeutic drug was calculated using Beer's Law:[61]

Equation 3.10

$$A = \varepsilon cl$$

where A is absorbance (unitless), ε is molar absorption coefficient (L*mol^{-1}*cm^{-1}), c is molar

concentration (mol/L), and l is optical path length (cm). The molar absorptivity was solved for

using the absorbance found at maximum wavelength for the stock therapeutic drug solution,

the known concentration of that solution, and a value of 1 cm for the length of the cuvette. The

molar absorptivities are listed in **Table 3.2**.

Table 3.2: Therapeutic drug calculated and published molar absorptivities.

Therapeutic Drug	Calculated Molar Absorptivity (ε) (L*mol^{-1}*cm^{-1})	Published Molar Absorptivity (ε)
Vancomycin[62]	5890.786	6690 dm^{3}mol^{-1}cm^{-1}
Bupivacaine[63]	399.989	473 M^{-1}cm^{-1}
Tobramycin	2.077	None published
Tranexamic Acid (w/ Fe(III)Cl)	18.6438	None published

Five concentrations with absorbances values between 0.2 and 0.8 Absorbance (A), the

linear range of a calibration curve, were calculated using Beer's Law and the determined molar

absorptivity for each therapeutic. These solution concentrations were created through serial

dilutions of the stock solution of therapeutic drug.

Each of these five diluted solutions were then pipetted into a cuvette and run against a

blank of DI H$_2$O. The absorbance values for the known therapeutic drug concentration solutions

were recorded. These absorbance values were plotted versus concentration to create the

calibration curve for each therapeutic drug.

The calibration curve for tranexamic acid required the addition of Iron (III) chloride. A 1% Iron (III) chloride solution was created by combining 1 g of Iron (III) chloride with 100 mL of DI H_2O. 600 μL of 1% Iron (III) chloride was added after each serial dilution for tranexamic acid. 600 μL was the volume added for the 5 mL volume of diluted solution. The amount of Iron (III) chloride was constant regardless of the change in concentration of tranexamic acid in the diluted solutions. This is based on published protocols for determining tranexamic acid using spectrophotometric techniques.[60]

3.5.2 Individual Therapeutic Drug Release Kinetic Studies

Hydrogels of 1 mL volume were created by combining in an Eppendorf tube 680 μL of 35.5 wt% PEG stock solution, 260 μL of DI H_2O/Drug Stock Solution, 30 μL of 1 M APS, and 30 μL of 1 M TEMED. The Eppendorf tube was then vortexed, and the solution removed using a glass pipette. The solution was dispensed onto a gel slicked glass slide with two glass slide spacers on either end, each spacer 1 mm thick, and a glass slide placed on top. This mold ensured all the hydrogels had equal thickness of 2 mm.

Once gelled, the hydrogels were then removed from the slide, punched with a 6 mm biopsy punch and placed into a 48 count well plate where 1000 μL of DI H_2O was pipetted into each well. The time of the DI H_2O addition was recorded to monitor the time it takes for the therapeutic drugs to diffuse out of the hydrogel. At set time intervals, aliquots from the well plate were taken. At each time interval an aliquot from one blank hydrogel and three therapeutic drug loaded hydrogels were taken. Once an aliquot was taken from the well, that specific hydrogel and its corresponding well were no longer used. New hydrogels were used for each time point. The aliquots were taken with a pipette and placed into a cuvette for UV Vis

analysis. The UV Visible Spectrometer determined the absorbance of the therapeutic drug loaded aliquots compared to the aliquot of a blank, non-drug loaded hydrogel.

3.6   Extended Therapeutic Drug Release using Sodium Polyacrylate

Hydrogels were prepared in a similar method to that described in 3.5.2, *Individual Therapeutic Drug Release Kinetic Studies.* A stock solution of 35.5 wt% PEG 700 was created. This PEG stock solution was then divided in known volumes into separate vials. Then, additional DI H_2O was added based on the volume needed to create a sodium polyacrylate (PAA) stock solution of known concentration. The concentrations of PAA varied between 1 mg/mL and 4 mg/mL. For each vial, the respective amounts of PAA powder was added to the vial and vortexed. The PAA was combined with both the PEG 700 and DI H_2O to prevent gelation of the superabsorbent PAA. Thus, the 680 µL of PEG stock solution and 260 µL of DI H_2O used in previous preparation methods was combined into one stock solutions. The hydrogel was made with 940 µL of PEG/PAA stock solution, 30 µL 1 M APS and 30 µL of 1 M TEMED.

3.7   Extended Therapeutic Drug Release using Acrylic Acid

For the incorporation of acrylic acid, 35.5 wt% PEG stock solution was created by adding DI H_2O to PEG of known molecular weight and vortexing. 1 M APS and 1 M TEMED were also prepared. Acrylic Acid stock solutions were created by adding a known amount of acrylic acid into a known volume of DI H_2O. These concentrations of acrylic acids stock solutions varied between 0.1 – 5 wt%. 260 µL of acrylic acid stock solution was then added to 680 µL of 35.5 wt% PEG stock solution, 30 µL of 1 M APS, and 30 µL of 1 M TEMED. Hydrogels with different wt% acrylic acid incorporation were then compared through their respective mass swelling ratios.

Therapeutic drugs were also incorporated into the hydrogel in junction with the acrylic acid stock solution. The number of moles of acrylic acid and the number of moles of therapeutic drug, were combined into the hydrogels in a 1:1 ratio for vancomycin and 5:1 ratio for bupivacaine. Thus, one stock solution was created that incorporated both the acrylic acid and therapeutic drug. This acrylic acid/drug stock solution replaced the 260 µL of DI H_2O in the previous protocols. The methods for gelation remained unchanged with 680 µL of PEG 35.5 wt% stock solution, 260 µL of acrylic acid/drug stock solution, 30 µL of 1 M APS, and 30 µL of 1 M TEMED.

4   Results and Discussion

The ultimate goal of this research is to design a hydrogel platform capable of sustained

release of antibiotics, analgesics, and hemostatic agent over a three-day period in order to seal

and passively protect a wound, actively decontaminate a wound, and locally deliver

therapeutics to prevent proliferation of limb-threatening infection. PEG hydrogels were

fabricated, characterized, and release kinetics of incorporated therapeutic drugs tested.

4.1   Hydrogel Gelation

Creating viable PEG hydrogels was the first step towards completing the project. Both

PEG 575 and PEG 700 were chosen as a result of the computational modeling. As the

computational models indicated, the lower the molecular weight PEG, the more extended the

release of the therapeutic drugs. Even the lowest molecular weight PEG hydrogels may not

result in the three-day extended release profile required. Thus, the low molecular weights PEGs

were chosen as the starting point for release kinetic examination. Additionally, PEG 2000 was

chosen as it is a solid powder prior to gelation whereas PEG 575 and PEG 700 are both liquids.

PEG in liquid form is not conducive to the ideal project design as the packaging of the final

product needs to be stable and have a long shelf life. All therapeutic drugs and other

components, macromers and initiators, need to share the same container without reacting until

potable water is added. Consequently, if some components are liquid, there is the potential for

polymerization to occur over time. Therefore, if possible, PEG in solid form, compared to liquid

form, would optimize the packaging process of the design.

A redox initiating system was used for the hydrogel preparation using APS and TEMED

as redox initiators. Both APS and TEMED are not active, producing radicals, until they are

combined together within the system. This redox crosslinking system has been used as the method to form hydrogels in the presence of live cells thus making it a viable option due to the biocompatibility. The redox initiators are biocompatible due to the low concentrations required for the system. One limit of the redox initiators, APS and TEMED, is the speed at which the reaction occurs once the initiators are combined. This crosslinking process occurs rapidly and can often result in the gelation of the hydrogel so quickly that it is not able to be removed from the container. Consequently, this would not be applicable as the individual requiring the wound dressing would have the hydrogel stuck in a container versus gelled and molded within the wound itself. This limitation is avoidable by adjusting the concentrations of both initiators, APS and TEMED, within the hydrogel system. Altering the concentration of redox initiators allows for temporal control of crosslinking which can be adjusted to meet the time constraint of approximately one minute. Therefore, the speed of the crosslinking is not a limiting factor in the use of a redox initiated system.

The first step was to optimize the weight percents of PEG, APS, and TEMED. The weight percents of PEG within the system were varied between 5 – 30 wt%, and the amounts of APS and TEMED were varied between 0.05 – 0.5 wt%. These variations were conducted in a systematic manner, ideally changing one variable at a time. The initial goal was to create a formed hydrogel, that was a fully formed solid hydrogel. Optimization for the weight percents of reagents were found through further experimentation and characterization of the hydrogels after ranges for the weight percents of each reagent that formed viable hydrogels were found. The ideal weight/weight percents and percent volume for the hydrogel reagents are shown in

Table 4.1 These values are the weight percents within the hydrogel and not the weight percents of the individual stock solutions.

Table 4.1: Percent volume of reagents in PEG hydrogel.

Reagent	w/w%	Percent Volume of Solution
35.5 wt% PEG	24.14%	68%
DI H$_2$O	N/A	26%
1M APS	0.556%	3%
1M TEMED	0.312%	3%

Once these weight percents were determined, the therapeutics were incorporated in the hydrogels. The therapeutic drugs were combined into the 26% volume of DI H$_2$O that is incorporated into the hydrogels. Initially, vancomycin was the only therapeutic drug added to the hydrogel to analyze the hydrogels physical properties and to determine the release kinetics. Vancomycin was chosen of the four therapeutic drugs because it is the largest of the four and thus will inherently have the longest sustained release from the hydrogel due to the size. Additionally, vancomycin is the most detectable by UV Vis when determining absorbance values for the release kinetics. Upon completion of this analysis with vancomycin, further analysis was conducted with hydrogels containing tranexamic acid, bupivacaine, and tobramycin. The concentrations for the stock solutions of the therapeutic drugs are shown in **Table 4.2**. These stock solutions replaced the 260 μL of DI H$_2$O when creating the hydrogels.

Table 4.2: Therapeutic drug stock solution concentrations.

Therapeutic Drug	Concentration
Bupivacaine	10.50 mg/mL
Vancomycin	5.20 mg/mL

The concentration of the stock solution for each therapeutic was determined based on the ability to be detectable by UV Vis when released from the hydrogels. Thus, the calibration curve for each therapeutic drug was a reference. A major contributing factor to the therapeutic drug stock solution concentration was the concentration required for detection from the initial aliquots from the well plate. The initial aliquots from the well plate, taken at the 30-minute time interval, needed to have a high enough concentration that the therapeutic drug was detectable. Therefore, the total amount of therapeutic drug released from the well into the 1000 µL sink must have a concentration high enough that when only a portion of the therapeutic drug has released it is still within the detectable range for the UV Vis. Too low of a concentration for the therapeutic drug stock solution will not produce reliable release kinetic graphs, because the concentration of therapeutic drug is outside the detectable range for the UV Vis. Consequently, in order to detect the release of the therapeutic drugs from the hydrogels into the 1000 µL well, the concentrations of therapeutic drug within the hydrogels are higher than the desired concentrations for in vivo application. In vivo applications will have a much larger hydrogel size and consequently the overall total amount of therapeutic drug loaded and released will be greater, thus making detection easier. However, for initial laboratory testing, small 6 mm hydrogels have a smaller amount of total loaded therapeutic

drug, and so a higher concentration of loaded therapeutic drug must be used to be within the detectable UV Vis range.

4.2   Characterization

Characterization indicates the physical properties of the hydrogels. This characterization was completed both with and without therapeutic drugs. This allows for the comparison and examination of the changes within the hydrogel when the therapeutics are incorporated.

4.2.1   Mass Swelling Ratio (q)

Swelling of the hydrogels in solvent was allowed for 30 minutes. No significant differences were noted when hydrogels were allowed to swell for 24 hours instead of 30 minutes. Therefore, maximum swelling occurs within the first 30 minutes of hydrogels being placed in DI H_2O. Accordingly, for all experiments 30 minutes was the standard swelling time. **Table 4.3** indicates the average mass swelling ratio and the standard deviation for each molecular weight PEG. These hydrogels do not include therapeutics. The swollen mass is taken 30 minutes after placing the hydrogels in DI H_2O. The dry mass does not include any DI H_2O as it was entirely removed from the polymer network through lyophilization. **Figure 4.1** displays the results shown in **Table 4.3**.

Table 4.3: Experimental mass swelling ratio (q_m) for varied molecular weight PEG hydrogels (n=12, 15, 45).

Molecular Weight PEG	Average q_m	Standard Deviation
575	4.005	0.050
700	3.910	0.123
2000	8.182	0.228
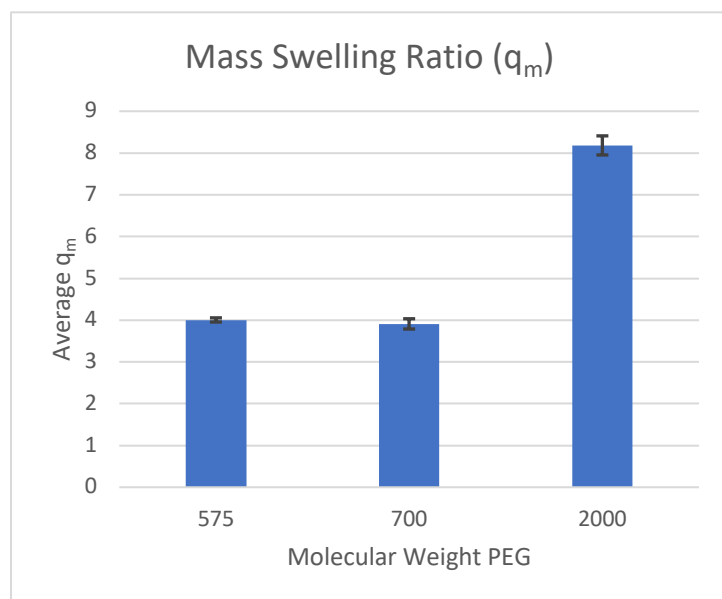
Figure 4.1: Mass swelling ratio (q_m) for varied molecular weight PEG hydrogels.

PEG 575 and PEG 700 have very similar experimentally determined mass swelling ratios. This would indicate that their mesh size and hence release kinetics would be very similar. However, the mass swelling ratio of PEG 2000 is significantly different than the PEG 575 and PEG 700, indicating that the release of therapeutics should be much faster. All PEG stock solution concentrations were held constant at 35.5 wt%. The higher molecular weight PEGs have larger swelling ratios, because the crosslink density decreases as a result of increased

chain length and consequently this increases the ability of the hydrogel network to swell. The computational model calculations treated the mass swelling ratio as a constant, and thus the value was chosen based on mass swelling ratio known to be achievable in hydrogel preparations. These values were able to range between 2-15. The computational modeling used to compare mesh sizes were rerun specifically for PEG 575, PEG 700, and PEG 2000 with the closest whole number mass swelling ratio to those found in **Table 4.3**. Computational models for PEG 575 and PEG 700 were rerun with a mass swelling ratio of 4, and PEG 2000 was rerun with a mass swelling ratio of 8. These computational modeling results were used to compare the experimental mesh size to the theoretical mesh size.

4.2.2   Volumetric Swelling Ratio (Q)

The volumetric swelling ratio is calculated from the mass swelling ratio using **Equation 3.2**. The volumetric swelling ratio also takes into account the density of DI H_2O, the solvent, and the density of PEG, the solute. **Table 4.4** shows the calculated volumetric swelling ratio for each molecular weight PEG based on the average mass swelling ratios from **Table 4.3**. **Figure 4.2** compares the mass swelling ratios shown in **Figure 4.1** to the volumetric swelling ratio data shown in **Table 4.4**.

Table 4.4: Calculated volumetric swelling ratio (Q) for varied molecular weight PEG hydrogels (n=12, 15, 45).

Molecular Weight PEG	Calculated Q
575	4.418
700	4.310
2000	9.749
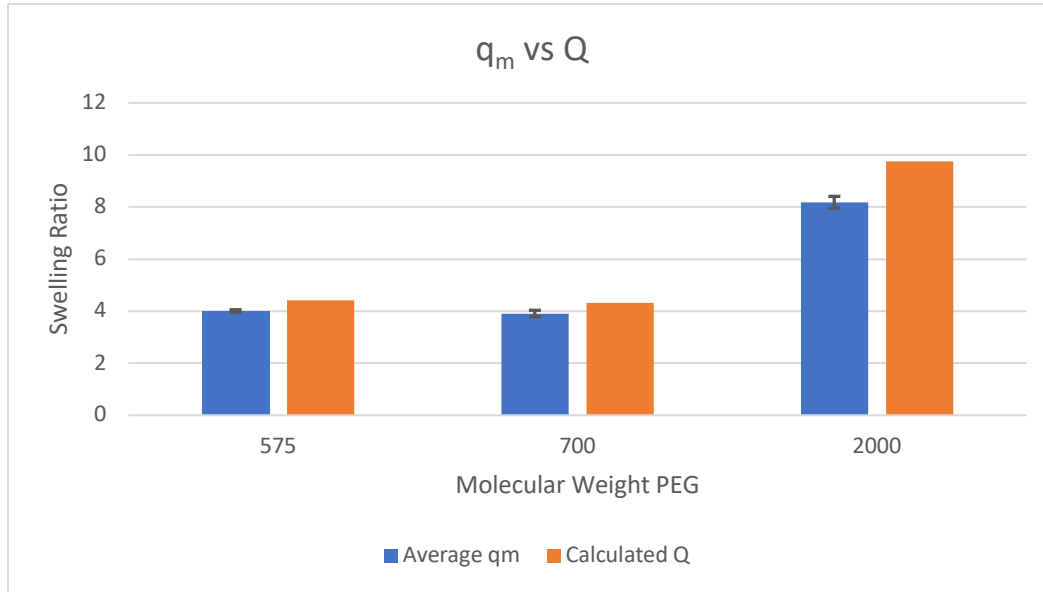
Figure 4.2: Experimental mass swelling ratio (q_m) versus calculated volumetric swelling ratio (Q) for varied molecualr weight PEG hydrogels (n=12, 15, 45).

As indicated in **Figure 4.2**, the volumetric swelling ratio is higher than the mass swelling ratio for all samples as the result of accounting for the density of both DI H_2O and PEG. Additionally, both the mass swelling ratio and the volumetric swelling ratio generally increase with increasing molecular weight PEG hydrogels.

4.2.3   Elastic Modulus (E)

The DMA produces a stress-strain curve for all samples upon completion of a uniaxial compression test. The modulus is found by taking the slope of the linear portion of the stress-strain curve. The ramp strain rate, the max strain, and the ramp de-strain rate were varied based on the molecular weight of the PEG hydrogel in order to produce a linear stress-strain plot from the DMA. For consistency of comparison, all slopes recorded from the stress-strain curves were taken between the -2% to -8% strain, which was within the linear portion of all graphs. **Table 4.5** indicates the average moduli of three PEG hydrogel samples run and the

standard deviation for each molecular weight PEG hydrogel. **Figure 4.3** displays the elastic

modulus for each molecular weight PEG hydrogel shown in **Table 4.5**.

Table 4.5: Elastic modulus and standard deviation for varied molecular weight PEG hydrogels (n=12, 15)

found using the DMA.

MW PEG	Average Moduli	Standard Deviation
575	87.717	6.252
700	111.6	8.675
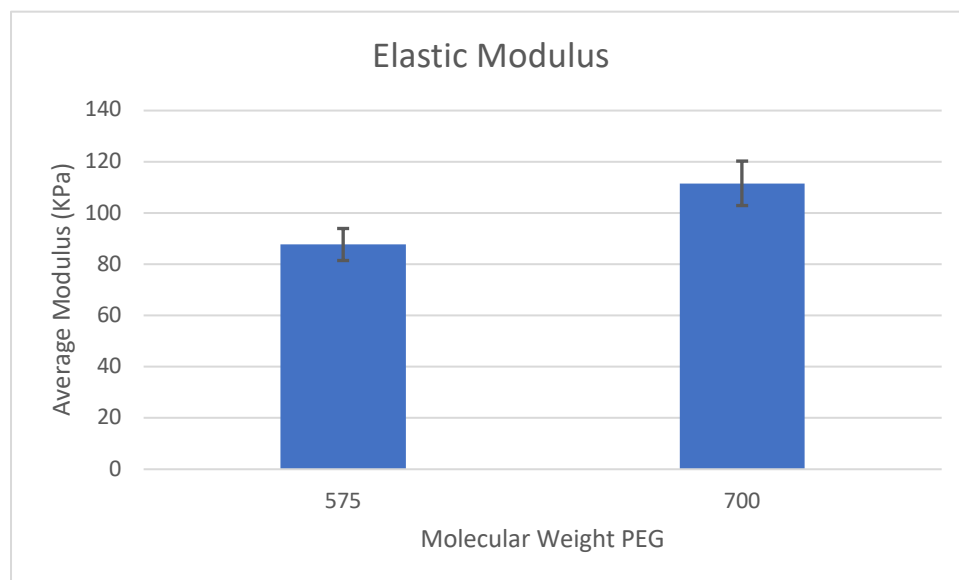
Figure 4.3: Elastic modulus for varied molecular weight PEG hydrogels (n=12, 15) found using the DMA.

As the graph indicates the higher the molecular weight, the higher the elastic modulus

as indicated by PEG 575 hydrogel having an elastic modulus of 90 KPa, and PEG 700 hydrogel

having an elastic modulus of 110 KPa. The modulus for each molecular weight PEG is another

qualitative predictive tool for the release kinetics of the therapeutic drugs. The modulus is

indicative of the mesh size of the hydrogel. The higher the elastic modulus the larger the mesh

size and hence the faster the release of therapeutic drug from the PEG hydrogel.

4.2.4 Mesh Size (ξ)

Mesh size was calculated as described in 3.4.3, *Mesh Size*. The mesh sizes were

calculated based on the mass swelling data for each molecular weight PEG hydrogel. **Table 4.6**

displays the average mesh size for each molecular weight PEG in addition to the theoretical

mesh size calculated via computational modeling. The computational models for theoretical

mesh size values were found using the whole number mass swelling ratio closest to the

experimental mass swelling ratio for each molecular weight hydrogel. The calculated mesh sizes

are then compared to the computational modeling mesh size values in **Figure 4.4**.

Table 4.6: Calculated experimental mesh size versus computational modeling of theoretical mesh size for varied molecular weight PEG hydrogels (n=12, 15, 45).

MW	Experimental Mesh Size (ξ)	Standard Deviation	q_m Computational Model	Theoretical Mesh Size
575	17.59	0.101	4	16.39
700	19.03	0.296	4	17.72
2000	41.93	0.161	8	41.31
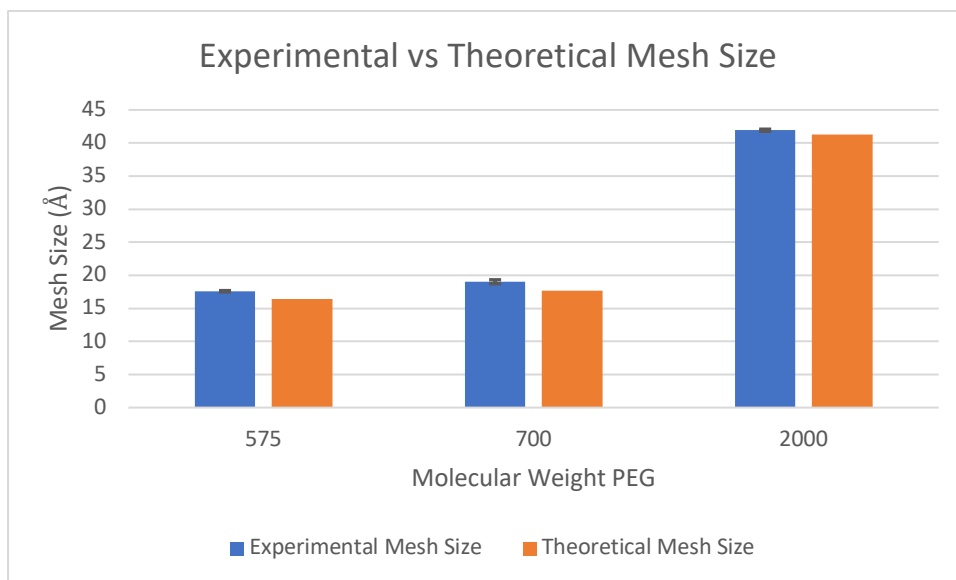
Figure 4.4: Experimentally determined mesh size versus theoretical mesh size from computational model for varied molecular weight PEG hydrogels (n=12, 15, 45).

Figure 4.4 indicates the higher the molecular weight, the larger the mesh size. Higher molecular weight PEG has more repeat units along the backbone, hence making the molecule longer. Therefore, the molecular weight of the polymer chain between two neighboring crosslinks (M_c) increases with the increase in molecular weight. Increasing M_c correlates to increases in the mesh size. When these PEG macromers crosslink and form a mesh, the space between the crosslinks is larger and thus, the size of the molecules that are able to fit between the crosslinks increase. Mesh size is indicative of the size of a solute that can pass through the crosslinked network.[50] Release kinetics of the therapeutic drugs are based on the rate of diffusion from the mesh. Larger mesh sizes will therefore have faster release kinetics and not sustain the release of the therapeutic drugs as well as lower molecular weight PEG hydrogels.

The values for theoretical mesh size determined through computational modeling were lower than the experimental mesh size values for all molecular weight PEGs. The theoretical

values were PEG 575 and PEG 700 were 17.588 Å and 19.026 Å respectively. The radius of a

solute (R_s) values for all four therapeutic drugs are found in **Table 2.2**. The largest of the

therapeutic drugs is vancomycin that has a R_s of approximately 10 Å. Therefore, vancomycin the

mesh size of PEG 575 or PEG 700 and the R_s of vancomycin are nearly identical. This may make

incorporation of vancomycin into the mesh difficult or it may allow for extremely difficult

diffusion from the mesh. The cumulative release kinetics of vancomycin from the PEG 575 and

PEG 700 hydrogels will give further indication. PEG 2000 has a larger mesh size of 41.929 Å.

Therefore, with the increase in mesh size, all therapeutic drugs will be able to fit within the

mesh.

4.3   Therapeutic Drug Release Kinetics

The release kinetics of the hydrogels were completed using a UV Visible

Spectrophotometer (UV Vis). The UV Visible Spectrophotometer returns the absorbance values

for a solution compared to a designated blank solution. The UV Vis experiments determined the

absorbance values for the aliquots of solution, of unknown concentration, from the hydrogel

well plate. The comparison between hydrogels with no drugs loaded, i.e. blanks, and drug

loaded hydrogels determined the concentration of the therapeutic drug in the solution. The

concentration at the time of the aliquot is able to determine the amount of therapeutic drug

released compared to the total amount of therapeutic drug able to be released from the

hydrogel. This comparison yields the cumulative release value of the therapeutic drug from the

hydrogel. The plot of the cumulative therapeutic drug release over time displays the release

kinetics of the therapeutic drug from a known molecular weight PEG hydrogel.

4.3.1 Calibration Curve

In order to use the UV-Visible Spectrometer, a calibration curve was prepared for each therapeutic drug. The first step was to find the maximum absorbance of the therapeutic drug using the scanning function on the UV-Vis. The purpose was to find the wavelength of light that has the maximum absorbance for the given therapeutic drug. This wavelength varied for each therapeutic drug due to the drugs ability to be able to absorb the energy of given wavelength of light. Once the maximum absorbance wavelength was determined, the UV-Vis was run only at that wavelength when determining the absorbance values of therapeutic drug solution. One issue with using UV-Vis was the therapeutic drugs had similar maximum absorbance wavelengths. The similar range of detection prevented multiple drugs from being combined into one hydrogel and then detected with UV-Vis. Since the wavelengths were so similar it is possible that the absorbance at one wavelength would pick up more than just the desired drug. Thus, individual drug release kinetics were necessary. Calibration curves were produced from known concentrations of therapeutic drug compared to a blank of DI H_2O. The concentration of solution was plotted along the x-axis and their respective absorbance values were plotted along the y-axis. The slope of the best fit line was then determined for each therapeutic drug. This best fit line produced a calibration curve that allowed for the determination of the therapeutic drug concentration when only the absorbance of the unknown aliquot is known.

The difficulty with tranexamic acid is that the drug itself is undetectable by the UV-Visible Spectrometer. Therefore, in order for the calibration curve to be created, the stock solution of tranexamic acid required the addition of ferric chloride (Fe(III)Cl). By adding in ferric chloride, the tranexamic acid solution turned a yellow-orange color that allowed for detection.

54

The calibration curves for tranexamic acid, bupivacaine, tobramycin, and vancomycin are shown in **Figures 4.5**, **4.6**, **4.7**, and **4.8** respectively.
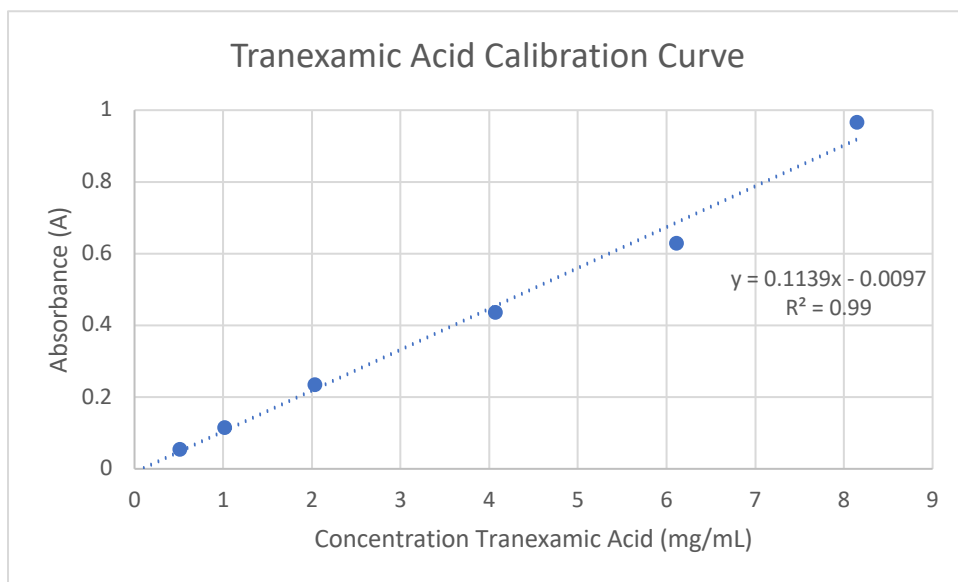
Figure 4.5: Tranexamic acid calibration curve at 366 nm using Fe(III) Cl for detection.
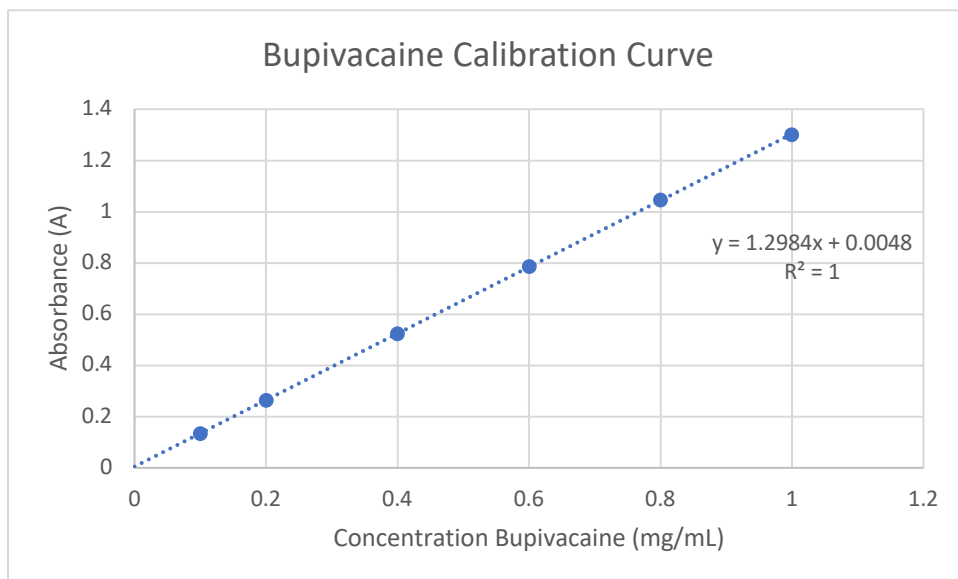
Figure 4.6: Bupivacaine calibration curve at 262 nm.
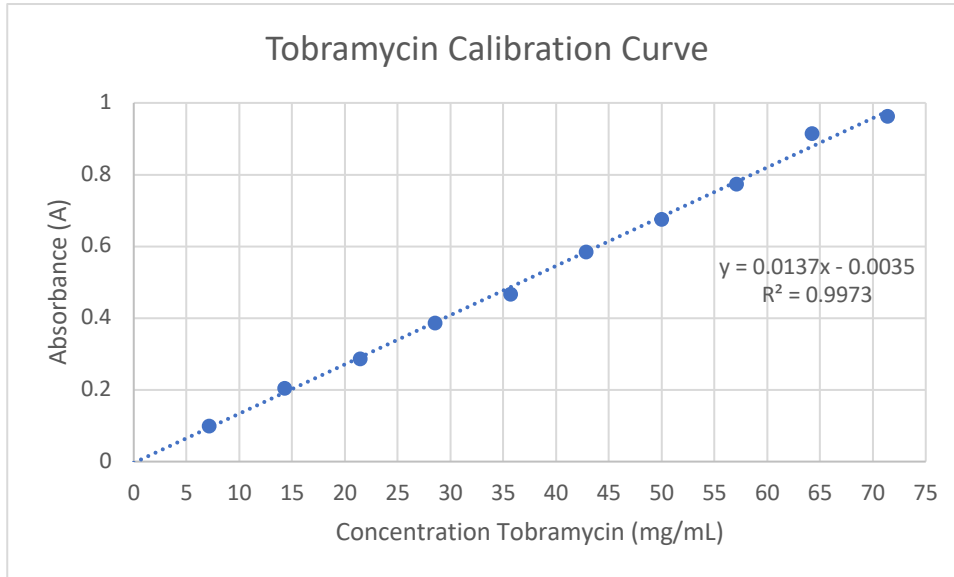
Figure 4.7: Tobramycin calibration curve at 254 nm.
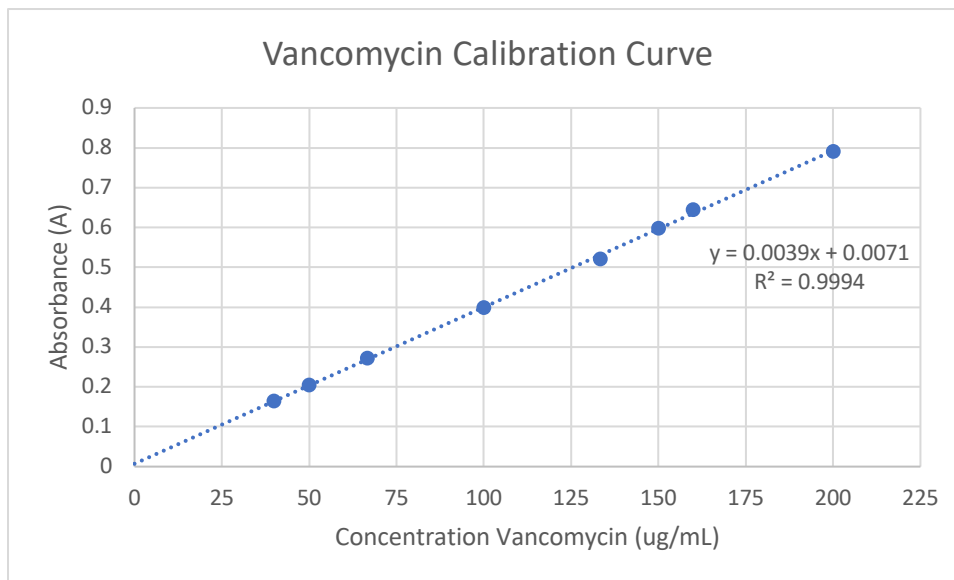
Figure 4.8: Vancomycin calibration curve at 281 nm.

It is important to note that **Figures 4.5**, **4.6**, and **4.7** all have units of mg/mL for the

concentration. However, the units of concentration for the calibration curve of vancomycin,

Figure 4.8, has units of µg/mL. The difference in concentrations is due to the ability of the

therapeutic drugs to be detected by the UV Vis. Vancomycin has a greater potential to absorb

56

light due to the increased number of chromophores, light absorbing groups, within its chemical structure.[64] Therefore, the highly detectable chemical structure of vancomycin indicates that a lower concentration of therapeutic drug is necessary for detection. The other therapeutics with less chromophores, absorb less light and thus are more difficult to detect using the UV Vis requiring higher concentrations of the therapeutics in solution.

4.3.2   Therapeutic Drug Stock Solutions

The calibration curves were created from serial dilutions of a known concentration of therapeutic drug. Each calibration curve had a minimum of six standard concentrations to ensure that the line of best fit was accurate. The calibration curves were run in a DI H_2O medium, the same medium as the therapeutic drug loaded hydrogels in the well plates. The stock solution concentrations for incorporation into the hydrogel were higher than the stock solutions used to create the calibration curves. This is because the detection of the therapeutic drug must be possible when released from the hydrogel into the 1000 µL of DI H_2O in the well plate. Values for therapeutic drug stock solution concentrations used when incorporated into the hydrogel are found in **Table 4.2**.

These concentration values for the incorporated therapeutic drugs are above the necessary effective therapeutic concentrations due to detection limitations from the UV Vis. The therapeutic drug concentrations necessary for effective drug application are shown in **Table 4.7.** These concentrations of therapeutic drugs will meet the effective dosage required for *in vivo* application of the hydrogel wound dressing.

Table 4.7: Required therapeutic drug concentrations necessary for the in vivo application.

Therapeutic Drug	Free Drug Incorporation in PEG Hydrogel
Tranexamic Acid	1 – 20 mg/mL
Bupivacaine	1.6 – 5 mg/mL
Tobramycin	4 µg/mL
Vancomycin	1 µg/mL

Due to the fact that the concentrations of therapeutic drugs incorporated in the PEG hydrogels for experimentation are significantly higher than the required concentrations, the cumulative therapeutic drug release plots are not representative of the appropriate daily drug dosage. The cumulative release plots for the therapeutic drugs shows the qualitative trends of the release over the three-day period. The exact therapeutic drug dosage in the initial payload and sustained release will be able to then be further altered in future research.

4.3.3   Individual Therapeutic Drug Release

The assumption was made that since the hydrogels are made from the same procedure and same reagents, that the hydrogels should be uniform in the amount of incorporated therapeutic drug and therefore have the same release kinetics. It is predicted that there will be an initial burst release of the therapeutic drug once the hydrogel is placed into the well plate. Following the burst release, the remaining therapeutic drug should release at a slower rate. All therapeutic drug should eventually diffuse from the hydrogel yielding 100% cumulative release. The ultimate goal is to have sustained release of the therapeutic drug over a three-day period. Samples were taken at set time intervals (approximately every 12 hours) over a three-day period in order to plot the cumulative release of the therapeutic drug.

The first set of experiments was designed to understand the cumulative release kinetics of a known mesh size with vancomycin. This initial analysis determined what further alterations

of the hydrogel were necessary in order to retard the therapeutics for the desired time interval for release. For all cumulative release plots, the trend line is the best fit logarithmic function of the form $y = a * ln(x) + b$, where x is the time in hours, y is the cumulative release, and a and b are constants. **Figures 4.9**, **4.10**, and **4.11** show the cumulative release of vancomycin from PEG 575, 700 and 2000 respectively. **Figure 4.12** overlays the curves from **Figures 4.9**, **4.10**, and **4.11** to compare the difference in release kinetics.
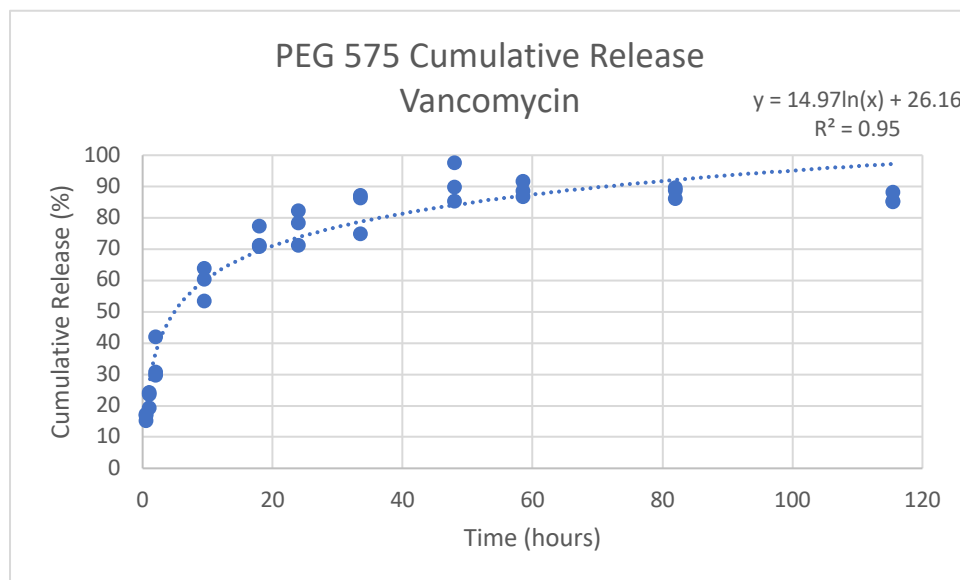
Figure 4.9: Cumulative release of vancomycin from PEG 575 (n=12) at 281 nm.
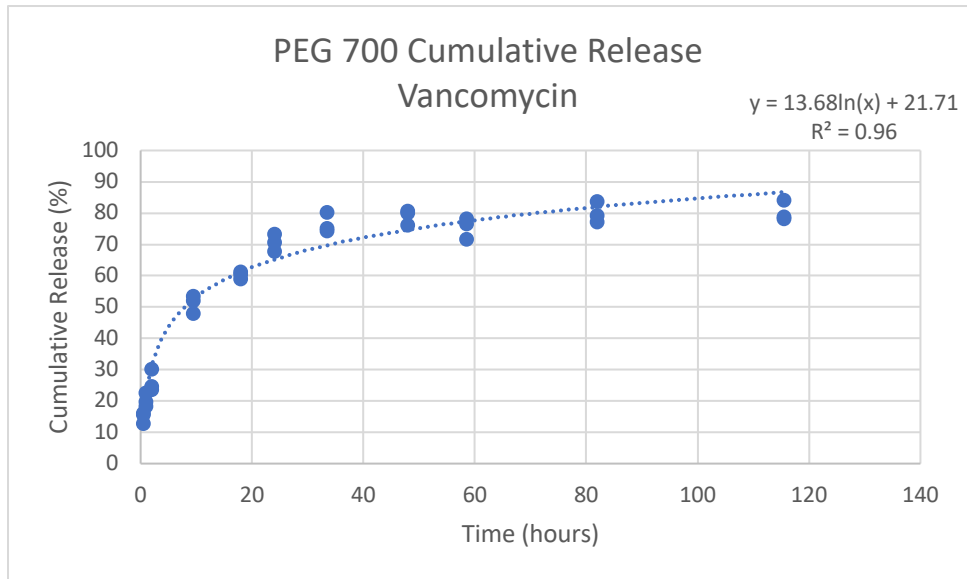
Figure 4.10: Cumulative release of vancomycin from PEG 700 (n=15) at 281 nm.
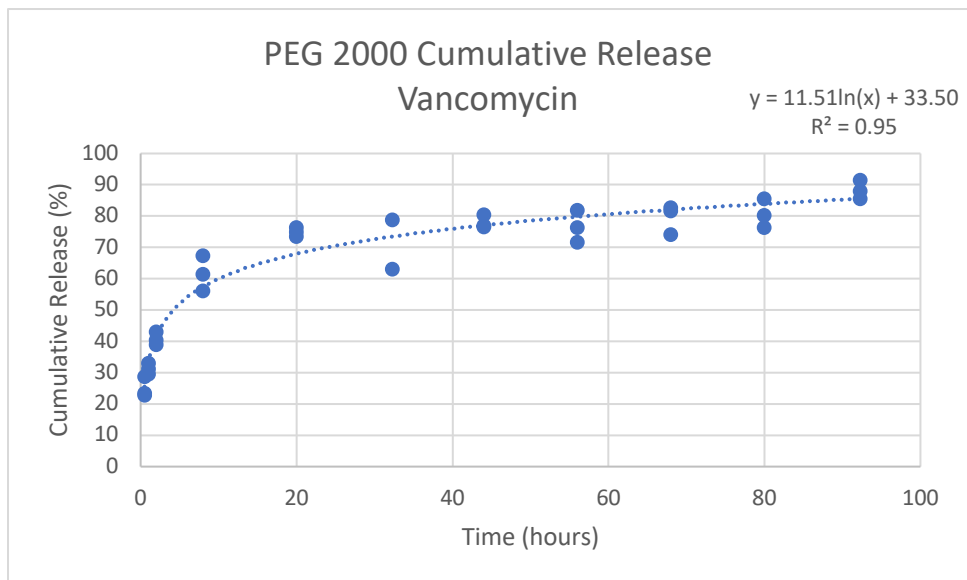
Figure 4.11: Cumulative release of vancomycin from PEG 2000 (n=45) at 281 nm.
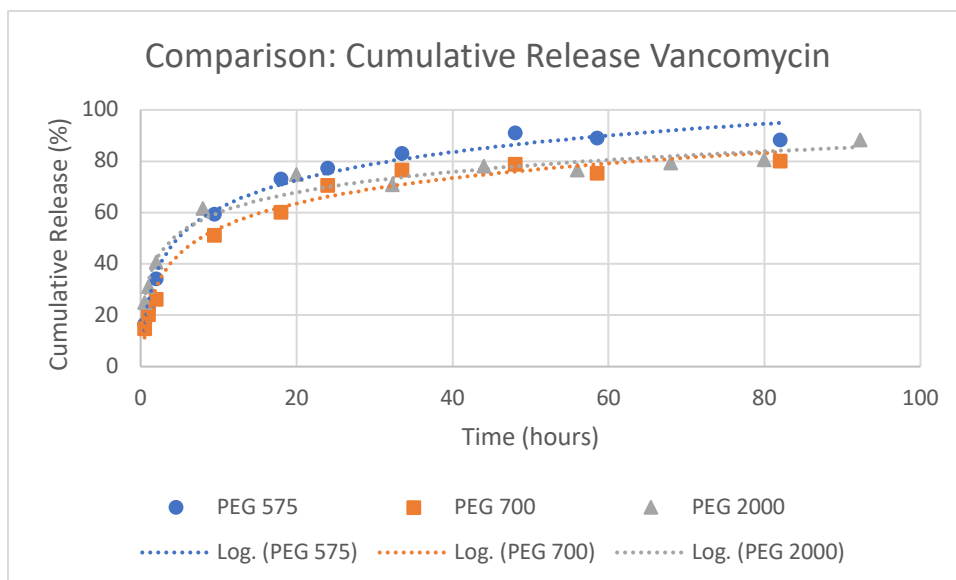
Figure 4.12: Cumulative release of vancomycin from different molecular weight PEG hydrogels (n=12, 15, 45) at 281 nm.

As **Figure 4.12** shows, the release of vancomycin does not vary significantly between PEG 575, PEG 700, and PEG 2000. The diffusion of vancomycin from the crosslinked mesh of the PEG 2000 hydrogel is expected to be faster due to the larger mesh size as there is less entanglements for the vancomycin. Therefore, these results vary from the theoretical release of vancomycin predicted in the computational modeling of Chapter 2.

The cumulative release kinetics of bupivacaine from PEG 575 and PEG 700 were also completed. **Figure 4.13** and **Figure 4.15** show the cumulative release of bupivacaine from PEG 575 and PEG 700 respectively. **Figure 4.14** and **Figure 4.16** show the cumulative release of bupivacaine compared to the release of vancomycin from PEG 575 or PEG 700 respectively.
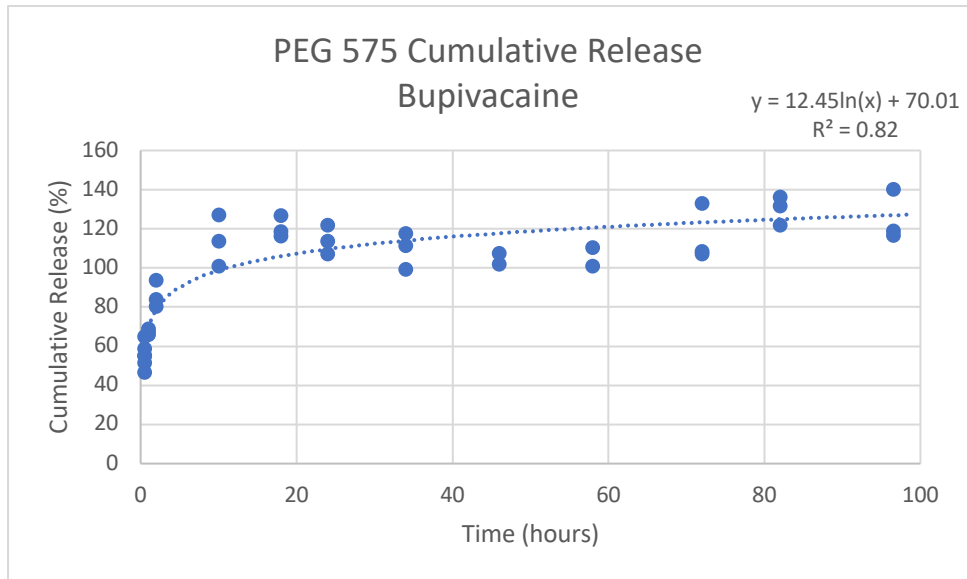
Figure 4.13: Cumulative release of bupivacaine from PEG 575 (n=12) at 262 nm.
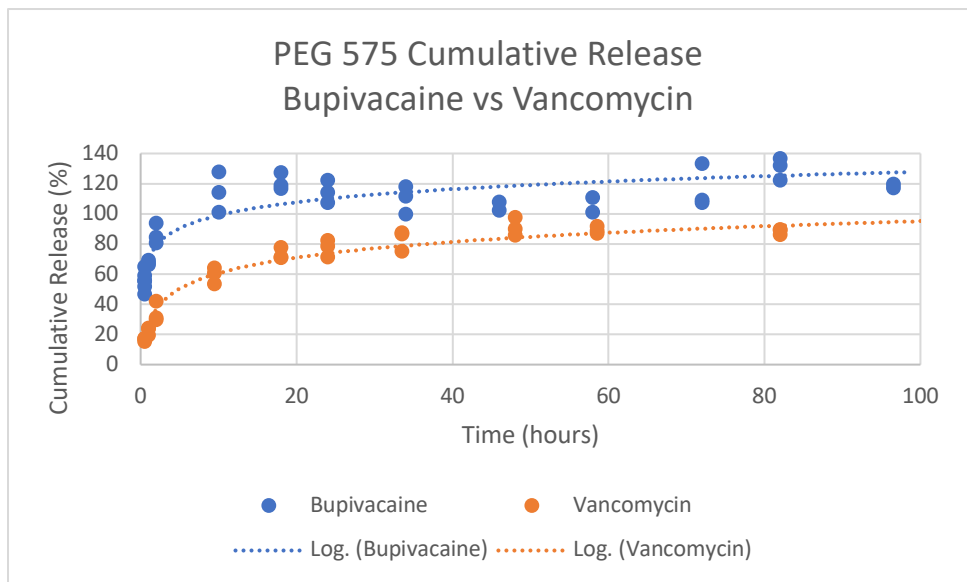
Figure 4.14: Cumulative release of bupivacaine versus vancomycin from PEG 575 (n=12).
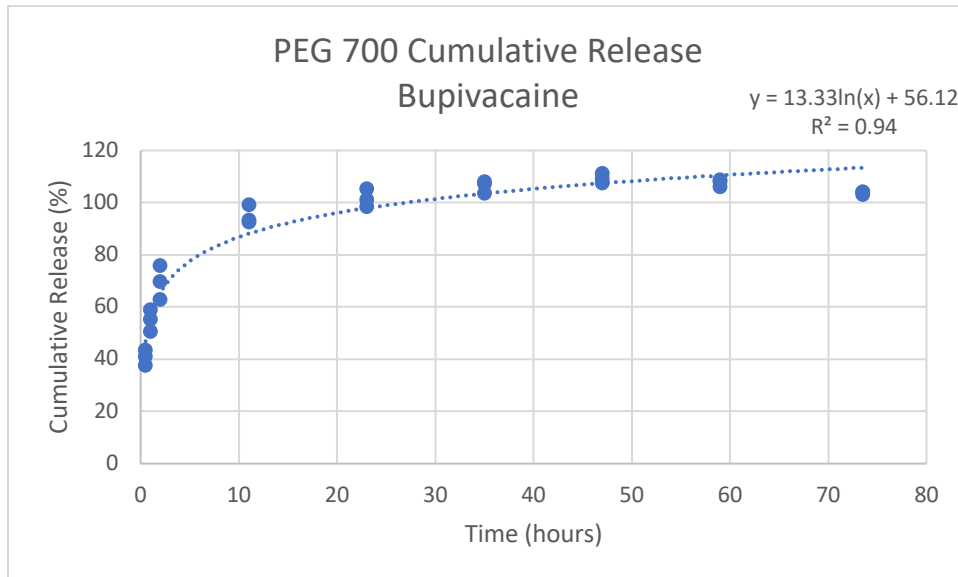
Figure 4.15: Cumulative release of bupivacaine from PEG 700 (n=15) at 262 nm.
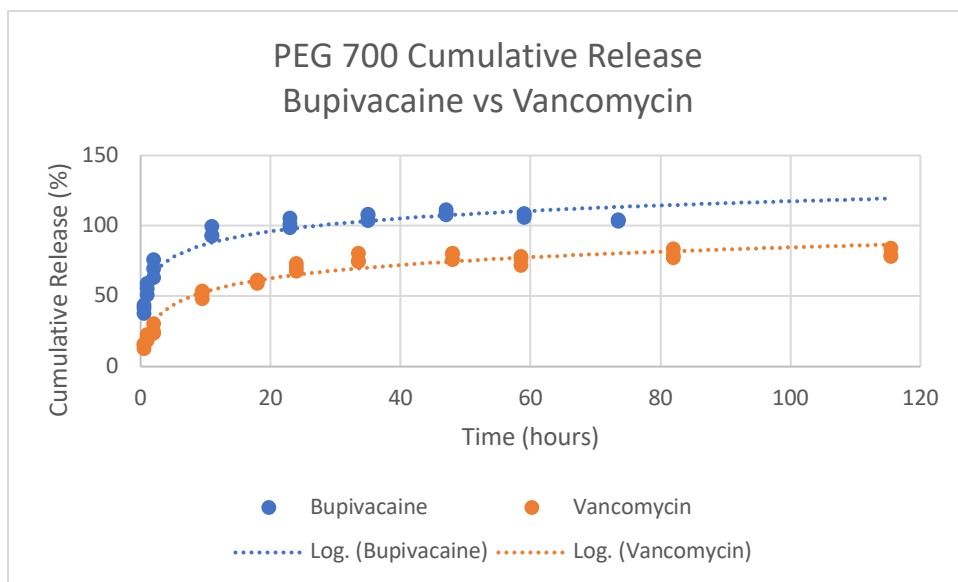
Figure 4.16: Cumulative release of bupivacaine versus vancomycin from PEG 700 (n=15).

Some burst release of each therapeutic drug is expected. However, the vancomycin, tobramycin, and bupivacaine need to be able to have extended release profiles in order to maintain the three-day sustained release. It is expected that tranexamic acid will have a large burst release as it is the smallest of the four therapeutic drugs and hence can easily escape the

physical entrapment by the hydrogel. The burst release of tranexamic acid is not a concern as the role of tranexamic acid is a hemostatic agent. Accordingly, it is not necessary for the hemostatic agent to release over the three days once hemostasis is achieved. Ideally, tranexamic acid would have a burst release to initially stop the wound bleeding. The antibiotics and analgesics need to obtain the three-day release profile. Modifications of macromer length, weight percent in solution, and changes to initiator concentrations were not sufficient to obtain the three-day release profile. Therefore, additional modifications to the hydrogel will be necessary to retard the diffusion of the therapeutics.

4.4   Extended Therapeutic Drug Release

The release of the therapeutic drugs from an unmodified PEG crosslinked network did not meet the time requirement of three days for sustained release. Therefore, the PEG hydrogel needed modification to obtain the sustained released profile. Modification of the hydrogel was attempted with two different mechanisms. The first mechanism is through the incorporation of sodium polyacrylate. The second mechanism is the incorporation of acrylic acid. These modifications alter the mesh of the hydrogel in two different ways with the goal of the alterations being to retard the diffusion of the therapeutic drugs.

4.4.1   Sodium Polyacrylate

The initial attempt at retarding the release of the therapeutic drugs was through the incorporation of sodium polyacrylate to extend the release. Sodium polyacrylate was desired over acrylic acid as sodium polyacrylate is a powder. The final product is intended to be a powder stored within a tube that then has potable water added. Accordingly, the reagent used for retardation would ideally be a solid. PAA should be able to alter the hydrogel by forming its

own polymerized mesh around the crosslinked PEG hydrogel network. The PEG crosslinked network sits within the PAA network and thus physically entraps the therapeutic drugs from diffusing. This physically entrapment would ideally slow the diffusion of the therapeutic drugs from the hydrogel.

However, after several different experiments, sodium polyacrylate was not found to be useful. One difficulty was its super absorbent properties, which made dissolving the sodium polyacrylate in DI H_2O very difficult. An extremely low concentration of PAA was necessary to keep PAA from forming a gel when combined with DI H_2O. The concentration of the solution was less than 4 mg/mL. This concentration was ultimately determined to be insufficient to alter the release of the therapeutic drugs from the hydrogel. Furthermore, the incorporation of sodium polyacrylate was not able to be uniform throughout the hydrogel as partial gelation would occur prior to the entire hydrogel slab gelation. The addition of PAA to PEG hydrogels should alter the mesh size slightly as there is an increase in negative charges at physiological pH that repel one another. Through mass swelling ratio, the mesh size was determined to be unchanged with the low concentration of PAA as shown in **Figure 4.17**.
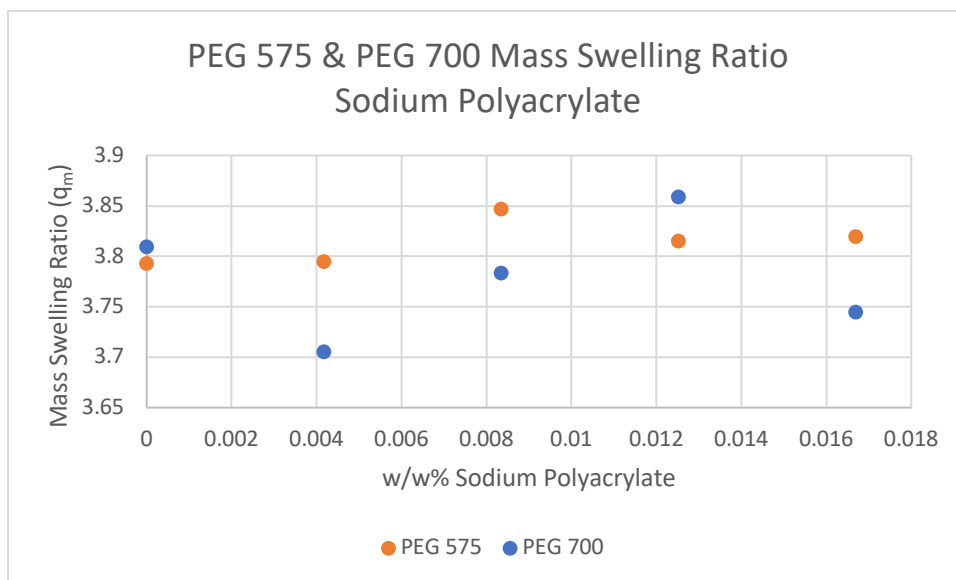
Figure 4.17: Mass swelling ratio (q_m) with sodium polyacrylate in PEG 575 (n=12) and PEG 700 (n=15) hydrogels.

Figure 4.17 displays the changes within the mass swelling ratio of both PEG 575 and PEG 700 hydrogels were not significant compared to hydrogels with 0 wt% PAA incorporated. Thus, PAA may not be the best method for retarding the release of the therapeutic drugs from the hydrogel.

Additionally, the release kinetics for vancomycin from a PAA altered hydrogel were examined. The concentration of PAA used within the hydrogels was 0.62 mg/mL. This concentration was low enough that the PAA did not form gels prior to the incorporation of all the reagents for the hydrogel itself. An issue within the hydrogel formation still remained that the PAA would partially gel when combined with all reagents. Consequently, the transfer from Eppendorf tube to slide to form the hydrogel slabs resulted in a loss of the PAA and hence non uniform incorporation. The vancomycin release kinetics data from the PAA incorporated hydrogels had large standard deviations between samples. This large variation was accredited

to the inconsistent and non-uniform incorporation of PAA into the hydrogel. Thus, the

cumulative release of the therapeutic drug, vancomycin, was inconsistent. The overall trendline

indicates a retarded release however the error is too large for it to be a reliable method of

retardation for therapeutic drug.
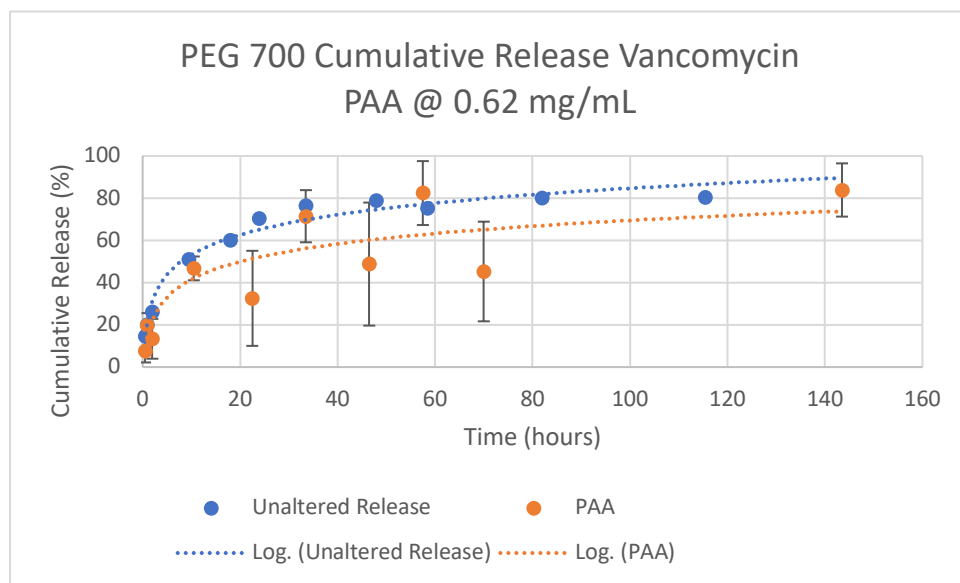
Figure 4.18: Cumulative release of vancomycin from PEG 700 (n=15) with and without sodium

polyacrylate at 281 nm.

4.4.2   Acrylic Acid

The second method for retarding the release of therapeutic drugs from the hydrogel is

through the incorporation of acrylic acid. Acrylic acid is a monomer that is able to be

incorporated into the PEG chains during crosslinking. Thus, the acrylic acid is bound into the

network. Bupivacaine has a tertiary amine that is protonated at physiological pH that could be

electrostatically sequestered through acrylic acid, an anionic monomer. Vancomycin also

contains a variety of amides, amines, alcohols, phenols, sugar groups, and aromatic rings that

can be utilized to retard the release from the PEG hydrogel. This increase in negative charges

due to the incorporation of acrylic acid interacts with the amine groups on the therapeutic

drugs. Hence, the interaction interferes with the diffusion of the therapeutic drug. The negative

charges also repel one another. As a result, this expands the crosslinked network further apart

from one another and thus should alter the mass swelling ratio of the hydrogel.

The experiments to analyze the cumulative release kinetics were designed identically to

the cumulative release kinetics for hydrogels without reagents for retardation. Therefore,

aliquots were taken at known time intervals from well plates and the absorbance determined

from UV Vis. **Figure 4.19** shows the release of bupivacaine from PEG 700 from hydrogels both

with and without the incorporation of acrylic acid. The acrylic acid was incorporated into the

PEG hydrogel in a 5:1 moles of acrylic acid to moles of bupivacaine ratio.
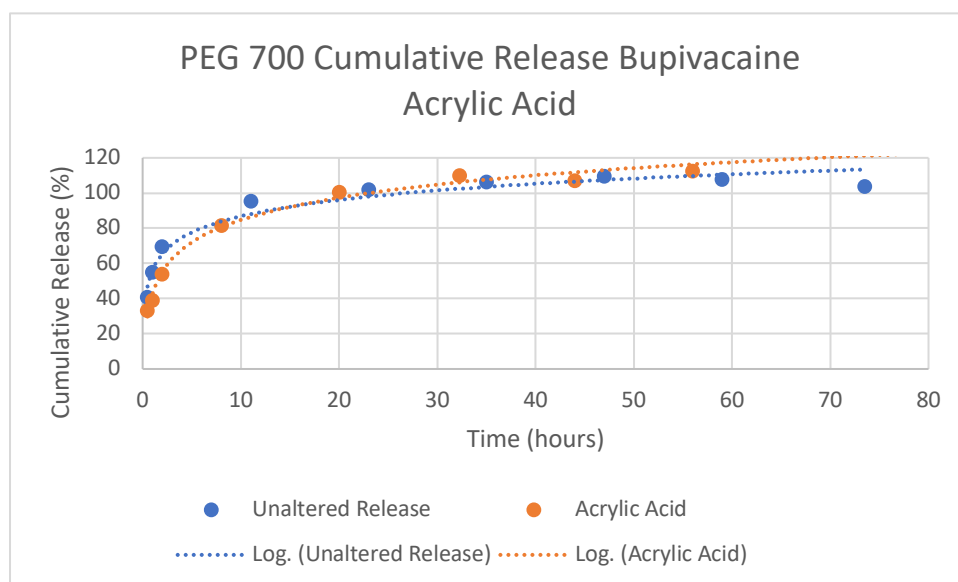
Figure 4.19: Cumulative release of bupivacaine from PEG 700 (n=15) with and without acrylic acid at 262

nm.

As **Figure 4.19** indicates, there is no conclusive evidence that the release of bupivacaine was retarded from the hydrogel. Additionally, it is unknown why the absorbance values for the cumulative release of bupivacaine indicates more than 100% release from the hydrogel network. Several different trials were run, and all bupivacaine leeching hydrogels ultimately yielded cumulative release values greater than 100%.

Vancomycin loaded hydrogels were also modified with the incorporation of acrylic acid. Acrylic acid was incorporated into the PEG hydrogels in a 1:1 moles of acrylic acid to moles of vancomycin ratio. Cumulative release of vancomycin from PEG 700 hydrogels both with and without acrylic acid incorporation are shown in **Figure 4.20**.
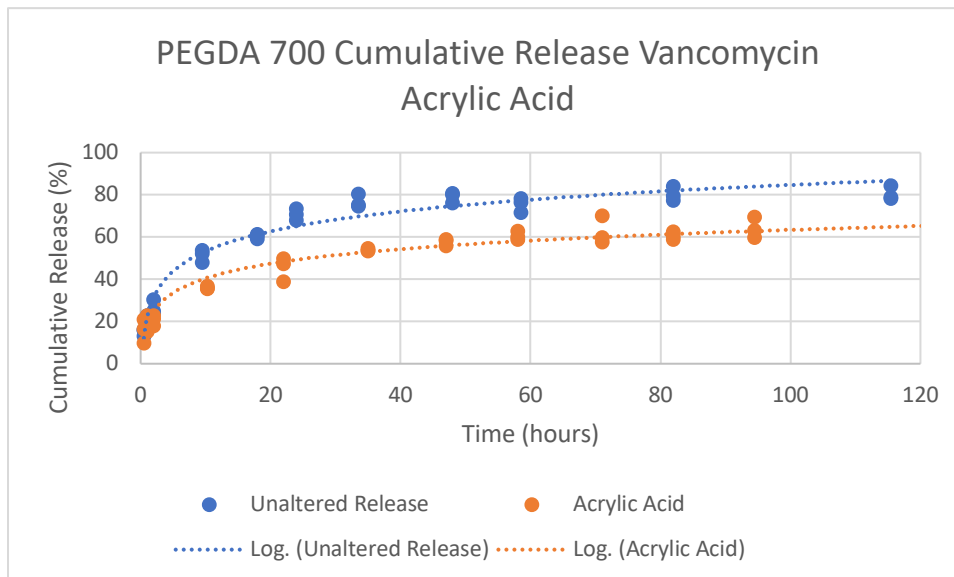
Figure 4.20: Cumulative release of vancomycin from PEG 700 (n=15) with and without acrylic acid.
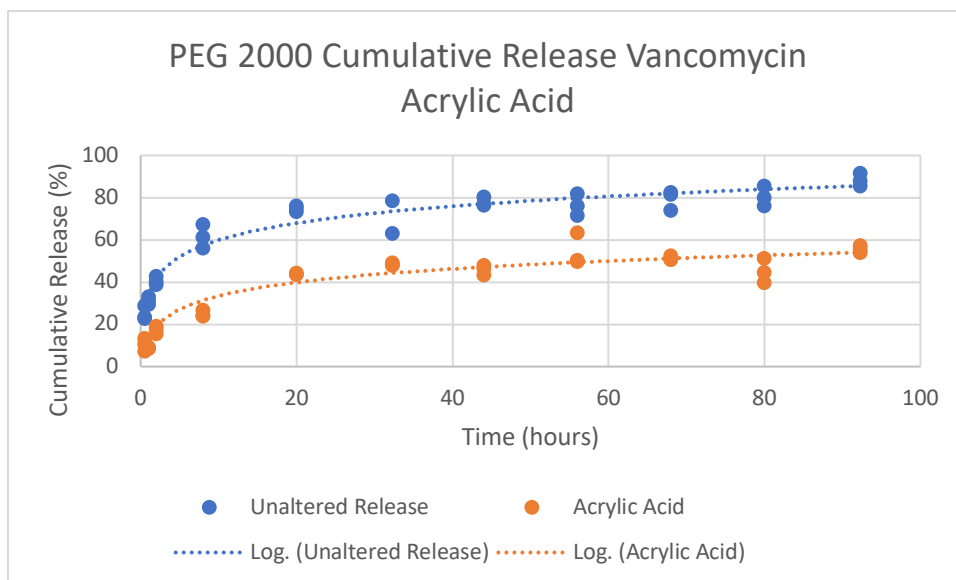
Figure 4.21: Cumulative release of vancomycin from PEG 2000 (n=45) with and without acrylic acid.

Figure 4.20 and **Figure 4.21** illustrate that acrylic acid incorporation alters the release kinetics of vancomycin. The burst release seen within the first 12 hours is decreased, and the overall release of vancomycin is slower.

Figure 4.22 compares the release of vancomycin from PEG 700 with acrylic acid to PEG 2000 with acrylic acid. Despite the differences in molecular weight, and thus the mesh size of the hydrogels, the incorporation of acrylic acid into PEG 2000 was actually able to retard the diffusion more than PEG 700 with acrylic acid incorporation. This is significant as this allows the optimization of release kinetics for the hydrogel to proceed with the use of PEG 2000. As previously discussed, this is desired as PEG 2000 is a powder compared to the liquid state of PEG 700.
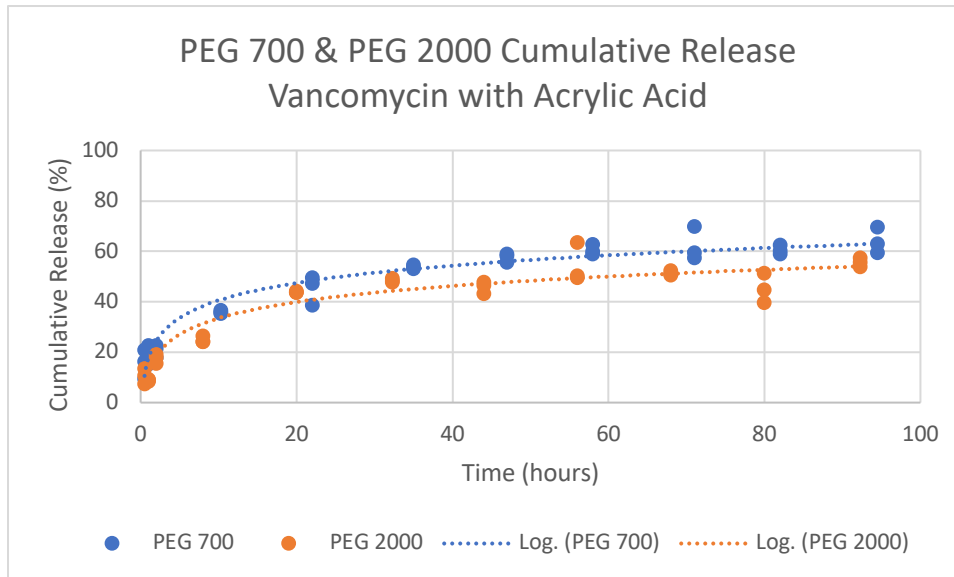
Figure 4.22: Cumulative release of vancomycin from PEG 700 (n=15) and PEG 2000 (n=45) with acrylic acid.

One potential issue with the use of acrylic acid to retard the diffusion of therapeutic drug from the hydrogel is the total amount of therapeutic drug released may be decreased. While the acrylic acid does retard the release of the therapeutic drug, it may also inhibit 100% release from the hydrogel. The cumulative release plots indicate that the burst release of the therapeutic drug is slowed when acrylic acid is incorporated. However, these experiments also never achieved 100% release within the desired time frame for sustained release. This may be able to be further altered by modifying the amount of acrylic acid incorporated into the system. Hence, these experiments demonstrate the feasibility of acrylic acid to retard the release, but further optimization of release kinetics is necessary.

71

5 Conclusions

The overall goal of the project was to create and characterize PEG hydrogels with varied mesh size to analyze therapeutic drug release properties and kinetics. Using this characterization of PEG, the therapeutic drugs, tranexamic acid, bupivacaine, tobramycin, and vancomycin, were able to be loaded into the hydrogel, and release of the therapeutic drugs extended for a sustained three-day release profile.

Chapter two discussed the computational modeling, conducted using MATLAB, to understand the correlation between mesh size and therapeutic drug release kinetics. The computational models examined the cumulative therapeutic drug release verse time and how the release can be altered based on changes in mesh size. Chapter three described the methods and materials for the in-lab verification of the computational models. PEG synthesis, hydrogel preparation, characterization, therapeutic drug release characterization, and extended therapeutic drug release were all described. Chapter four discussed the results from the mesh size characterization and therapeutic drug release kinetics.

5.1 Computational Modeling

The computational models produced qualitative information on the release kinetics of each therapeutic drug relative to each other. In addition, the models displayed the release kinetics of a single therapeutic drug from varied molecular weight hydrogels. The larger the size of the therapeutic drug, the slower the cumulative release. Thus, vancomycin had the slowest cumulative release followed by tobramycin, then bupivacaine, and tranexamic acid had the fastest release regardless of the molecular weight of the PEG hydrogel. The lower the molecular weight PEG hydrogel, the slower the cumulative release of the therapeutic drug. Computational

models indicated that even the lowest molecular weight PEG hydrogels may have mesh sizes too large to sustain the release of therapeutic drug over a three-day period. The models also demonstrated the relationship between mass swelling ratio and mesh size. Based on the computational models run, incorporation of additional reagents for retardation of therapeutic drug may be necessary. The computational models allowed for a guided approach to laboratory experiments. The lowest molecular weight PEG hydrogels release kinetics should be analyzed first to determine the experimental release kinetics of the therapeutic drugs. The computational models also were used as a comparison for the theoretical versus the experimental mesh size.

5.2   PEG Hydrogel Characterization

Experimental mesh size was determined through evaluating the mass swelling ratio. The overall trend was as the molecular weight of PEG increased, the mass swelling ratio increased. Hence, the mesh size also increased as the mass swelling ratio increased with increasing molecular weight PEG. Large mesh sizes predict faster release of the therapeutic drug incorporated into the PEG hydrogel.

5.3   PEG Hydrogel Release

PEG hydrogels of molecular weight 575, 700 and 2000 were used to analyze the release kinetics of bupivacaine and vancomycin. The experimental cumulative release of vancomycin from all three different molecular weight hydrogels did not vary significantly. However, the release of vancomycin was significantly slower than the cumulative release of bupivacaine. The release of therapeutics from the hydrogels were ultimately still too fast to meet the three-day

sustained release requirement. Consequently, further alterations of the hydrogel were necessary to retard the diffusion.

5.4   PEG Hydrogel Retarded Release

Retardation of therapeutic drug release form PEG hydrogels was attempted with two different mechanisms. The incorporation of PAA did not provide conclusive evidence for retarded release as the PAA was not able to be incorporated uniformly. The retarded release of therapeutic drugs using acrylic acid was successful for vancomycin. The burst release in both PEG 700 and PEG 2000 hydrogels were decreased for vancomycin when acrylic acid was incorporated.

5.5   Research Translated to the Combat Zone

Ultimately, both the PEG macromers and its initiators, and therapeutic drugs will be stored in powder form in a plastic centrifuge like a tube with a screw on lid. The powder reagents are then able to be combined with potable water and mixed into a liquid solution that is able to be poured into a bleeding wound. The liquid solution will solidify rapidly, within 60 seconds, and form a hydrogel fitting exactly within the unique wound shape. This hydrogel will be able to seal the traumatic wound, prevent bleeding with hemostatic agents, begin wound decontamination through sustained release of antibiotics, and provide pain management with analgesic release. This biochemical tool aims to improve patient outcome after battlefield and trauma injuries in the austere combat environments in the case of delayed medical evacuation.

6   Future Work

This research is the first step towards designing and completing a hydrogel wound dressing that is able to release antibiotics, analgesics, and hemostatic agents over a three-day period. This work set the foundation by designing a hydrogel with proper mesh size, diffusion kinetics, and mechanical characteristics. This work also considers the ease for the user while designing this hydrogel.

Following this work, it will be necessary to determine the best detection methods for tranexamic acid and tobramycin. Individual therapeutic drug release studies were not possible with these two drugs as unmodified drug is not detectable using UV Vis technology. A microBCA kit may be able to be used to aid in this detection.

Additionally, combined therapeutic drug release kinetics must be examined. The addition of all four therapeutic drugs into one hydrogel may alter the release kinetics of the individual therapeutic drugs. The release of the individual therapeutic drugs will need to be detected using HPLC as the wavelengths for detection using UV Vis are too similar that detection would overlap between therapeutic drugs thus giving errored absorbance values.

Leak pressure testing is the next step in optimizing the hydrogel wound dressing. Leak pressure testing will require a unique testing device composed of a sensor assembled and connected to a cylindrical reservoir that evaluates the pressures able to be withstood by the hydrogel. This will be conducted according to literature protocols.[65] With the assembled sensor, the pressure can be applied in either a continuous or a pulsed manners. A continuous manner will mimic venous blood flow, while a pulsed manner will mimic arterial blood flow. The variation in flow will be possible by using either a pressure infuser or a peristaltic pump. The

leak pressure will be quantified given the thickness of the hydrogel, the crosslink density, and the encapsulated therapeutic drugs. All three of these factors will have an effect on the leak pressure. Altering these factors can enhance the leak pressure of the hydrogel.

Subsequently, the hydrogel will undergo ruggedization testing. The ruggedization of the wound hydrogel dressing is a key factor to its success as a wound dressing used in combat. Ruggedization of the hydrogel will require that the components be able to withstand a variety of extreme environments. This includes elevated temperatures and vibration. The ultimate goal is to have the wound dressing hydrogel form in situ and have properties similar to that of human skin tissue. Therefore, this wound dressing should be able to withstand similar stressors as living human tissue. In order to test the ruggedization of this hydrogel wound dressing, the individual components will need to each undergo their own testing. One of the tests will be the thermal stability. This will be conducted by characterizing the changes to the chemical structure of the individual components of the hydrogel after prolonged storage at elevated temperatures. Cure time of the hydrogel wound dressing system will be quantified as the effect of extreme temperature storage conditions. The mechanical stability will also be characterized for both the precursor components and the formed hydrogel wound dressing. The mechanical stability will be analyzed with both temperature and mechanical vibrations. This will be possible by using a dynamic mechanical analyzer varying both the frequency and the temperature on the material modulus.

Following both the leak pressure and ruggedization testing, validation of the released therapeutic drugs is necessary. This validation will ensure that the incorporation and release, in addition to the ruggedization testing, does not alter the therapeutic drugs themselves. Mass

spectrometry will be used to ensure the therapeutic drugs remain intact. It will also be possible to test the therapeutic drug activity of the antibiotics, vancomycin and tobramycin, in *in vitro* release experiments using the antibiotics released from the hydrogels against *E. coli* and *S. aureus* for tobramycin and vancomycin respectively.[66] This will complete the first aim of the project of understanding and optimizing the release profile for the therapeutic drugs.

The second aim for the project requires the hydrogel to undergo both small and large animal *in vivo* testing. Animal model testing will allow for the *in vivo* efficiency of the hydrogels to be examined. The ultimate goal of the hydrogel is to prevent wound infection. Therefore, modeled infections must be tested in both small animals, such as a mouse model, and in large animals, such as a goat model, to best predict the *in vivo* efficacy for human patients.

Mouse model testing will require bacteria placed into a controlled wound and cultured. The hydrogel wound dressing will then be applied to the infected mouse wound and wrapped with a bandage. The response of the bacteria to the wound dressing will be able to be examined through the bioluminescence in the controlled bacteria. Different groups required for testing will include subjects with no hydrogel, subjects with hydrogel only, and subjects with hydrogel and different combinations of therapeutics. Imaging to detect the bioluminescence of the bacteria will be performed for five days following the application of the hydrogel wound dressing. In addition to the *in vivo* efficacy of the hydrogel, it is also important to detect the *in vivo* immune response to the hydrogel by looking at the neutrophils and macrophages at the site of infection. Furthermore, *in vivo* toxicity must also be assessed as the hydrogel dressing cannot be toxic *in vivo*. Lastly, it is important to assess the efficacy of the hemostasis agent, tranexamic acid. This will be examined by checking for bleeding at the wound site on one-

minute intervals post application of the wound dressing simply by removing the bandage covering the hydrogel and observing the rate, if any, of bleeding.

The *in vivo* study using the goat model will provide further information about the effectiveness of the hydrogel. Similar to the mouse model, the goat model will look at the efficacy and safety of the hydrogel on an infected wound by creating a contaminated musculoskeletal wound. Within this model of testing there will be an assessment on the infection, a histological evaluation looking for toxins, an assessment of the hemostasis, and an assessment of the analgesic effect. These results should correlate to the results conducted in the mice study. However, if when conducting the *in vivo* studies, the therapeutic drug release is altered or the initiation or application process needs revision, then further optimization of the hydrogel will be necessary.

7   Appendices

7.1   Appendix A: MATLAB Code for Theoretical Mesh Size and Release Kinetics

Table of Contents

Molecular Weight of PEG

Table:

```
opts = spreadsheetImportOptions("NumVariables", 3);

% Specify sheet and range
opts.Sheet = "Molecular Weight PEG";
opts.DataRange = "A17:C19";

% Specify column names and types
opts.VariableNames = ["Mn_g_mol", "n_repeats", "BulkDensity"];
opts.VariableTypes = ["double", "double", "double"];

% Import the data
ThesisResearch_1 = readtable("/Users/kaitlyncook/OneDrive/UCLA/Thesis/Thesis
Research 1.xlsx", opts, "UseExcel", false)
```

ThesisResearch_1 = 3×3 table

	Mn_g_mol	n_repeats	BulkDensity
1	575	12.6443	1.1300
2	700	15.4820	1.1300
3	2000	44.9939	1.2100

Q and $v_{2,s}$

Q= volumetric swelling ratio

Q_M is swelling ratio based on hydrogel mass (varied from 2 to 15)

```
Q_M=4
```

Q_M = 4

p_s is density of solvent (water at 80 deg) (g/cm3)

```
p_s=0.993329
```

p_s = 0.9933

Q_v is volume swelling ratio

```
BD=ThesisResearch_1{:,3}
```

BD = 3×1
    1.1300

```
    1.1300
    1.2100
```

```
Q_v=1+(BD/p_s)*(Q_M-1)
```

```
Q_v = 3×1
    4.4128
    4.4128
    4.6544
```

v2,s is polymer volume fraction in equilibrium swollen hydrogel

```
v2s=1./Q_v
```

```
v2s = 3×1
    0.2266
    0.2266
    0.2149
```

M~c~

v is the specific volume of polymer

```
v=(p_s./BD)
```

```
v = 3×1
    0.8791
    0.8791
    0.8209
```

V1 is the molar volume of water (cm^3/mol)

```
V1=18
```

```
V1 = 18
```

X1 is the polymer water interaction parameter

```
X1=0.426
```

```
X1 = 0.4260
```

Mn is the average molecular weight of linear polymer chains

```
Mn=ThesisResearch_1{:,"Mn_g_mol"}
```

```
Mn = 3×1
         575
         700
        2000
```

Mc where 1/Mc is the MW of polymer chains between 2 neighboring crosslinks

```
Mc=1./((2./Mn)-(((v./V1).*(log(1-v2s)+v2s+X1.*v2s.^2))./(v2s.^(1/3)-(v2s/2))))
```

```
Mc = 3×1
   231.8456
   270.8488
   593.9942
```

r_o^2

RMS end-to end distance of polymer chains between 2 neighboring crosslinks (units = Angstroms)

l is length of bond along polymer backbone (units = Angstroms)

```
l=1.54
```

```
l = 1.5400
```

Cn is the Flory characteristic ratio

```
Cn=4
```

```
Cn = 4
```

Mc is molecular weight of polymer chains between 2 neighboring crosslinks; measure of degree of crosslinking of polymer (g/mol)

```
Mc
```

```
Mc = 3×1
   231.8456
   270.8488
   593.9942
```

Mr is molecular weight of repeating units from which polymer chain is composed (g/mol)

```
Mr=44.05
```

```
Mr = 44.0500
```

N is the number of links

```
N=(2.*Mc)./Mr
```

```
N = 3×1
   10.5265
   12.2973
   26.9691
```

(ro2)^1/2

```
ro2=l.*(Cn.*N).^(1/2)
```

```
ro2 = 3×1
    9.9929
   10.8008
   15.9950
```

Mesh Size

ξ (units = Angstroms)

```
E=v2s.^(-1/3).*ro2
```

```
E = 3×1
   16.3906
   17.7158
   26.7057
```

Drug Properties

```
opts = spreadsheetImportOptions("NumVariables", 6);

% Specify sheet and range
opts.Sheet = "Drug Properties";
opts.DataRange = "A4:F7";

% Specify column names and types
opts.VariableNames = ["drug", "drugeffect", "solubility", "MW_gmol", "MW_kDA",
"Rs_angstoms"];
opts.VariableTypes = ["string", "string", "string", "double", "double",
"double"];

% Specify variable properties
opts = setvaropts(opts, ["drug", "drugeffect", "solubility"], "WhitespaceRule",
"preserve");
opts = setvaropts(opts, ["drug", "drugeffect", "solubility"], "EmptyFieldRule",
"auto");

% Import the data
ThesisResearch1S8 = readtable("/Users/kaitlyncook/OneDrive/UCLA/Thesis/Thesis
Research 1.xlsx", opts, "UseExcel", false)
```

`ThesisResearch1S8 = 4×6 table`

	drug	drugeffect	solubility	MW_gmol	MW_kDA	Rs_angstoms
1	"tranexamic acid"	"hemostatic agent"	"water soluble at 167 mg/mL"	157.2100	0.1572	4.8600
2	"bupivacaine"	"analgesic"	"freely water soluble"	288.4350	0.2884	5.9200
3	"tobramycin"	"cationic antibiotic"	"water soluble"	467.5150	0.4675	6.9300
4	"vancomycin"	"antibiotic"	"water soluble >100 g/mol"	1.4493e+03	1.4493	10.0000

Drug Diffusion Coefficient

solved using Stokes Einstein:

KB is the Boltzmann's constant (J/K) (m^2kg/s^2K)

```
KB=1.38064852*10^-23
```

KB = 1.3806e-23

T is the temperature in Kelvin

```
Temp=310.15
```

Temp = 310.1500

η is the viscosity of the solution (water) at 37 C (Ns/m^2)

```
w=0.0006915
```

w = 6.9150e-04

rs is the Stokes Einstein hydrodynamic radius of solute (drug) (m)

```
rs=ThesisResearch1S8{:,"Rs_angstoms"}
```

rs = 4×1
```
    4.8600
    5.9200
    6.9300
   10.0000
```

```
rs_m=rs.*10^-10
```

rs_m = 4×1
10^{-9} ×
```
    0.4860
    0.5920
    0.6930
    1.0000
```

D0_m is solute diffusivity (m^2/s)

```
D0_m=(KB*Temp)./(6*pi*w*rs_m)
```

D0_m = 4×1
10^{-9} ×
```
    0.6760
    0.5549
    0.4741
    0.3285
```

D0_cm is solute diffusivity (cm^2/s)

```
D0_cm=D0_m.*100^2
```

```
D0_cm = 4×1
10⁻⁵ ×
    0.6760
    0.5549
    0.4741
    0.3285
```

Diffusion from Gel

Constants

Y is the ratio of critical volume required for successful translational movement of solute molecule to average free volume per molecule of liquid; approximated to 1

```
Y=1
```

```
Y = 1
```

rs is the Stokes Einstein hydrodynamic radius of solute (drug) (Angstroms)

```
rs
```

```
rs = 4×1
    4.8600
    5.9200
    6.9300
   10.0000
```

v2s is polymer volume fraction in equilibrium swollen hydrogel

```
v2s
```

```
v2s = 3×1
    0.2266
    0.2266
    0.2149
```

E is mesh size; ξ (units = Angstroms)

```
E
```

```
E = 3×1
   16.3906
   17.7158
   26.7057
```

Tranexamic Acid

Dg_TA is the diffusion coefficient from gel for Tranexamic Acid

```
Dg_TA=D0_cm(1,1).*(1-(rs(1,1)./E)).*exp(-Y.*(v2s./(1-v2s)))
```

```
Dg_TA = 3×1
```

10⁻⁵ ×
```
    0.3548
    0.3659
    0.4206
```

Bupivacaine

Dg_B is the diffusion coefficient from gel for Bupivacaine

```
Dg_B=D0_cm(2,1).*(1-(rs(2,1)./E)).*exp(-Y.*(v2s./(1-v2s)))
```

Dg_B = 3×1
10⁻⁵ ×
```
    0.2645
    0.2756
    0.3285
```

Tobramycin

Dg_To is the diffusion coefficient from gel for Tobramycin

```
Dg_To=D0_cm(3,1).*(1-(rs(3,1)./E)).*exp(-Y.*(v2s./(1-v2s)))
```

Dg_To = 3×1
10⁻⁵ ×
```
    0.2041
    0.2153
    0.2670
```

Vancomycin

Dg_V is the diffusion coefficient from gel for Vancomycin

```
Dg_V=D0_cm(4,1).*(1-(rs(4,1)./E)).*exp(-Y.*(v2s./(1-v2s)))
```

Dg_V = 3×1
10⁻⁵ ×
```
    0.0956
    0.1067
    0.1563
```

Summation to solve for diffusion from thin film

Constants:

symbolic variables

- n is for summation from 0 to infinity
- t is for time (ideally release over 5 days)

```
syms n t
```

Diffusion coefficients from gel for the drugs

```
 Dg_TA
```

```
Dg_TA = 3×1
10⁻⁵ ×
     0.3548
     0.3659
     0.4206
```

```
 Dg_B
```

```
Dg_B = 3×1
10⁻⁵ ×
     0.2645
     0.2756
     0.3285
```

```
 Dg_To
```

```
Dg_To = 3×1
10⁻⁵ ×
     0.2041
     0.2153
     0.2670
```

```
 Dg_V
```

```
Dg_V = 3×1
10⁻⁵ ×
     0.0956
     0.1067
     0.1563
```

Height of the thin film (cm)

   varies from 0.1 to 3 cm

```
 L= 0.2
```

```
L = 0.2000
```

Tranexamic Acid

Summation Tranexamic Acid:

```
 f_TA_1(t)=(8/((2*n+1)^2*pi^2))*exp((-Dg_TA(1)*(2*n+1)^2*pi^2*t)/L^2)
```

```
f_TA_1(t) =
```

$$
\frac{2251799813685248\, e^{\frac{-5817497521573904532246519227758625\, t\ (2\,n+1)^2}{6646139978924579364519035301401722288}}}{27780466668940015\ (2\,n+1)^2}
$$

```
 M_TA_1(t)=1-symsum(f_TA_1,n,0,inf)
```

`M_TA_1(t) =`

$$1 - \frac{2251799813685248 \left(\sum_{n=0}^{\infty} \frac{e^{-\frac{58174975215739045322465192275862 5\, t\,(2\,n+1)^2}{6646139978924579364519035301401722 88}}}{(2\,n+1)^2} \right)}{2778046668940015}$$

`f_TA_2(t)=(8/((2*n+1)^2*pi^2))*exp((-Dg_TA(2)*(2*n+1)^2*pi^2*t)/L^2)`

`f_TA_2(t) =`

$$\frac{2251799813685248 \, e^{-\frac{300045230467355052273639679195375\, t\,(2\,n+1)^2}{33230699894622896822595176507008614 4}}}{2778046668940015\,(2\,n+1)^2}$$

`M_TA_2(t)=1-symsum(f_TA_2,n,0,inf)`

`M_TA_2(t) =`

$$1 - \frac{2251799813685248 \left(\sum_{n=0}^{\infty} \frac{e^{-\frac{300045230467355052273639679195375\, t\,(2\,n+1)^2}{3323069989462289682259517650700861 44}}}{(2\,n+1)^2} \right)}{2778046668940015}$$

`f_TA_3(t)=(8/((2*n+1)^2*pi^2))*exp((-Dg_TA(3)*(2*n+1)^2*pi^2*t)/L^2)`

`f_TA_3(t) =`

$$\frac{2251799813685248 \, e^{-\frac{344845409008280270090615244551625\, t\,(2\,n+1)^2}{33230699894622896822595176507008614 4}}}{2778046668940015\,(2\,n+1)^2}$$

`M_TA_3(t)=1-symsum(f_TA_3,n,0,inf)`

`M_TA_3(t) =`

$$1 - \frac{2251799813685248 \left(\sum_{n=0}^{\infty} \frac{e^{-\frac{344845409008280270090615244551625\, t\,(2\,n+1)^2}{3323069989462289682259517650700861 44}}}{(2\,n+1)^2} \right)}{2778046668940015}$$

Solved Data Tranexamic Acid:

`T_TA=[0:300:5400]`

T_TA = 1×19

| 0 | 300 | 600 | 900 | 1200 | 1500 ⋯ |

`mt_minf_TA_1=double(M_TA_1(T_TA))`

mt_minf_TA_1 = 1×19

```
  -0.0000    0.3681    0.5198    0.6312    0.7165    0.7819    0.8323 ⋯
```

```
mt_minf_TA_2=double(M_TA_2(T_TA))
```

```
mt_minf_TA_2 = 1×19
  -0.0000    0.3739    0.5278    0.6403    0.7257    0.7908    0.8404 ⋯
```

```
mt_minf_TA_3=double(M_TA_3(T_TA))
```

```
mt_minf_TA_3 = 1×19
  -0.0000    0.4008    0.5648    0.6814    0.7667    0.8291    0.8748 ⋯
```

Solved Data Tranexamic Acid Combined Plot:

change in time scale to match for all therapeutics

```
T_TA1=[0:1000:20000]
```

```
T_TA1 = 1×21
          0       1000       2000       3000       4000       5000 ⋯
```

```
mt_minf_TA1_1=double(M_TA_1(T_TA1))
```

```
mt_minf_TA1_1 = 1×21
  -0.0000    0.6622    0.8592    0.9413    0.9756    0.9898    0.9958 ⋯
```

```
mt_minf_TA1_2=double(M_TA_2(T_TA1))
```

```
mt_minf_TA1_2 = 1×21
  -0.0000    0.6714    0.8668    0.9460    0.9781    0.9911    0.9964 ⋯
```

```
mt_minf_TA1_3=double(M_TA_3(T_TA1))
```

```
mt_minf_TA1_3 = 1×21
  -0.0000    0.7128    0.8983    0.9640    0.9872    0.9955    0.9984 ⋯
```

Plot Tranexamic Acid Different MW PEG:

```
figure('Name','Tranexamic Acid')
    xlabel('time (hours)')
    ylabel('Mt/Minf')
    title('Diffusion of Tranexamic Acid')
    set (gca,'FontSize', 16)
    hold on

    plot(T_TA/3600,mt_minf_TA_1)
    plot(T_TA/3600,mt_minf_TA_2)
    plot(T_TA/3600,mt_minf_TA_3)

    hold off
```

```
legend({'575','700','2000'}, 'location','southeast')
lgd=legend;
lgd.Title.String='Molecular Weight PEG';
```

Diffusion of Tranexamic Acid
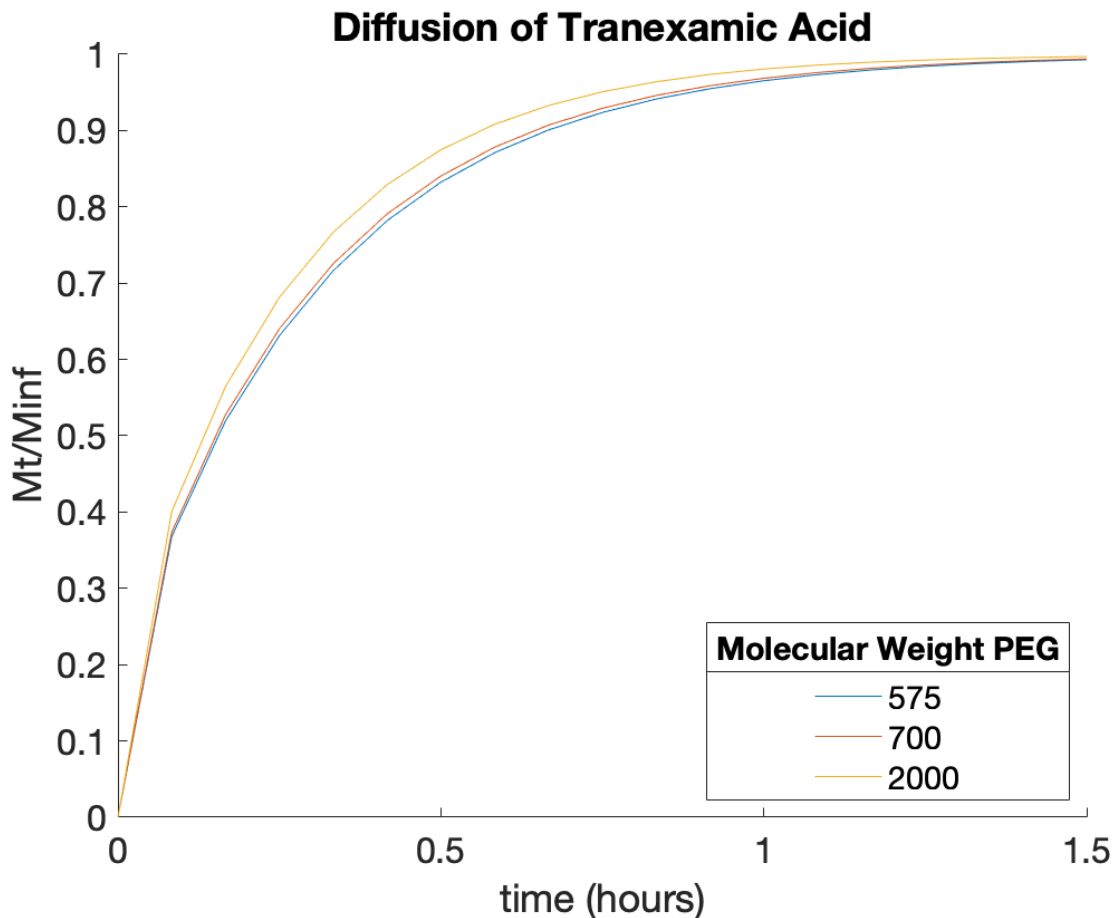
Bupivacaine

Summation Bupivacaine:

```
f_B_1(t)=(8/((2*n+1)^2*pi^2))*exp((-Dg_B(1)*(2*n+1)^2*pi^2*t)/L^2)
```

f_B_1(t) =

$$\frac{2251799813685248 \, e^{-\frac{10842029441587645149730152433 6625 \, t \, (2\,n+1)^2}{16615349947311448411297588253 5043072}}}{2778046668940015 \, (2\,n+1)^2}$$

```
M_B_1(t)=1-symsum(f_B_1(t),n,0,inf)
```

M_B_1(t) =

$$1 - \frac{2251799813685248 \left(\sum_{n=0}^{\infty} \frac{e^{-\frac{1084202944158764514973015243 36625 \, t \, (2\,n+1)^2}{1661534994731144841129758825 35043072}}}{(2\,n+1)^2} \right)}{2778046668940015}$$

```
f_B_2(t)=(8/((2*n+1)^2*pi^2))*exp((-Dg_B(2)*(2*n+1)^2*pi^2*t)/L^2)
```

f_B_2(t) =

$$2251799813685248\,\mathrm{e}^{\frac{-4520218864408254573118335329786 25\,t\,(2\,n+1)^2}{6646139978924579364519035301 40172288}} \Big/ 2778046668940015\,(2\,n+1)^2$$

```
M_B_2(t)=1-symsum(f_B_2(t),n,0,inf)
```

M_B_2(t) =

$$1-\frac{2251799813685248\left(\sum_{n=0}^{\infty}\dfrac{\mathrm{e}^{\frac{-45202188644082545731183353297 8625\,t\,(2\,n+1)^2}{66461399789245793645190353 0140172288}}}{(2\,n+1)^2}\right)}{2778046668940015}$$

```
f_B_3(t)=(8/((2*n+1)^2*pi^2))*exp((-Dg_B(3)*(2*n+1)^2*pi^2*t)/L^2)
```

f_B_3(t) =

$$2251799813685248\,\mathrm{e}^{\frac{-538725736906983910222441706143 875\,t\,(2\,n+1)^2}{6646139978924579364519035301 40172288}} \Big/ 2778046668940015\,(2\,n+1)^2$$

```
M_B_3(t)=1-symsum(f_B_3(t),n,0,inf)
```

M_B_3(t) =

$$1-\frac{2251799813685248\left(\sum_{n=0}^{\infty}\dfrac{\mathrm{e}^{\frac{-53872573690698391022244170614 3875\,t\,(2\,n+1)^2}{66461399789245793645190353 0140172288}}}{(2\,n+1)^2}\right)}{2778046668940015}$$

Solved Data Bupivacaine:

```
T_B=[0:500:9000]
```

T_B = 1×19

0	500	1000	1500	2000	2500	⋯

```
mt_minf_B_1=double(M_B_1(T_B))
```

mt_minf_B_1 = 1×19

-0.0000	0.4103	0.5777	0.6954	0.7802	0.8414	0.8855 ⋯

```
mt_minf_B_2=double(M_B_2(T_B))
```

mt_minf_B_2 = 1×19

-0.0000	0.4189	0.5892	0.7078	0.7920	0.8520	0.8946 ⋯

```
mt_minf_B_3=double(M_B_3(T_B))
```

```
mt_minf_B_3 = 1×19
   -0.0000    0.4572    0.6396    0.7597    0.8398    0.8932    0.9288 ⋯
```

Solved Data Bupivacaine Combined Plot:

change in time scale to match for all therapeutics

```
T_B1=[0:1000:20000]
```

```
T_B1 = 1×21
         0       1000       2000       3000       4000       5000 ⋯
```

```
mt_minf_B1_1=double(M_B_1(T_B1))
```

```
mt_minf_B1_1 = 1×21
   -0.0000    0.5777    0.7802    0.8855    0.9404    0.9690    0.9838 ⋯
```

```
mt_minf_B1_2=double(M_B_2(T_B1))
```

```
mt_minf_B1_2 = 1×21
   -0.0000    0.5892    0.7920    0.8946    0.9466    0.9730    0.9863 ⋯
```

```
mt_minf_B1_3=double(M_B_3(T_B1))
```

```
mt_minf_B1_3 = 1×21
   -0.0000    0.6396    0.8398    0.9288    0.9683    0.9859    0.9937 ⋯
```

Plot Bupivacaine Different MW PEG:

```
figure('Name','Bupivacaine')
    xlabel('time (hours)')
    ylabel('Mt/Minf')
    title('Diffusion of Bupivacaine')
    set (gca,'FontSize', 16)
    hold on

    plot(T_B/3600,mt_minf_B_1)
    plot(T_B/3600,mt_minf_B_2)
    plot(T_B/3600,mt_minf_B_3)

    hold off
    legend({'575','700','2000'}, 'location','southeast')
    lgd=legend;
    lgd.Title.String='Molecular Weight PEG';
```

Diffusion of Bupivacaine
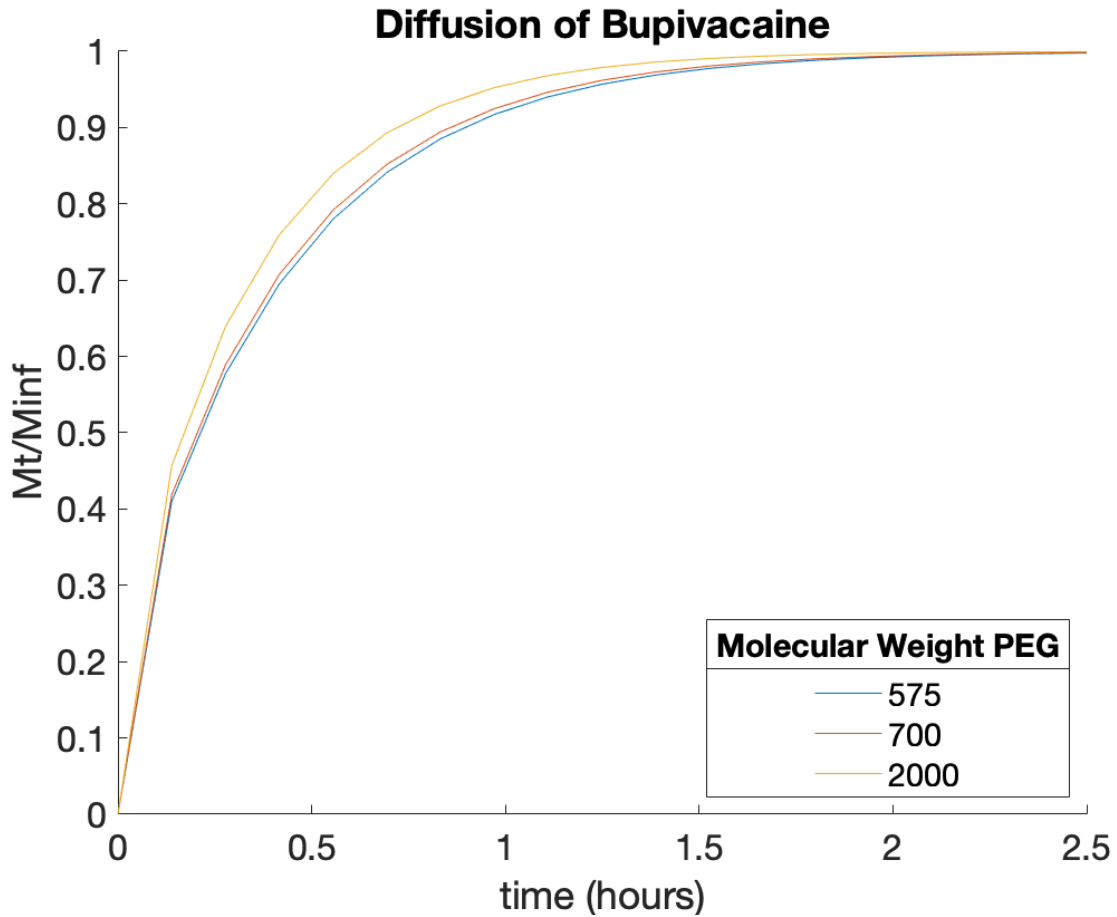
Tobramycin

Summation Tobramycin:

```
f_To_1(t)=(8/((2*n+1)^2*pi^2))*exp((-Dg_To(1)*(2*n+1)^2*pi^2*t)/L^2)
```

f_To_1(t) =

$$\frac{2251799813685248\, e^{\frac{-83684751494728274181940228947125\, t\, (2\,n+1)^2}{166153499473114484112975882535043072}}}{2778046668940015\, (2\,n+1)^2}$$

```
M_To_1(t)=1-symsum(f_To_1(t),n,0,inf)
```

M_To_1(t) =

$$1-\frac{2251799813685248\left(\sum_{n=0}^{\infty}\frac{e^{\frac{-83684751494728274181940228947125\, t\, (2\,n+1)^2}{166153499473114484112975882535043072}}}{(2\,n+1)^2}\right)}{2778046668940015}$$

```
f_To_2(t)=(8/((2*n+1)^2*pi^2))*exp((-Dg_To(2)*(2*n+1)^2*pi^2*t)/L^2)
```

93

```
f_To_2(t) =
```

$$\frac{2251799813685248\,e^{-\frac{17653985737811633929961081396012 5\,t\,(2\,n+1)^2}{3323069989462289682259517650700861 44}}}{2778046668940015\,(2\,n+1)^2}$$

```
  M_To_2(t)=1-symsum(f_To_2(t),n,0,inf)
```

```
M_To_2(t) =
```

$$1-\frac{2251799813685248\left(\sum_{n=0}^{\infty}\frac{e^{-\frac{17653985737811633929961081396012 5\,t\,(2\,n+1)^2}{3323069989462289682259517650700861 44}}}{(2\,n+1)^2}\right)}{2778046668940015}$$

```
  f_To_3(t)=(8/((2*n+1)^2*pi^2))*exp((-Dg_To(3)*(2*n+1)^2*pi^2*t)/L^2)
```

```
f_To_3(t) =
```

$$\frac{2251799813685248\,e^{-\frac{21892403285121126354361487859537 5\,t\,(2\,n+1)^2}{3323069989462289682259517650700861 44}}}{2778046668940015\,(2\,n+1)^2}$$

```
  M_To_3(t)=1-symsum(f_To_3(t),n,0,inf)
```

```
M_To_3(t) =
```

$$1-\frac{2251799813685248\left(\sum_{n=0}^{\infty}\frac{e^{-\frac{21892403285121126354361487859537 5\,t\,(2\,n+1)^2}{3323069989462289682259517650700861 44}}}{(2\,n+1)^2}\right)}{2778046668940015}$$

Solved Data Tobramycin:

```
  T_To=[0:500:9000]
```

```
T_To = 1×19
         0        500       1000       1500       2000       2500 …
```

```
  mt_minf_To_1=double(M_To_1(T_To))
```

```
mt_minf_To_1 = 1×19
    -0.0000     0.3605     0.5092     0.6191     0.7040     0.7699     0.8211 …
```

```
  mt_minf_To_2=double(M_To_2(T_To))
```

```
mt_minf_To_2 = 1×19
    -0.0000     0.3702     0.5227     0.6346     0.7199     0.7852     0.8353 …
```

```
  mt_minf_To_3=double(M_To_3(T_To))
```

```
mt_minf_To_3 = 1×19
```

```
     -0.0000     0.4123     0.5803     0.6983     0.7829     0.8439     0.8877 ···
```

Solved Data Tobramycin Combined Plot:

change in time scale to match for all therapeutics

```
T_To1=[0:1000:20000]
```

```
T_To1 = 1×21
             0        1000        2000        3000        4000        5000 ···
```

```
mt_minf_To1_1=double(M_To_1(T_To1))
```

```
mt_minf_To1_1 = 1×21
   -0.0000     0.5092     0.7040     0.8211     0.8919     0.9347     0.9605 ···
```

```
mt_minf_To1_2=double(M_To_2(T_To1))
```

```
mt_minf_To1_2 = 1×21
   -0.0000     0.5227     0.7199     0.8353     0.9032     0.9431     0.9665 ···
```

```
mt_minf_To1_3=double(M_To_3(T_To1))
```

```
mt_minf_To1_3 = 1×21
   -0.0000     0.5803     0.7829     0.8877     0.9419     0.9699     0.9844 ···
```

Plot Tobramycin Different MW PEG:

```
figure('Name','Tobramycin')
    xlabel('time (hours)')
    ylabel('Mt/Minf')
    title('Diffusion of Tobramycin')
    set (gca,'FontSize', 16)
    hold on

    plot(T_To/3600,mt_minf_To_1)
    plot(T_To/3600,mt_minf_To_2)
    plot(T_To/3600,mt_minf_To_3)

    hold off
    legend({'575','700','2000'}, 'location','southeast')
    lgd=legend;
    lgd.Title.String='Molecular Weight PEG';
```
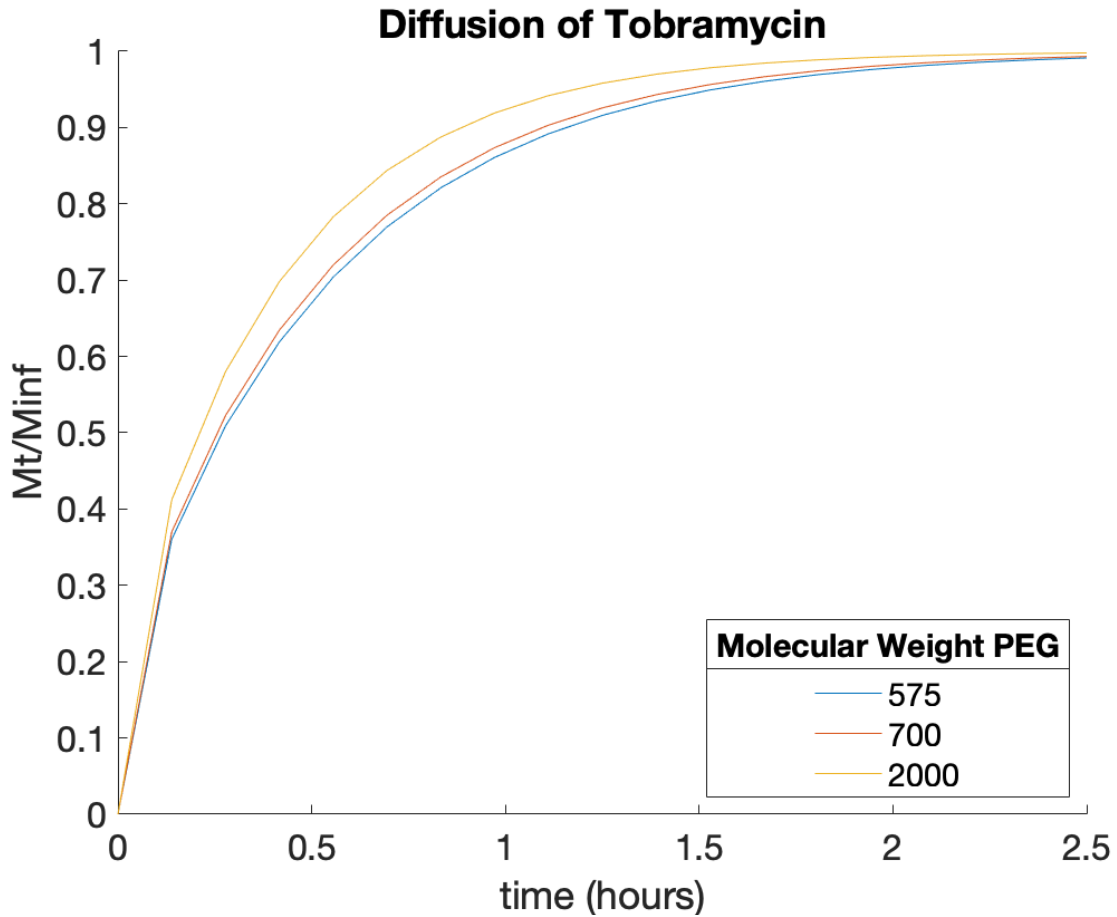
Vancomycin

Summation Vancomycin:

```
f_V_1(t)=(8/((2*n+1)^2*pi^2))*exp((-Dg_V(1)*(2*n+1)^2*pi^2*t)/L^2)
```

f_V_1(t) =

$$\frac{2251799813685248 \, e^{\frac{-313395911945060656662520637062875 \, t \, (2\,n+1)^2}{1329227995784915872903807060280344576}}}{2778046668940015 \, (2\,n+1)^2}$$

```
M_V_1(t)=1-symsum(f_V_1(t),n,0,inf)
```

M_V_1(t) =

$$1 - \frac{2251799813685248 \left(\sum_{n=0}^{\infty} \frac{e^{\frac{-313395911945060656662520637062875 \, t \, (2\,n+1)^2}{1329227995784915872903807060280344576}}}{(2\,n+1)^2} \right)}{2778046668940015}$$

```
f_V_2(t)=(8/((2*n+1)^2*pi^2))*exp((-Dg_V(2)*(2*n+1)^2*pi^2*t)/L^2)
```

```
f_V_2(t) =
```

$$2251799813685248\,e^{\frac{-3500773294996998204054420613263755\,t\,(2n+1)^2}{13292279957849158729038070602803445776}} \over 2778046668940015\,(2\,n+1)^2$$

```
M_V_2(t)=1-symsum(f_V_2(t),n,0,inf)
```

```
M_V_2(t) =
```

$$1-\frac{2251799813685248\left(\sum_{n=0}^{\infty}\frac{e^{\frac{-3500773294996998204054420613263755\,t\,(2n+1)^2}{13292279957849158729038070602803445776}}}{(2\,n+1)^2}\right)}{2778046668940015}$$

```
f_V_3(t)=(8/((2*n+1)^2*pi^2))*exp((-Dg_V(3)*(2*n+1)^2*pi^2*t)/L^2)
```

```
f_V_3(t) =
```

$$2251799813685248\,e^{\frac{-5126483794166898281202567617186255\,t\,(2n+1)^2}{13292279957849158729038070602803445776}} \over 2778046668940015\,(2\,n+1)^2$$

```
M_V_3(t)=1-symsum(f_V_3(t),n,0,inf)
```

```
M_V_3(t) =
```

$$1-\frac{2251799813685248\left(\sum_{n=0}^{\infty}\frac{e^{\frac{-5126483794166898281202567617186255\,t\,(2n+1)^2}{13292279957849158729038070602803445776}}}{(2\,n+1)^2}\right)}{2778046668940015}$$

Solved Data Vancomycin:

```
T_V=[0:1000:20000]
```

```
T_V = 1×21
         0       1000       2000       3000       4000       5000 ···
```

```
mt_minf_V_1=double(M_V_1(T_V))
```

```
mt_minf_V_1 = 1×21
   -0.0000    0.3488    0.4929    0.6003    0.6843    0.7506    0.8030 ···
```

```
mt_minf_V_2=double(M_V_2(T_V))
```

```
mt_minf_V_2 = 1×21
   -0.0000    0.3686    0.5205    0.6321    0.7173    0.7828    0.8331 ···
```

```
mt_minf_V_3=double(M_V_3(T_V))
```

```
mt_minf_V_3 = 1×21
```

```
    -0.0000      0.4460      0.6251      0.7451      0.8267      0.8822      0.9199 ···
```

Solved Data for Vancomycin Combined Plot:

change in time scale to match for all therapeutics

```
T_V1=[0:1000:20000]
```

```
T_V1 = 1×21
           0        1000        2000        3000        4000        5000 ···
```

```
mt_minf_V1_1=double(M_V_1(T_V1))
```

```
mt_minf_V1_1 = 1×21
    -0.0000      0.3488      0.4929      0.6003      0.6843      0.7506      0.8030 ···
```

```
mt_minf_V1_2=double(M_V_2(T_V1))
```

```
mt_minf_V1_2 = 1×21
    -0.0000      0.3686      0.5205      0.6321      0.7173      0.7828      0.8331 ···
```

```
mt_minf_V1_3=double(M_V_3(T_V1))
```

```
mt_minf_V1_3 = 1×21
    -0.0000      0.4460      0.6251      0.7451      0.8267      0.8822      0.9199 ···
```

Plot Vancomycin Different MW PEG:

```
figure('Name','Vancomycin')
    xlabel('time (hours)')
    ylabel('Mt/Minf')
    title('Diffusion of Vancomycin')
    set (gca,'FontSize', 16)
    hold on

    plot(T_V/3600,mt_minf_V_1)
    plot(T_V/3600,mt_minf_V_2)
    plot(T_V/3600,mt_minf_V_3)

    hold off
    legend({'575','700','2000'}, 'location','southeast')
    lgd=legend;
    lgd.Title.String='Molecular Weight PEG';
```

Diffusion of Vancomycin
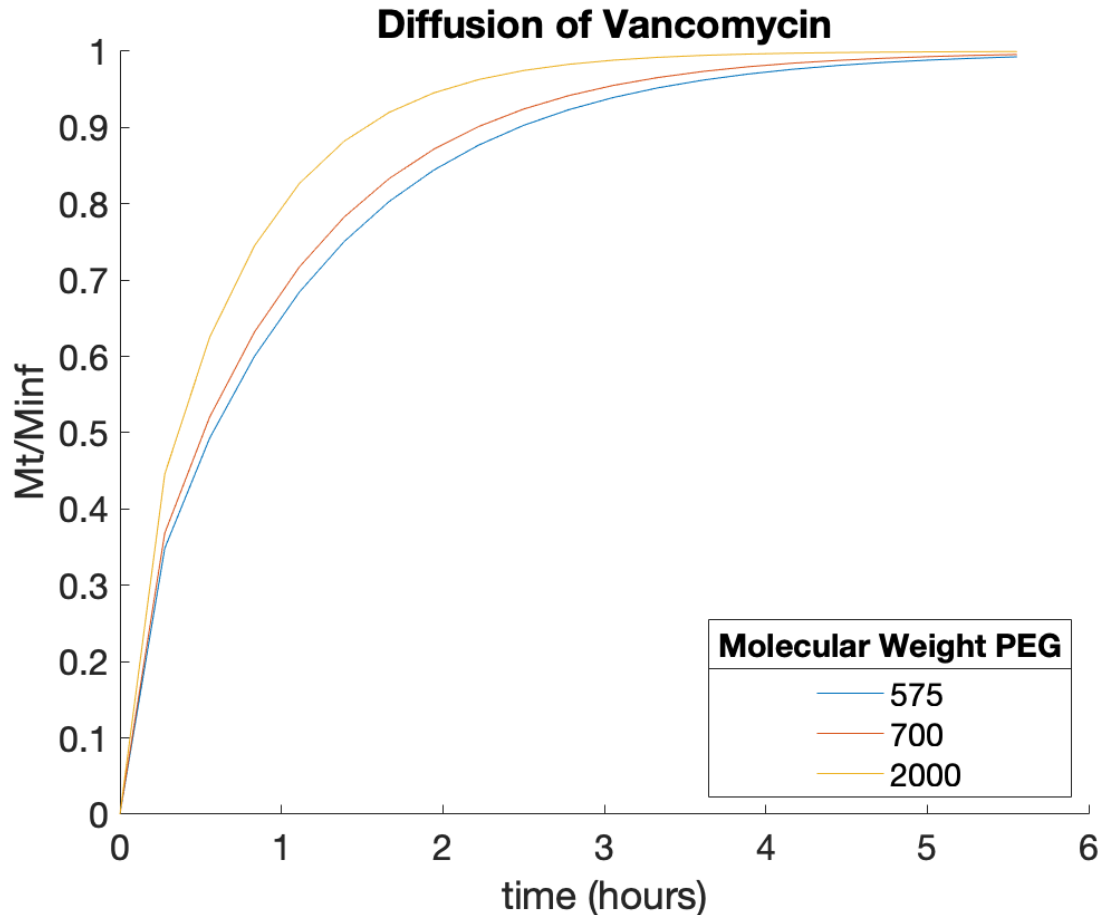
Combined Plots

plots with the release kinetics for all 4 therapeutic drugs

PEG 575

```
figure ('Name','PEG 575_1')
xlabel ('time (hours)')
ylabel ('Mt/Minf')
title ('Diffusion of Therapeutic Drugs in PEG 575')
set (gca,'FontSize', 16)
hold on
plot(T_TA1/3600,mt_minf_TA1_1)
plot(T_B1/3600,mt_minf_B1_1)
plot(T_To1/3600,mt_minf_To1_1)
plot(T_V1/3600,mt_minf_V1_1)
hold off

legend({'Tranexamic
Acid','Bupivacaine','Tobramycin','Vancomycin'},'location','southeast')
lgd=legend;
```

```
lgd.Title.String='Therapeutic Drug';
```

Diffusion of Therapeutic Drugs in PEG 575

PEG 700

```
figure ('Name','PEG 700_2')
xlabel ('time (hours)')
ylabel ('Mt/Minf')
title ('Diffusion of Therapeutics in PEG 700')
set (gca,'FontSize', 16)
hold on
plot(T_TA1/3600,mt_minf_TA1_2)
plot(T_B1/3600,mt_minf_B1_2)
plot(T_To1/3600,mt_minf_To1_2)
plot(T_V1/3600,mt_minf_V1_2)
hold off

legend({'Tranexamic
Acid','Bupivacaine','Tobramycin','Vancomycin'},'location','southeast')
lgd=legend;
lgd.Title.String='Therapeutic Drug';
```
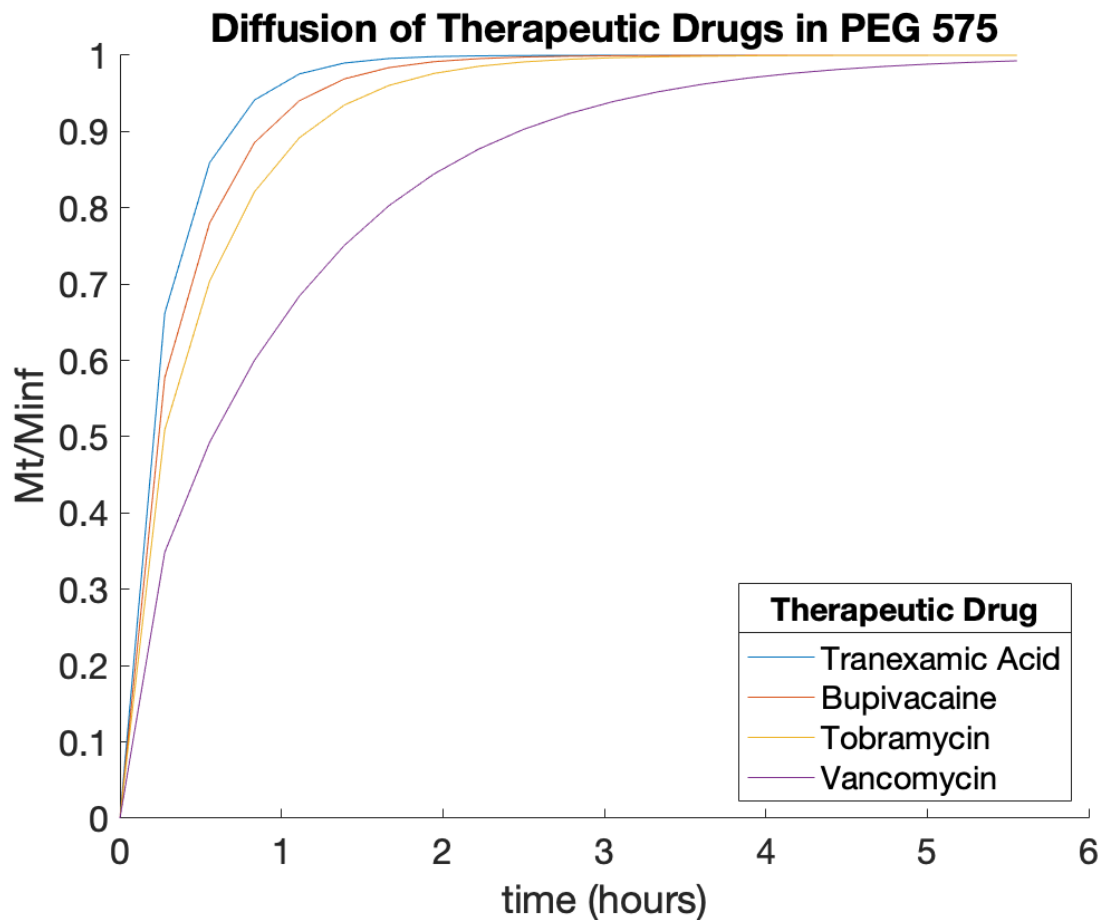
Diffusion of Therapeutics in PEG 700

PEG 2000

```
figure ('Name','PEG 2000_3')
xlabel ('time (hours)')
ylabel ('Mt/Minf')
title ('Diffusion of Therapeutics in PEG 2000')
set (gca,'FontSize', 16)
hold on
plot(T_TA1/3600,mt_minf_TA1_3)
plot(T_B1/3600,mt_minf_B1_3)
plot(T_To1/3600,mt_minf_To1_3)
plot(T_V1/3600,mt_minf_V1_3)
hold off

legend({'Tranexamic
Acid','Bupivacaine','Tobramycin','Vancomycin'},'location','southeast')
lgd=legend;
lgd.Title.String='Therapeutic Drug';
```
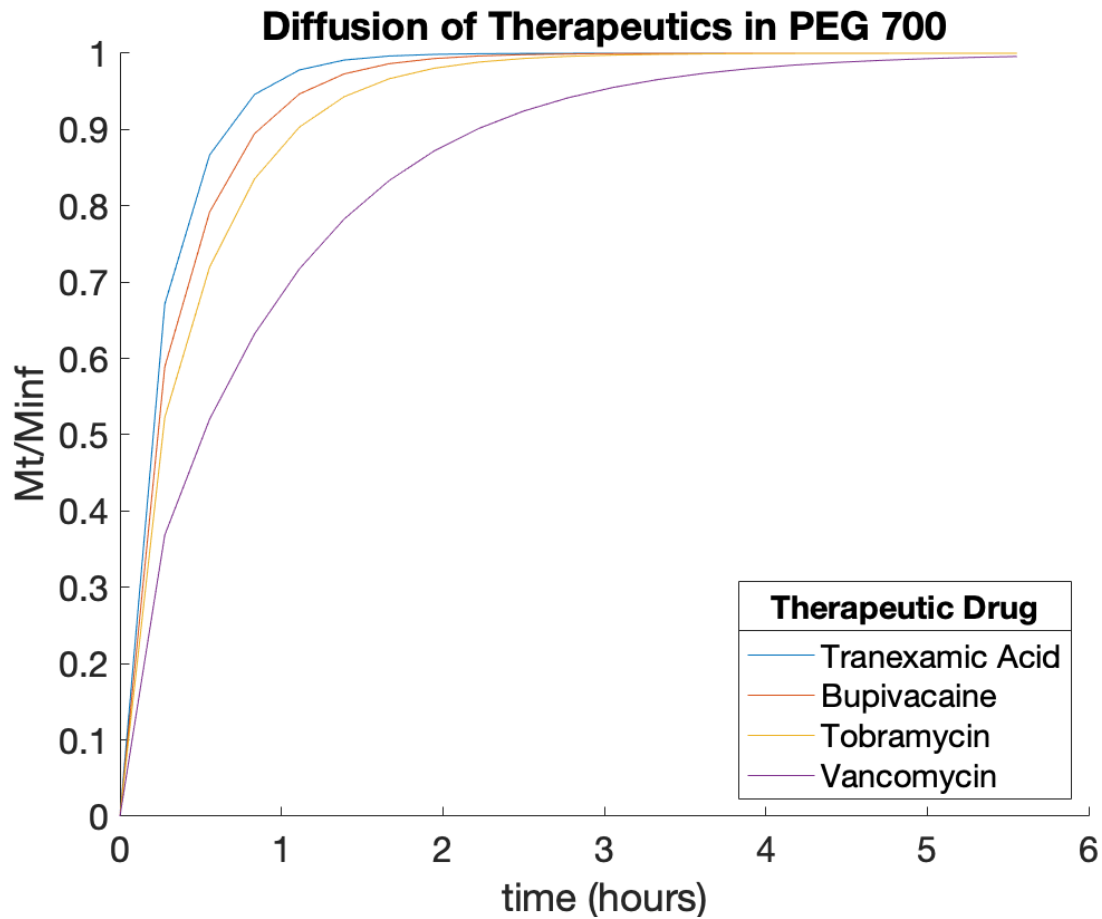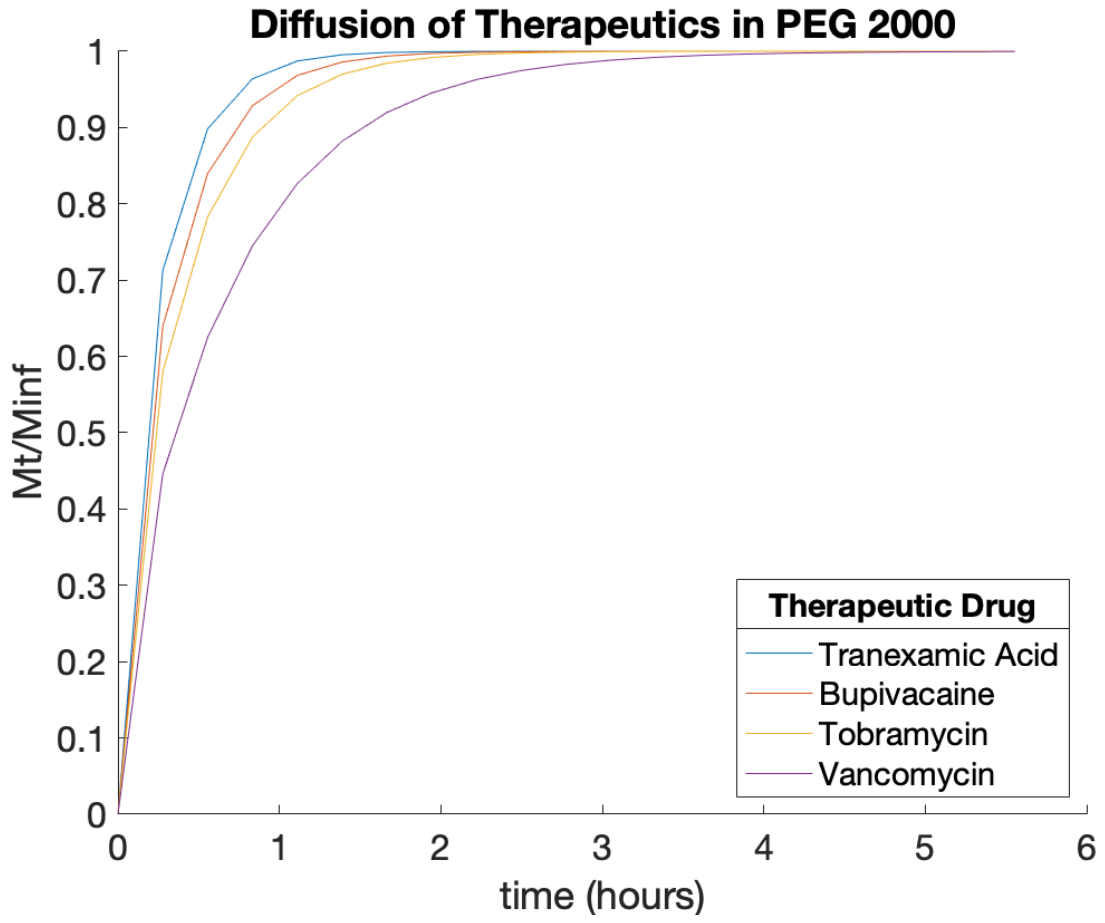
Diffusion of Therapeutics in PEG 2000

References

1. Green, B. Challenges of Aeromedical Evacuation in the Post-Cold-War Era. *Aerosp. Power J.* **15**, 14 (2001).

2. Cross, J. D., Ficke, J. R., Hsu, J. R., Masini, B. D. & Wenke, J. C. Battlefield orthopaedic injuries cause the majority of long-term disabilities. *J. Am. Acad. Orthop. Surg.* **19**, 1–7 (2011).

3. Murray, C. K., Obremskey, W. T., Hsu, J. R., Andersen, R. C., Calhoun, J. H., Clasper, J. C., Whitman, T. J., Curry, T. K., Fleming, M. E., Wenke, J. C. & Ficke, J. R. Prevention of Infections Associated With Combat-Related Extremity Injuries. *J. Trauma Inj. Infect. Crit. Care* **71**, S235–S257 (2011).

4. Murray, C. K., Hsu, J. R., Solomkin, J. S., Keeling, J. J., Andersen, R. C., Ficke, J. R. & Calhoun, J. H. Prevention and Management of Infections Associated With Combat-Related Extremity Injuries. *J. Trauma Inj. Infect. Crit. Care* **64**, S239–S251 (2008).

5. Patzakis, M. J. & Wilkins, J. Factors influencing infection rate in open fracture wounds. *Clin. Orthop. Relat. Res.* 36–40 (1989) doi:10.1097/00003086-198906000-00006.

6. Stansbury, L. G., Lalliss, S. J., Branstetter, J. G., Bagg, M. R. & Holcomb, J. B. Amputations in U.S. Military Personnel in the Current Conflicts in Afghanistan and Iraq. *J. Orthop. Trauma* **22**, 43–46 (2008).

7. Napierala, M. A., Rivera, J. C., Burns, T. C., Murray, C. K., Wenke, J. C. & Hsu, J. R. Infection reduces return-to-duty rates for soldiers with Type III open tibia fractures. *J. Trauma Acute Care Surg.* **77**, S194–S197 (2014).

8. Kragh, J. F., Walters, T. J., Baer, D. G., Fox, C. J., Wade, C. E., Salinas, J. & Holcomb, J. B. Survival With Emergency Tourniquet Use to Stop Bleeding in Major Limb Trauma. *Ann. Surg.* **249**, 1–7 (2009).

9. Kragh, J. F., Baer, D. G. & Walters, T. J. Extended (16-Hour) Tourniquet Application After Combat Wounds: A Case Report and Review of the Current Literature. *J. Orthop. Trauma* **21**, 274–278 (2007).

10. Gegel, B. T., Austin, P. N., Don, A. " & Johnson, ". *An Evidence-Based Review of the Use of a Combat Gauze (QuikClot) for Hemorrhage Control. AANA Journal   December* vol. 81 www.aana.com/aanajournalonline (2013).

11. Kotwal, R. S., O'Connor, K. C., Johnson, T. R., Mosely, D. S., Meyer, D. E. & Holcomb, J. B. A novel pain management strategy for combat casualty care. *Ann. Emerg. Med.* **44**, 121–127 (2004).

12. Metaxotos, N. G., Asplund, O., Hayes, M. & Nikolaos, N. G. The efficacy of bupivacaine

with adrenaline in reducing pain and bleeding associated with breast reduction: A prospective trial. *Br. J. Plast. Surg.* **52**, 290–293 (1999).

13.   Dhivya, S., Vijaya Padma, V. & Santhini, E. Wound dressings-a review. **5**, 24–28 (2015).

14.   INTRASITE Gel Hydrogel Wound Dressing | Smith & Nephew - US Professional. https://www.smith-nephew.com/professional/products/advanced-wound-management/intrasite-gel/.

15.   NU-GEL^TM Hydrogel with Alginate · GDM. https://www.gdm-medical.nl/en/product/nu-gel-hydrogel/.

16.   Timmons, J., Bertram, M., Pirie, G. & Duguid, K. Aquaform hydrogel - a new formulation for an improved wound care performance. *Wounds UK* **4**, (2008).

17.   Tsou, T.-L., Tang, S.-T., Huang, Y.-C., Wu, J.-R., Young, J.-J. & Wang, H.-J. *Poly(2-hydroxyethyl methacrylate) wound dressing containing ciprofloxacin and its drug release studies*.

18.   Laverty, G., Gorman, S. P. & Gilmore, B. F. Antimicrobial peptide incorporated poly(2-hydroxyethyl methacrylate) hydrogels for the prevention of Staphylococcus epidermidis-associated biomaterial infections. *J. Biomed. Mater. Res. Part A* **100A**, 1803–1814 (2012).

19.   Zumbuehl, A., Ferreira, L., Kuhn, D., Astashkina, A., Long, L., Yeo, Y., Iaconis, T., Ghannoum, M., Fink, G. R., Langer, R. & Kohane, D. S. Antifungal hydrogels. *Proc. Natl. Acad. Sci.* **104**, 12994–12998 (2007).

20.   Hudson, S. P., Langer, R., Fink, G. R. & Kohane, D. S. Injectable in situ cross-linking hydrogels for local antifungal therapy. *Biomaterials* **31**, 1444–1452 (2010).

21.   Xia, Q., Qing, J., Zhao, S., Deng, J. & Lü, R. A novel injectable chlorhexidine thermosensitive hydrogel for periodontal application: preparation, antibacterial activity and toxicity evaluation. doi:10.1007/s10856-010-4098-1.

22.   Cheng, G., Xue, H., Li, G. & Jiang, S. Integrated Antimicrobial and Nonfouling Hydrogels to Inhibit the Growth of Planktonic Bacterial Cells and Keep the Surface Clean. *Langmuir* **26**, 10425–10428 (2010).

23.   Ghobril, C., Charoen, K., Rodriguez, E. K., Nazarian, A. & Grinstaff, M. W. A Dendritic Thioester Hydrogel Based on Thiol-Thioester Exchange as a Dissolvable Sealant System for Wound Closure. *Angew. Chemie Int. Ed.* **52**, 14070–14074 (2013).

24.   Krsko, P. & Libera, M. Biointeractive hydrogels. *Mater. Today* **8**, 36–44 (2005).

25.   Herrick, W. G., Nguyen, T. V., Sleiman, M., McRae, S., Emrick, T. S. & Peyton, S. R. PEG-phosphorylcholine hydrogels as tunable and versatile platforms for mechanobiology.

Biomacromolecules **14**, 2294–2304 (2013).

26. Chen, S.-L., Fu, R.-H., Liao, S.-F., Liu, S.-P., Lin, S.-Z. & Wang, Y.-C. A PEG-Based Hydrogel for Effective Wound Care Management. doi:10.1177/0963689717749032.

27. Lokhande, G., Carrow, J. K., Thakur, T., Xavier, J. R., Parani, M., Bayless, K. J. & Gaharwar, A. K. Nanoengineered injectable hydrogels for wound healing application. *Acta Biomater.* **70**, 35–47 (2018).

28. Annabi, N., Yue, K., Tamayol, A. & Khademhosseini, A. Elastic sealants for surgical applications. *Eur. J. Pharm. Biopharm.* **95**, 27–39 (2015).

29. Ausman, J. I., Schiariti, M., Acerbi, F., Broggi, M., Tringali, G., Raggi, A., Broggi, G. & Ferroli, P. Surgical Neurology International Two alternative dural sealing techniques in posterior fossa surgery: (Polylactide-co-glycolide) self-adhesive resorbable membrane versus polyethylene glycol hydrogel. doi:10.4103/2152-7806.146154.

30. Elefteriades, J. A. 'How I do it: utilization of high-pressure sealants in aortic reconstruction'. (2009) doi:10.1186/1749-8090-4-27.

31. Konieczynska, M. D., Villa-Camacho, J. C., Ghobril, C., Perez-Viloria, M., Blessing, W. A., Nazarian, A., Rodriguez, E. K. & Grinstaff, M. W. A hydrogel sealant for the treatment of severe hepatic and aortic trauma with a dissolution feature for post-emergent care HHS Public Access. **4**, 222–227 (2017).

32. Elbert, D. L., Pratt, A. B., Lutolf, M. P., Halstenberg, S. & Hubbell, J. A. Protein delivery from materials formed by self-selective conjugate addition reactions. *J. Control. Release* **76**, 11–25 (2001).

33. Axpe, E., Chan, D., S. Offeddu, G., Chang, Y., Merida, D., Lopez Hernandez, H. & A. Appel, E. A Multiscale Model for Solute Diffusion in Hydrogels. *Macromolecules* **52**, 6889–6897 (2019).

34. Cruise, G. M., Scharp, D. S. & Hubbell, J. A. Characterization of permeability and network structure of interfacially photopolymerized poly(ethylene glycol) diacrylate hydrogels. *Biomaterials* (1998) doi:10.1016/S0142-9612(98)00025-8.

35. Weber, L. M., Lopez, C. G. & Anseth, K. S. Effects of PEG hydrogel crosslinking density on protein diffusion and encapsulated islet survival and function. *J. Biomed. Mater. Res. A* **90**, 720–729 (2009).

36. Zustiak, S. P. & Leach, J. B. Hydrolytically degradable poly(ethylene glycol) hydrogel scaffolds with tunable degradation and mechanical properties. doi:10.1021/bm100137q.

37. Molina, I., Li, S., Martinez, M. B. & Vert, M. Protein release from physically crosslinked hydrogels of the PLA/PEO/PLA triblock copolymer-type. *Biomaterials* **22**, 363–369 (2001).

38. Caliceti, P., Salmaso, S., Elvassore, N. & Bertucco, A. Effective protein release from PEG/PLA nano-particles produced by compressed gas anti-solvent precipitation techniques. *J. Control. Release* **94**, 195–205 (2004).

39. Merrill, E. W., Dennison, K. A. & Sung, C. Partitioning and diffusion of solutes in hydrogels of poly(ethylene oxide). *Biomaterials* (1993) doi:10.1016/0142-9612(93)90154-T.

40. Chesko, J., Kazzaz, J., Ugozzoli, M., O'Hagan, D. T. & Singh, M. An investigation of the factors controlling the adsorption of protein antigens to anionic PLG microparticles. *J. Pharm. Sci.* **94**, 2510–2519 (2005).

41. Seo, B. B., Park, M. R., Chun, C. J., Lee, J. Y. & Song, S. C. The biological efficiency and bioavailability of human growth hormone delivered using injectable, ionic, thermosensitive poly(organophosphazene)-polyethylenimine conjugate hydrogels. *Biomaterials* **32**, 8271–8280 (2011).

42. Wissink, M. J. B., Beernink, R., Pieper, J. S., Poot, A. A., Engbers, G. H. M., Beugeling, T., Van Aken, W. G. & Feijen, J. Binding and release of basic fibroblast growth factor from heparinized collagen matrices. *Biomaterials* **22**, 2291–2299 (2001).

43. Sakiyama, S. E., Schense, J. C. & Hubbell, J. A. Incorporation of heparin-binding peptides into fibrin gels enhances neurite extension: an example of designer matrices in tissue engineering. *FASEB J.* **13**, 2214–2224 (1999).

44. Lin, C. C. & Metters, A. T. Hydrogels in controlled release formulations: Network design and mathematical modeling. *Advanced Drug Delivery Reviews* (2006) doi:10.1016/j.addr.2006.09.004.

45. Siepmann, J. & Siepmann, F. Mathematical modeling of drug delivery. *Int. J. Pharm.* **364**, 328–343 (2008).

46. Lee, P. I. Modeling of drug release from matrix systems involving moving boundaries: Approximate analytical solutions. *International Journal of Pharmaceutics* (2011) doi:10.1016/j.ijpharm.2011.01.019.

47. PEG | Sigma-Aldrich. https://www.sigmaaldrich.com/catalog/search?term=PEG&interface=All&N=0&mode=match partialmax&lang=en&region=US&focus=product.

48. Browe, D. P., Wood, C., Sze, M. T., White, K. A., Scott, T., Olabisi, R. M. & Freeman, J. W. Characterization and optimization of actuating poly(ethylene glycol) diacrylate/acrylic acid hydrogels as artificial muscles. *Polymer (Guildf).* **117**, 331–341 (2017).

49. Tanaka, M., Girard, G., Davis, R., Peuto, A. & Bignell, N. Recommended table for the density of water between 0 °C and 40 °C based on recent experimental reports. *Metrologia* **38**, 301 (2001).

50. Canal, T. & Peppas, N. A. Correlation between mesh size and equilibrium degree of swelling of polymeric networks. *J. Biomed. Mater. Res.* **23**, 1183–1193 (1989).

51. Griffith Cima, L. & T. Lopina, S. Network structures of radiation-crosslinked star polymer gels. *Macromolecules* **28**, 6787–6794 (2002).

52. Gilbert, D. L., Teruo Okano, Teruo Miyata & Sung Wan Kim. Macromolecular diffusion through collagen membranes. *Int. J. Pharm.* (1988) doi:10.1016/0378-5173(88)90217-7.

53. Holland, T. A., Tabata, Y. & Mikos, A. G. In vitro release of transforming growth factor-β1 from gelatin microparticles encapsulated in biodegradable, injectable oligo(poly(ethylene glycol) fumarate) hydrogels. *J. Control. Release* (2003) doi:10.1016/S0168-3659(03)00258-X.

54. Hydrodynamic Radius Calculator. https://www.fluidic.com/resources/Toolkit/hydrodynamic-radius-Converter/.

55. Loll, P. J., Derhovanessian, A., Shapovalov, M. V, Kaplan, J., Yang, L. & Axelsen, P. H. Vancomycin forms ligand-mediated supramolecular complexes. *J Mol Biol* **385**, 200–211 (2009).

56. Peppas, N. A., Bures, P., Leobandung, W. & Ichikawa, H. Hydrogels in pharmaceutical formulations. *European Journal of Pharmaceutics and Biopharmaceutics* (2000) doi:10.1016/S0939-6411(00)00090-4.

57. Pande, S. & Parikh, J. R. Development and Validation of UV- Spectrophotometric Method for estimation of Vancomycin Hydrochloride. *J. Drug Deliv. Ther.* **9**, 116–118 (2019).

58. Ruckmani, K., Shaikh, S. Z., Khalil, P. & Muneera, M. S. A simple and rapid high-performance liquid chromatographic method for determining tobramycin in pharmaceutical formulations by direct UV detection. *Pharm. Methods* **2**, 117–123 (2011).

59. Corciova, A. Spectrophotometric method for determination of bupivacaine hydrochloride in pharmaeutical preparations. *Eur. Chem. Bull* **2**, 554–557 (2012).

60. Arayne, M. S., Sultana, N., Siddiqui, F. A., Mirza, A. Z. & Zuberi, M. H. Spectrophotometric techniques to determine tranexamic acid: Kinetic studies using ninhydrin and direct measuring using ferric chloride. *J. Mol. Struct.* **891**, 475–480 (2008).

61. Swinehart, D. F. The Beer-Lambert law. *J. Chem. Educ.* **39**, 333–335 (1962).

62. Mcphail, D. & Cooper, A. Thermodynamics and kinetics of dissociation of ligand-induced dimers of vancomycin antibiotics. *J. Chem. Soc. Faraday Trans.* **93**, 2283–2289 (1997).

63. Florey, K. & Wilson, T. D. *Analytical Profiles of Drug Substances*. (1990).

64. Reusch, W. Visible and Ultraviolet Spectroscopy. *MSU.edu* https://www2.chemistry.msu.edu/faculty/reusch/VirtTxtJml/Spectrpy/UV-Vis/spectrum.htm (2013).

65. Villa-Camacho, J. C., Ghobril, C., Anez-Bustillos, L., Grinstaff, M. W., Rodríguez, E. K. & Nazarian, A. The efficacy of a lysine-based dendritic hydrogel does not differ from those of commercially available tissue sealants and adhesives: An ex vivo study Orthopedics and biomechanics. *BMC Musculoskelet. Disord.* **16**, 1–6 (2015).

66. Wiegand, I., Hilpert, K. & Hancock, R. E. W. Agar and broth dilution methods to determine the minimal inhibitory concentration (MIC) of antimicrobial substances. *Nat. Protoc.* **3**, 163–175 (2008).